L SHIP RESEARCH AND DEVELOPMENT CENTER
Bethesda, Maryland 20034

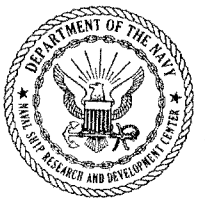

INCREMENTAL ANALYSIS OF NONLINEAR STRUCTURAL MECHANICS PROBLEMS WITH APPLICATIONS TO GENERAL SHELL STRUCTURES

by

Rembert F. Jones, Jr.

STRUCTURES DEPARTMENT
RESEARCH AND DEVELOPMENT REPORT

September 1973

Report 4142

INCREMENTAL ANALYSIS OF NONLINEAR STRUCTURAL MECHANICS PROBLEMS WITH APPLICATIONS TO GENERAL SHELL STRUCTURES

The Naval Ship Research and Development Center is a U. S. Navy center for laboratory effort directed at achieving improved sea and air vehicles. It was formed in March 1967 by merging the David Taylor Model Basin at Carderock, Maryland with the Marine Engineering Laboratory at Annapolis, Maryland.

Naval Ship Research and Development Center
Bethesda, Md. 20034

MAJOR NSRDC ORGANIZATIONAL COMPONENTS

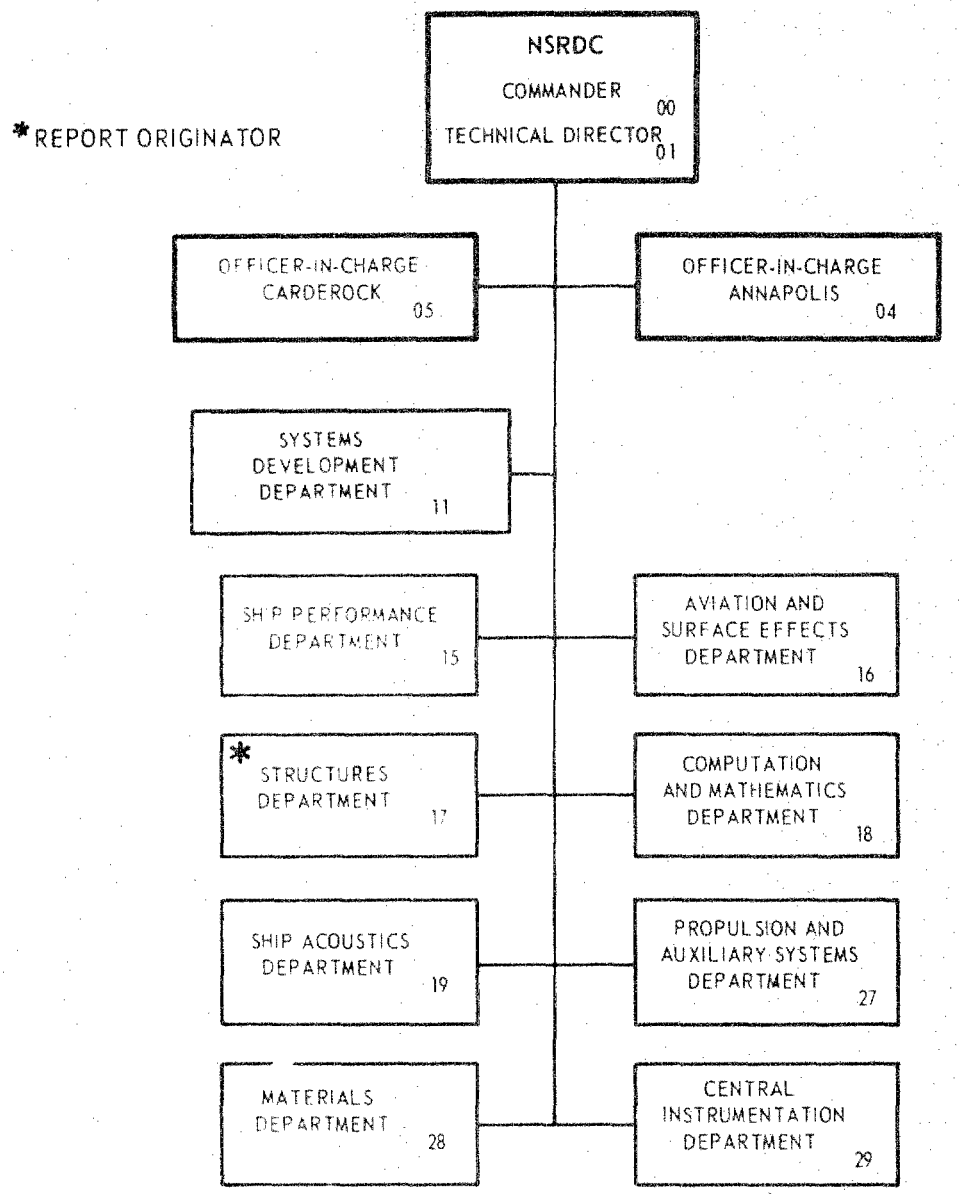

NDW-NSRDC 3960/44 (REV. 8/71)
GPO 917-872

DEPARTMENT OF THE NAVY
NAVAL SHIP RESEARCH AND DEVELOPMENT CENTER
BETHESDA, MARYLAND 20034

INCREMENTAL ANALYSIS OF NONLINEAR STRUCTURAL MECHANICS PROBLEMS WITH APPLICATIONS TO GENERAL SHELL STRUCTURES

by

Rembert F. Jones, Jr.

September 1973

Report 4142

TABLE OF CONTENTS

TABLE OF CONTENTS (Contd.)

LIST OF FIGURES

LIST OF TABLES

ABSTRACT

The primary theme is the nonlinear behavior of shell structures. A general formulation that can be applied to all structures is derived and then specialized for application to shells through the development of a quadrilateral shell finite element.

The formulation is in incremental form and is derived in terms of the material coordinate system. The procedure evolved to solve the nonlinear equilibrium equations allows for the inclusion of all terms as opposed to previous incremental procedures where the equations are linearized. The derivation of the formulation and solution procedure is independent of the finite element method, but it is this method that is used to exercise and apply the formulation. An elementary nonlinear problem is first solved and then more complex problems are studied by using the formulation and solution procedure.

The quadrilateral shell element which is introduced uses the exact geometry of the shell surface in the computation of stiffness matrices and loads. A consistent method is used for transforming the element and its properties; this improves element effectiveness for application to branched and reinforced shells. The shell surface geometry is used in the enforcement of the continuity of displacements for satisfying the convergence requirements. The ability of the element to undergo rigid body motion without causing strains is examined by studying the eigenvalues of the stiffness matrix of an element.

ADMINISTRATIVE INFORMATION

The study was conducted at the Naval Ship Research and Development Center (NSRDC) under the sponsorship of the Naval Ships Systems Command. Funding was provided by Subproject SF 43.422.210, Task 15053, Work Unit 1-1725-395. This report is based on the dissertation submitted to the faculty of The Catholic University of America in partial fulfillment of the requirements for the Doctor of Philosophy degree. The format is that of Catholic University rather than NSRDC.

CHAPTER 1
INTRODUCTION

1.1 GENERAL REMARKS

The mathematical description of large finite deformations is well founded. Unfortunately, it is also very complicated and difficult to apply to complex practical problems. Writers have presented the elegant theory for finite deformations but have been hampered in the solution of other than very basic problems. The present availability of high-speed computers, coupled with numerical methods, now makes it feasible to exploit the significant fundamental work that has been accomplished by pioneers in the field.

The most prominent numerical approach for solving complex structural problems is the finite element method. There has been a great deal of development and application of the method within the last 15 years. More investigators in the solid mechanics and structural engineering fields are probably devoted to this subject than to any other. Significant progress has been made. The requirements that must be satisfied to achieve adequate solutions have been recognized and methods have been conceived to satisfy a large number of these requirements. Progress on the most difficult of problems has been significant.

The need for a comprehensive analysis of general shell structures prompted investigators to turn to the finite element method. The early work was directed to developing linear analyses for shells, which is now well in hand. Small deflection, elastic analyses of shells with arbitrary geometry and reinforcement can now be conducted routinely. Research is currently being conducted to extend these shell analyses into the nonlinear geometry and nonlinear material range. Significant work has already been done but reasonable accuracy is obtained at the expense of very high computing costs.

The research reported herein is directed to a better understanding of the nonlinear behavior of structures, in particular, that of shell structures. A general formulation for conducting nonlinear incremental analyses is introduced and a quadrilateral shell finite element is developed. It is hoped that both will contribute to the more efficient solution of nonlinear structural problems.

1.2 NONLINEAR ANALYSES

The evolution of the procedures for handling material and geometrical nonlinearities by the finite element method has followed two separate and distinct paths. This has been possible because the formulation of one type of nonlinearity does not depend on the other and their effects can be included independently.

1.2.1 Nonlinear Material Behavior

Two successful techniques have been used to include the effects of time-independent isothermal, small strain plasticity behavior. Both are based on the incremental theory of

plasticity which has more physical meaning than the deformation or total strain theory. The classical approaches to solving plasticity problems were primarily restricted to using the deformation theory, but this is no longer necessary.

The first approach for solving plasticity problems numerically takes advantage of the analogy between plastic strain and body forces first recognized by Ilyushin [1]*. The total strain is decomposed into the elastic and the plastic portions. Element stiffness matrices are computed on the assumption of full elastic behavior in the element while the plastic strains are converted to equivalent pseudo forces at the nodes. The plastic strain increments used in the plastic load vector are those that were computed in the previous increment. Applications of this approach are described by Armen et al. [2] and Argyris et al. [3].

The second approach used to incorporate inelastic material behavior is the tangent stiffness method. This is the formulation that is used in the present study and will be described in detail subsequently. Briefly, the element stiffness matrices are recomputed at each load step by using the current transformation of total strain increment to total stress increment.

The important difference to note between the above two approaches is that in the initial strain method, element stiffness matrices are computed only at the beginning of the analysis whereas for the tangent stiffness method, they have to be computed at each load increment. Thus, if only inelastic material is being studied and it can be safely assumed that the displacements will remain small, the initial strain approach is found to be much more economical. However, if nonlinear geometric behavior must be incorporated in the analysis, the usual procedure has been to recompute element stiffness matrices at each load step. Thus there would be no particular advantage in using the initial strain approach. However, we shall discuss this point later.

1.2.2 Large Deformations

Mallet and Marcal [4] have described the three alternative formulations that have been used in the past for solving geometric nonlinear structural problems by the finite element stiffness method. The first approach seeks a displacement state which minimizes the total potential energy. The second method is a direct one where the equilibrium equations are solved for the desired displacements. Since these equations are nonlinear, such techniques as the Newton-Raphson, or modified Newton-Raphson, method have been used. The final and most popular approach is the linear incremental method. The equilibrium equations are linearized in each increment of loading to obtain stiffness matrices which are dependent on the current state of the structure. This is the approach used here and will be described in detail.

It is important to note that the above description of approaches for solving nonlinear geometric problems is the first line classification of the available methods. That is, the three approaches are fundamental and any solution procedure is applied to the total potential

*Numbers in brackets designate references listed on page 94.

energy, the nonlinear equilibrium equations, or the incremental equations obtained by linearizing the equilibrium equations.

The wide popularity of the linearized incremental formulation is apparently due to its computational advantage over the other two formulations. Efficient linear equation solvers have been developed and can be easily applied to the linearized formulation. Moreover, the incremental formulation allows the straightforward inclusion of constitutive relationships which are path dependent.

The development of a correct linear incremental formulation did not come easily. Martin surveyed the progress up to 1965 at the first Wright-Patterson meeting on matrix methods [5] and provided a derivation which helped to clarify matters. Since then, the formulations have stabilized and the correct forms are understood quite well.

The early derivations of the incremental formulation were based, more or less, on intuitive approaches where equilibrium was examined at individual nodal points by using local coordinate frames which translated and rotated with the deformation of the structure. The result was that the derivation of the geometrical or initial stress matrix for the same element varied from author to author. Martin pointed out these inconsistencies and derived the correct formulation for the initial stress matrix for several elements by using an initial configuration reference frame. However, Martin truncated the expressions, dropping terms which proved later to be significant.

If the Lagrangian description is used in the derivation, as was done by Martin, it was determined later that an additional matrix, termed by Marçal [6], the initial displacement matrix must be included in the stiffness equation. Marçal showed the importance of including this additional matrix and presented a formulation for its derivation.

Hibbitt, Rice, and Marçal [7] included the effects of following loads in the Lagrangian formulation by introducing the initial load matrix. This term was later derived by other investigators, e.g., Oden and Keys [8], but apparently its effect has not been determined because of the awkwardness of introducing the terms.

The most recent addition to the incremental stiffness equation has been the equilibrium correction term, apparently first introduced by Hofmeister, Greenbaum, and Evensen [9]. A formulation was introduced later by Stricklin et al. [10]. It will be shown subsequently that the term is needed because the pointwise equilibrium requirement within the element is not satisfied. The addition of the term in the linearized incremental stiffness equation can be viewed as including the zeroth term in a Taylor expansion as opposed to dropping the term in a simple Euler integration.

Hibbitt [11] pointed out that when the equilibrium correction term is included in the linear formulation, care must be taken to ensure that the incremental stresses are summed properly. He showed the importance of using the expression for strain (which is quadratic in the computed incremental displacements) in calculating the incremental stresses. Otherwise, the equilibrium correction term obtained by using the linearized formulation can give very poor results.

1.3 GENERAL SHELL FINITE ELEMENTS

The application of the finite element method to shell structures occurred early after the original development of the method; see Greene et al. [12]. This was a natural application since solutions for a large number of practical problems could be obtained only by some other numerical means such as the finite difference method. These early applications used flat plate elements to model the curved surface; these proved to be adequate if one was willing to pay the price for inordinate amounts of computing time. No known attempts have been made to apply these flat elements to nonlinear shell problems, and that is just as well since the results would probably have been disastrous.

The previous application of flat plate elements to shell problems revealed that the potential for solving very difficult problems was there [13, 14]. It remained to improve the method so that it could be applied with reduced computing time and cost and to other than linear elastic problems. The most logical improvement needed was the development of an adequate curved shell element with reasonable convergence characteristics. Unfortunately, this proved not to be easy. Although elements have been developed that are certainly more than adequate, there is still no one curved shell element that is accepted universally.

Gallagher [15] has outlined the four difficulties that have impeded the derivation of curved shell elements:

a. The choice of an appropriate shell theory – both shallow and nonshallow shell theories have been used. The choice of a particular shell theory should be preceded by the decision on whether to compute element stiffnesses in local element coordinates or in global coordinates. A direction that is often taken is to use shallow shell theory and then compute individual element stiffnesses in global coordinates, that is, element displacements and strains are in terms of global coordinates. This limits the application, then, to shells that are reasonably shallow and thus restricts their application. On the other hand, nonshallow shell theory can cause other problems because of the degrees of freedom used for the element. These problems arise when branched shells are being studied.

b. Description of the geometry of the element – depending on which shell theory is used, various geometrical quantities are required in the strain-displacement relationships. Curvatures are usually required but not always. Few investigators have recognized the importance of having these geometric quantities as accurate as possible. The approaches have been varied, but one feature seems common to most developments that have been reported previously. Along with assuming a certain displacement distribution in the element, the surface is taken to be some polynomial form with undetermined coefficients. The values of these coefficients are determined by evaluating geometric quantities within the element and on the boundary. The form of the polynomial can be determined uniquely taking a sufficient number of these points, depending on the order. There apparently has been only one report of an investigation being conducted to determine the magnitude of errors that are introduced by taking the above approach [16].

c. Representation of rigid body modes of behavior – many of the elements that have been developed to date are seriously deficient in that the assumed displacement patterns do not include all rigid body modes. The result is that strains are induced when the element undergoes a rigid body rotation or translation. This problem is usually associated with elements that are represented in curvilinear coordinates where rigid body motion is represented only by a coupling of the individual displacements.

d. Satisfaction of requirements related to continuity of displacements – to achieve this, the u, v, and w displacements must be represented by the same order of ploynomials. For flexure requirements, the first derivative of the displacements across element boundaries must be continuous. The early applications of flat plate elements did not satisfy either of these requirements but could be achieved in the limit as the grid pattern was made finer.

There has been an extensive development of curved shell elements for axisymmetric and arbitrary shells [16-35]. The various approaches can best be described by discussing representative examples; the remaining elements are variations on these basic types.

One of the more sophisticated elements developed to date is that by Argyris and Scharph [17]. They used fifth order polynomials to develop a triangular element with 18 degrees of freedom at each vertex node and three degrees at each midside node. The formulation for the element is derived in triangular surface coordinates. The particular form of differential geometry is derived for determining the metric of the undeformed and deformed surface. These are used to obtain the strain displacement relationships. The authors report that the element satisfies continuity requirements and that no strains are induced in the element under rigid body motion.

The triangular element developed by Dupuis [18], based on a previous formulation by Dupuis and Goel [19], has been used for a wide range of practical applications. The element has nine degrees of freedom at each node, and third order Lagrange polynomials are used to interpolate the displacements within the element. The accurate shell theory due to Koiter [36] and Budiansky and Sanders [37] is used for the strain displacement expressions. This element satisfies the continuity and rigid-body strain requirements.

The elements that probably have received the most attention are those developed by Zienkiewicz [20, 21]. The elements were originally reported for applications to thick shells and have since been specialized for anlayses of thin shells. Both triangular and quadrilateral shapes have been developed. The elements evolved from the original isoparametric concept where geometry and displacement modes are assumed to have the same functional form. The superparametric concept is used for this particular application; the geometry of the element is defined by higher order polynomials than those used in defining the displacements within the element. No shell theory, as such, is used in developing the element. The basic three-dimensional state of stress is assumed to exist throughout the element except that the normal stress through the thickness is set equal to zero to conform to shell behavior. There are five degrees of freedom at each of the nodes which may be arbitrary in number, depending on the order of the polynomials assumed for the displacements. The rigid-body condition is

satisfied by the element. There has been some difficulty in applying the element since it has a tendency to be too stiff. This problem has been circumvented by arbitrarily reducing the number of points used in the numerical integration procedure for computing the element stiffness matrix.

Appropriate shell theory has been employed to develop elements that include deformation due to transverse shear. This approach was used by Key and Beisinger [16] to develop a quadrilateral element where the shell theory is that given by Washizu [38]. The advantage of this approach is that the continuity requirements demand only that u, v, and w be continuous. The usual shell theory requirement that normals must remain normal is relaxed, and thus the first derivative of the normal displacement w does not have to be continuous across element boundaries. This approach makes the selection of displacement interpolation polynomials easier and Hermite polynomials are used. There are seven degrees of freedom at each of the four corner nodes. A mapping similar to that due to Zienkiewicz is used, and the element is limited to shells of revolution. It does not satisfy the rigid-body mode requirement.

The approach of using shallow shell theory in global coordinates is given by Cowper et al. [22]. The strain displacement expressions of Novozhilov [39] are employed in the element along with cubic distribution of the displacements in the surface of the shell and fifth-order polynomial distribution for the normal displacement. There are twelve degrees of freedom at each node. The surface of the shell is assumed to be quadratic in form; this dictates that the element must have constant curvatures. The primary disadvantage of this method is that complete shells cannot be studied.

A variation on the above approach was also presented by Cowper et al. [23]. The element was assembled in a global system on the shell surface, that is, the element stiffness was first computed in its own local system and then rotated on the shell surface to line up with the Gaussian coordinate system. This is different from the first developed where the elements were rotated to line up with the coordinate system in the projected plane of the total shell. Thus this second approach removed the restriction that only parts of complete shells could be studied. The same degrees of freedom were used as those reported for the initial Cowper approach [22].

The development of an additional triangular shell element was also reported by Cowper et al. [23]. Few details were given, but the development followed previous approaches where the degrees of freedom and stiffness were expressed in terms of the curvilinear coordinates in the shell surface. In all, 36 degrees of freedom are used in the element with 12 at each of the three nodes. The authors state that exact rigid-body modes are not obtained with the element and that this point has often been overemphasized. This is contrary to a majority of the research reported previously; see Gallagher [15].

The method of using shallow shell equations in local element coordinates and transforming to the surface was also reported in Strickland and Loden [24] where a triangular element is developed. The primary difference between this work and that reported by Cowper et al. [23] is that the order of displacement functions is less and thus results in fewer degrees

of freedom at the nodes. Linear functions are used for the membrane displacements and a cubic function for the normal displacement. There are a total of 15 degrees of freedom, five at each node. As expected, the convergence rate to the correct solution for increasing number of elements is less than that reported in Cowper et al. [22 and 23].

CHAPTER 2
GENERAL INCREMENTAL FORMULATION

We turn now to the derivation of the incremental formulation that will eventually be implemented by the finite element method. Although we will show how the formulation can be applied in terms of finite elements, it is not limited to this method but could be implemented by another numerical approach such as the finite difference method. The derivation in the beginning will be independent both of the magnitude of deflection or strain and of the constitutive relationship between stress and strain. The limitations on material behavior will be described later.

2.1 DEFINITION OF STRAIN AND STRESS

The motion of a point in a body is described by a one-to-one mapping of the type

$$x_i = X_i + u_i \tag{2.1}$$

where X_i is the initial position of the point and x_i is its position at a later time. For our work here, we will say that they are both in the same Cartesian coordinate system. The amount that the point moves is u_i. There are two classical methods by which the motion is described, the Lagrangian, or material description, and the Eulerian, or spatial description. In the first, various quantities are described in terms of X as the independent variable whereas in the second, x is the independent variable.

For the measure of strain, the square of a line segment before and after deformation is required. These are given respectively by

$$\begin{aligned} dS^2 &= dX_i dX_i = \delta_{ij}\, dX_i dX_j \\ ds^2 &= dx_i dx_i = \left(\frac{\partial x_i}{\partial X_j}\, dX_j\right)\left(\frac{\partial x_i}{\partial X_k}\, dX_k\right) \end{aligned} \tag{2.2}$$

where δ_{ij} is the Kronecker delta and the summation convention is used with the range from 1 to 3 over the indices. Thus the expression for strain becomes

$$ds^2 - dS^2 = dx_i dx_i - dX_i dX_i = 2e_{ij}\, dx_i dx_j = 2E_{ij}\, dX_i dX_j \tag{2.3}$$

The symbol e_{ij} is the Eulerian or Almansi strain tensor and E_{ij} is the Lagrangian or Green strain tensor.

In the later numerical implementation of the theory, it is more convenient to work with the material description and thus the Green strain tensor will be applied. Using equations (2.1), (2.2), and (2.3), the expression for Green strain becomes

$$E_{ij} = 1/2\,(u_{i,j} + u_{j,i} + u_{k,i}\,u_{k,j}) \tag{2.4}$$

where the comma indicates differentiation with respect to the material independent variable X.

Since the derivation and application of the methods to follow will be performed in the material coordinates, it will be necessary to have a stress measure which is in terms of the undeformed configuration. This will be the Kirchoff, or Piola, stress tensor.

We consider a force vector $d\underset{\sim}{f}$ acting on an element of area in the strained configuration and want to assign a correspondence rule between that vector and one, $d\underset{\sim}{F}$, acting on the element of area in the unstrained configuration. In component form, we write the Kirchoff rule for the correspondence [40] as

$$dF_i = \frac{\partial X_i}{\partial x_j}\, df_j \tag{2.5}$$

which is the same form as that for transforming from spatial to material coordinates.

Using equation (2.5), we can obtain the result that we actually need, i.e., the relationship between true or Cauchy stress and the nominal or Kirchoff stress. The derivation is given in many continuum mechanics text books and will not be repeated here. The transformation of Cauchy stress to Kirchoff stress is

$$S_{ij} = \frac{\rho_o}{\rho}\,\frac{\partial X_i}{\partial x_k}\,\frac{\partial X_j}{\partial x_\ell}\,\sigma_{k\ell} \tag{2.6}$$

where S_{ij} is the Kirchoff stress, $\sigma_{k\ell}$ is the Cauchy stress, ρ is the density in the deformed configuration, and ρ_o is the density in the original configuration. The Kirchoff stress tensor is symmetric. This can be seen above since the Cauchy stress tensor and the transformation are symmetric.

2.2 PRINCIPLE OF VIRTUAL WORK – INCREMENTAL THEORY

The method under consideration for solving the nonlinear problems will have to be incremental, i.e., obtained in finite steps, since we will be including inelastic material effects which are path dependent. The derivation given will be independent of material properties but can be applied to bodies which undergo plastic deformation, as will be described. Although we will eventually be considering problems that are characterized by small strains, the following derivation is not subject to that limitation.

The three configurations in the deformation path that are of interest are shown in Figure 2.1: the original undeformed reference configuration, the intermediate deformed configuration, and the current deformed configuration for which the virtual work equation will be written. The intermediate configuration is taken as the one just before the current configuration.

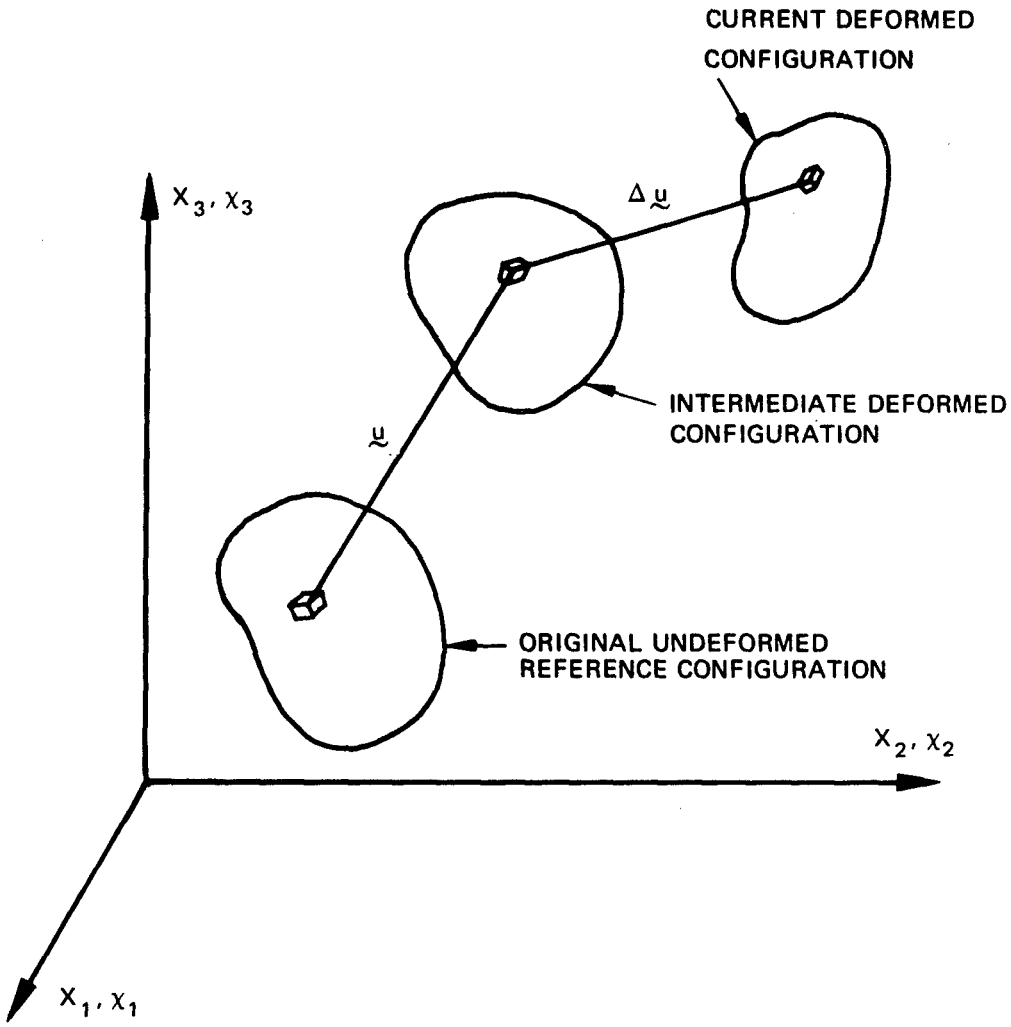

Figure 2.1 -- Original and Deformed Configurations

Over the surface of the body, there are specified displacements and surface tractions, $\underset{\sim}{F}$, in terms of the original undeformed reference configuration. There are also body forced, $\underset{\sim}{P}$, expressed in terms of the density and volume of the undeformed reference configuration.

The virtual work equation is now written for the current configuration

$$\int_V (S_{ij} + \Delta S_{ij})\delta(\Delta E_{ij})dV - \int_S (\rho_o P_i + \rho_o \Delta P_i)\delta(\Delta u_i)dV - \int_S (F_i + \Delta F_i + \Delta_G F_i)\delta(\Delta u_i)dS = 0 \tag{2.7}$$

which is referenced to the original undeformed state, i.e., all integrals are performed over that configuration and the conditions stated above with respect to loads hold true. The symbols S_{ij} and E_{ij} have been defined previously and are the Kirchoff stress tensor and the Green strain tensor, respectively. The prefix Δ indicates the change in the quantity that occurs in the body in going from the intermediate deformed configuration to the current configuration. The difference in the surface loading caused by this change is indicated by the symbol $\Delta_G F_i$. The subscript G means that the change in force is associated with the change in geometry.

In writing equation (2.7), it is assumed that the body is in equilibrium in the current configuration under the body forces, the external applied surface tractions, and the specified displacements. The body is then assumed to execute an infinitesimal virtual displacement $\delta(\Delta u)$ from the equilibrium configuration without violating the specified displacements. It is important to note that the variation is only on the displacements with the prefix Δ since the displacements occurring up to and including the intermediate deformed configuration just before the current configuration are assumed to be constants in the equation.

The value of the Green strain that occurs in the current configuration is

$$E_{ij} = 1/2\,(u_i + \Delta u_i)_{,j} + 1/2\,(u_j + \Delta u_j)_{,i} + 1/2\,(u_m + \Delta u_m)_{,i}\,(u_m + \Delta u_m)_{,j} \tag{2.8}$$

with the variation resulting from a variation in Δu_i given by

$$\delta(\Delta E_{ij}) = \delta E_{ij} = 1/2\,\delta(\Delta u_i)_{,j} + 1/2\,\delta(\Delta u_j)_{,i} + 1/2\,u_{m,i}\,\delta(\Delta u_m)_{,j} + 1/2\,u_{m,j}\,\delta(\Delta u_m)_{,i} + 1/2\,(\Delta u_m)_{,i}\,\delta(\Delta u_m)_{,j} + 1/2\,(\Delta u_m)_{,j}\,\delta(\Delta u_m)_{,i} \tag{2.9}$$

Now, substituting equation (2.9) into equation (2.7) and recognizing the symmetry of the strain tensor, we may write

$$\int_V (S_{ij} + \Delta S_{ij})[1/2\,(\delta(\Delta u_i)_{,j} + \delta(\Delta u_j)_{,i}) + u_{m,i}\,\delta(\Delta u_m)_{,j} + (\Delta u_m)_{,i}\,\delta(\Delta u_m)_{,j}]\,dV - \int_V (\rho_o P_i + \rho_o \Delta P_i)\delta(\Delta u_i)dV - \int_S (F_i + \Delta F_i + \Delta_G F_i)\delta(\Delta u_i)dS = 0 \tag{2.10}$$

This equation can now be rearranged to obtain

$$\underset{(1)}{\int_V \Delta S_{ij}[1/2\,(\delta(\Delta u_i)_{,j} + \delta(\Delta u_j)_{,i} + u_{m,i}\,\delta(\Delta u_m)_{,j}]\,dV} + \underset{(2)}{\int_V S_{ij}(\Delta u_m)_{,i}\,\delta(\Delta u_m)_{,j}\,dV}$$

$$+ \underset{(3)}{\int_V \Delta S_{ij}(\Delta u_m)_{,i}\,\delta(\Delta u_m)_{,j}\,dV} - \underset{(4)}{\int_S \Delta_G F_i \delta(\Delta u_i)dS} = \underset{(5)}{\int_V (\rho_o P_i + \rho_o \Delta P_i)\delta(\Delta u_i)dV} \qquad (2.11)$$

$$+ \underset{(6)}{\int_S (F_i + \Delta F_i)\delta(\Delta u_i)dS} - \underset{(7)}{\int_V S_{ij}[1/2\,(\delta(\Delta u_i)_{,j} + \delta(\Delta u_j)_{,i}) + u_{m,i}\delta(\Delta u_m)_{,j}]dV}$$

At this point it is convenient to discuss the form of equation (2.11). We will substitute shortly for an increment of stress in the first and third integrals and eliminate the virtual displacements when the above equation is cast into the form for the finite element method. The present form of the equation is such that we may compare the various terms with the linearized incremental formulations that have been derived by other investigators.

Except for term 3, each of the above numbered terms in equation (2.11) is an equivalent term of the linearized incremental stiffness equation of the finite element method. Term 1 can be shown to be the small displacement plus initial displacement matrix due to Marçal [6]. Term 2 is the initial stress or geometric stiffness matrix [5]. Term 4 is the initial load matrix of Hibbitt et al. [7] and Oden and Keys [8]. Terms 5 and 6 are the body force load plus increment of load and the surface load plus increment of load, respectively. Term 7 is the equilibrium load correction term of Hofmeister et al. [9] and Stricklin et al. [10]. Apparently, term 3 has never been included and applied in previous incremental nonlinear finite element analyses.

When we substitute for an increment of stress in equation (2.11), we will obtain a form of the incremental equations that is altogether different from the linear form that has been used by previous investigators. It is primarily term 3 although that is lost in the linearization process.

Before we go on, note one further point concerning equation (2.11). The equilibrium load correction term, term 7, can be written as

$$\int_V S_{ij}\,\delta(\Delta u_i)_{,j} + S_{ij}\,u_{m,i}\,\delta(\Delta u_m)_{,j}\,dV = \int_V S_{ij}\,(\delta_{im} + u_{m,i})\delta(\Delta u_m)_{,j}\,dV;$$

but

$$x_{m,i} = \delta_{im} + u_{m,i}$$

So term 7 becomes

$$\int_V S_{ij}\, x_{m,i}\, \delta(\Delta u_m)_{,j}\, dV$$

Now consider

$$\int_V (S_{ij}\, x_{m,i}\, \delta(\Delta u_m))_{,j}\, dV = \int (S_{ij}\, x_{m,i})_{,j}\, \delta(\Delta u_m)\, dV + \int_V S_{ij}\, x_{m,i}\, \delta(\Delta u_m)_{,j}\, dV$$

and by the Gauss integral theorem

$$\int_V [S_{ij}\, x_{m,i}\, \delta(\Delta u_m)]_{,j}\, dV = \int_S S_{ij}\, x_{m,i}\, \nu_j\, \delta(\Delta u_m) dS$$

where ν_j is the component of the unit normal to the surface. Thus, term 7 may be written

$$\int_V S_{ij}\, x_{m,i}\, \delta(\Delta u_m)_{,j}\, dV = -\int_V (S_{ij}\, x_{m,i})_{,j}\, \delta(\Delta u_m) + \int_S S_{ij}\, x_{m,i}\, \nu_j\, \delta(\Delta u_m)\, dS$$

We now take term 7 and add it to the first part of term 5 and the first part of term 6; regrouping and paying particular attention to the signs, we can write the expression

$$\int_V [(S_{ij}\, x_{m,i})_{,j} + \rho_o\, P_m]\, \delta(\Delta u_m)\, dV + \int (-S_{ij}\, x_{m,i}\, \nu_j + F_m)\, \delta(\Delta u_m)\, dS$$

At each step of the loading, we assume a displacement pattern which results in an assumed strain and stress distribution. If this resulting stress pattern satisfied the equations of equilibrium at each point in the body and at the surface, we could write the following equations (expressed in the Lagrangian description)

$$\begin{aligned} (S_{ij}\, x_{m,i})_{,j} + \rho_o\, P_m &= 0 \\ S_{ij}\, x_{m,i}\, \nu_j &= F_m \end{aligned} \qquad (2.12)$$

The point is that these conditions are not, in general, satisfied and that is why the above-considered terms have to be included in equation (2.11). This close examination of the virtual work equation points out the necessity of including all of the terms considered. It is often stated that equilibrium is not satisfied at any given load level in the incremental solution to nonlinear problems. Specifically, it is the pointwise equilibrium requirements of equation (2.12) that are not being satisfied.

We now propose to rearrange equation (2.11) into a form which will allow a different solution method to nonlinear incremental problems. This is shown as follows

$$\int_V \Delta S_{ij}\,[1/2\,(\delta(\Delta u_i)_{,j} + \delta(\Delta u_j)_{,i}) + (u_{m,i} + \Delta u_{m,i})\delta(\Delta u_m)_{,j}]\,dV$$

$$= \int_S (\rho_o P_i + \rho_o \Delta P_i)\delta(\Delta u_i)dV + \int_S (F_i + \Delta F_i + \Delta_G F_i)\delta(\Delta u_i)\,dS \qquad (2.13)$$

$$- \int_V S_{ij}\,[1/2\,(\delta(\Delta u_i)_{,j} + \delta(\Delta u_j)_{,i}) + (u_{m,i} + \Delta u_{m,i})\delta(\Delta u_m)_{,j}]\,dV$$

The first difference to be noted between equations (2.11) and (2.13) is that term 3 of equation (2.11) is put into the first term of that equation. Secondly, the initial stress term, term 2, of equation (2.11) is moved to the right side and put into term 7. Finally, the initial load term of equation (2.11) is put into term 6 of that equation.

The initial load term of equation (2.11) is a function of the change in area which is a function of the change in displacements that occur in each increment. When it is kept on the left side and its contribution added to the stiffness matrix, the matrix is nonsymmetric and causes problems in the solution process. Thus it is more convenient to move the term to the right side and include its contribution as part of the iteration on displacements that is performed to reach convergence. This is suggested in Hibbitt [11].

We now complete the formulation of equation (2.13) by first expressing an increment of stress in terms of an increment of strain by the constitutive relationship

$$\Delta S_{ij} = D_{ijab}\,\Delta E_{ab} \qquad (2.14)$$

where D_{ijab} is a known function of the current state. As described previously, both the stress and strain are measured with respect to the undeformed configuration. In writing equation (2.14), no limitation is put on the magnitude of strain. We ask only that the relationship between stress and strain remain linear. If the material goes plastic, then we will require the strain to be small and will use the constitutive relationship derived in the next chapter.

The increment of strain can be computed by

$$\Delta E_{ab} = 1/2\,(u_a + \Delta u_a)_{,b} + 1/2\,(u_b + \Delta u_b)_{,a} + 1/2\,(u_m + \Delta u_m)_{,a}\,(u_m + \Delta u_m)_{,b}$$

$$- 1/2\,(u_{a,b} + u_{b,a}) - 1/2\,u_{m,a}\,u_{m,b}$$

where the increment of strain is that in the current configuration minus the strain in the intermediate state just before the current state. The above reduces to

$$\Delta E_{ab} = 1/2\,(\Delta u_{a,b} + \Delta u_{b,a}) + 1/2\,u_{m,a}\,\Delta u_{m,b} + 1/2\,\Delta u_{m,a}\,u_{m,b} + 1/2\,\Delta u_{m,a}\,\Delta u_{m,b} \qquad (2.15)$$

After recognizing the symmetry in a and b, the expression for an increment of stress now becomes

$$\Delta S_{ij} = D_{ijab}[1/2(\Delta u_{a,b} + \Delta u_{b,a}) + u_{m,a}\Delta u_{m,b} + 1/2\,\Delta u_{m,a}\Delta u_{m,b}] \tag{2.16}$$

Now substituting equation (2.16) into the left side of equation (2.13), we obtain

$$\begin{aligned}
&\int_V \overset{(1)}{D_{ijab}}[1/2(\Delta u_{a,b} + \Delta u_{b,a}) + (u_{m,a} + 1/2\,\Delta u_{m,a})\Delta u_{m,b}] \\
&\qquad [1/2(\delta(\Delta u_i)_{,j} + \delta(\Delta u_j)_{,i}) + (u_{n,i} + \Delta u_{n,i})\delta(\Delta u_n)_{,j}] \\
&= \int_V \overset{(2)}{(\rho_o P_i + \rho_o \Delta P_i)}\delta(\Delta u_i)dV + \int_S \overset{(3)}{(F_i + \Delta F_i + \Delta_G F_i)}\delta(\Delta u_i)dS \\
&- \int_V \overset{(4)}{S_{ij}}[1/2(\delta(\Delta u_i)_{,j} + \delta(\Delta u_j)_{,i}) + (u_{m,i} + \Delta u_{m,i})\delta(\Delta u_m)_{,j}]\,dV
\end{aligned} \tag{2.17}$$

which is the final form of the virtual work equation. Note that the left side of the equation, which corresponds to the stiffness matrix, is nonsymmetric. Since we will want to use the efficiency of a symmetric equation solver, it will be convenient to separate the term into a symmetric part and a nonsymmetric part. This will be described subsequently.

2.3 FINITE ELEMENT FORMULATION OF THE EQUILIBRIUM EQUATION

Equation (2.7) was written without mentioning the origin and orientation of the material reference frame. It is often convenient to have a reference frame for each individual element when the finite element method is used. Thus, the previous derivation could be thought of as being done for a single element with its own coordinate system. Eventually we will want to be able to assemble all of the elements into a single system. This causes no problem since all of the quantities in equation (2.7) can be transformed easily because they are tensor quantities. Thus we will not make a distinction between the local element system and the common global system. This is necessary only when we start to apply the method to a particular problem.

The finite element stiffness approach is based on the approximation of representing the displacment at any point in an element in terms of polynomials. For our application here, the polynomials will be written in terms of the material coordinates. The coefficients in the polynomials are represented as linear combinations of the displacements that occur at the nodal points. Thus we seek a relationship where the displacement at any point in the element can be determined in terms of the displacements that occur at the nodes.

To determine the relationship between the displacements at the nodes and interior points, we start by selecting the polynomial form that will be used for the three u, v, and w displacements at the interior points. We represent this by

$$u_i = r_{ij}\,a_j \tag{2.18}$$

where r_{ij} is an array of polynomial terms and a_j are unknown coefficients. The range on i is one to three and the range on j is from one to the number of nodal points in the element times the number of displacements, i.e., degrees of freedom at each nodal point.

Next a set of generalized displacements is introduced [41] such that:

a. The connection of one element to another element along a common boundary is expressed by equating each of the respective generalized displacements pertaining to the boundary.

b. The displacement field along the common boundary is uniquely defined in terms of the generalized displacements that occur at the nodal points on the boundary and thus ensures the continuity of displacements across the boundary.

c. The number of generalized displacements is equal to the number of unknown coefficients in equation (2.18).

The set of generalized displacements is expressed by

$$v_i = R_{ij}\, a_j \tag{2.19}$$

The set of generalized displacements v_i is composed of the displacements u_i and, in general, their derivatives. Thus, the terms of the array R_{ij} are composed of the terms of r_{ij} plus terms created by taking the derivatives of the terms with respect to the material coordinates. The introduction of the generalized displacements sets the form of generalized forces which evolve in the process when the consistent loading vectors are derived.

An expression is required for the coefficients a_j in terms of the generalized displacements at the nodes. This is obtained by first substituting the coordinates of the nodal points into equation (2.19) to obtain a set of equations equal in number to the number of coefficients a_j:

$$\bar{v}_i = \bar{R}_{ij}\, a_j \tag{2.20}$$

where the bar indicates that the equations are written at the nodal points. This set of equations is then solved to obtain

$$a_i = \bar{R}_{ij}^{-1}\, \bar{v}_j = A_{ij}\, \bar{v}_j \tag{2.21}$$

and is the desired result which expresses the coefficients of the polynomials of equation (2.18) as linear combinations of the generalized displacements that occur at the nodes. Each term in A_{ij} is a constant. Substituting (2.21) into (2.18), we obtain

$$u_i = r_{ij}\, A_{jk}\, \bar{v}_k \tag{2.22}$$

the displacements u, v, and w at any point in the element expressed in terms of the generalized displacements at the nodes.

Using equation (2.22), we may now obtain the finite element stiffness equation from the virtual work equation (2.17). But first we need the following expressions

$$u_{i,\ell} = r_{ij,\ell} A_{jk} \bar{v}_k \tag{2.23}$$

$$\Delta u_{i,\ell} = r_{ij,\ell} A_{jk} \Delta\bar{v}_k \tag{2.24}$$

$$\delta(\Delta u_{i,\ell}) = r_{ij,\ell} A_{jk} \delta(\Delta\bar{v}_k) \tag{2.25}$$

each of which is obtained from (2.22). Equation (2.25) is the result of r_{ij} being a function of the initial position only.

Substituting (2.23) through (2.25) into (2.17), the following is obtained for each of the terms of that equation

Term 1

$$\int_V D_{ijab}[1/2(r_{ae,b} + r_{be,a}) + (\bar{v}_d + 1/2\,\Delta\bar{v}_d) r_{hc,a} r_{he,b} A_{cd}]$$
$$[1/2(r_{in,j} + r_{jn,i}) + (\bar{v}_\ell + \Delta\bar{v}_\ell) r_{mk,i} r_{mn,j} A_{k\ell}]\, dV\, A_{nq} A_{ef} \Delta\bar{v}_f \delta(\Delta\bar{v}_q) \tag{2.26}$$

Term 2

$$\int_V (\rho_o P_i + \rho_o \Delta P_i) r_{ij}\, dV\, A_{jq}\, \delta(\Delta\bar{v}_q) \tag{2.27}$$

Term 3

$$\int_S (F_i + \Delta F_i + \Delta_G F_i) r_{ij}\, dS\, A_{jq}\, \delta(\Delta\bar{v}_q) \tag{2.28}$$

Term 4

$$\int_V S_{ij}[1/2(r_{in,j} + r_{jn,i}) + (\bar{v}_\ell + \Delta\bar{v}_\ell) r_{mk,i} r_{mn,j} A_{k\ell}]\, dV\, A_{nq}\, \delta(\Delta\bar{v}_q) \tag{2.29}$$

The virtual displacements, $\delta(\Delta\bar{v}_q)$, of the nodal points are arbitrary and thus can be eliminated. In other words, since they are arbitrary, an equation in just the coefficients of the virtual displacements must hold true. The result of equating the coefficients is the stiffness equation.

An important point to remember at this stage is that the virtual displacement of a nodal point generalized displacement may be thought of as causing virtual displacements within all of the elements that are connected to the nodal point. Thus all of these elements are represented in the stiffness equation that is written to eliminate the generalized virtual

displacements at the nodes. We noted earlier that the equations may be transformed easily – so there is no problem in writing an equation in a single coordinate system in the coefficients of the virtual displacements.

The matrix form of the stiffness equation can finally be obtained by letting the first bracketed part in (2.26) be represented by the matrix [B1] and the second bracketed part by the matrix [B2]. The resulting matrix form is

$$\begin{aligned}([A]^T\int_V [B2]^T[D][B1]dV[A])\{\Delta\bar{v}\} &= [A]^T\int_V [r]^T(\rho_0\{P\}+\rho_0\{\Delta P\})dV \\ &+ [A]^T\int_S [r]^T(\{F\}+\{\Delta F\}+\{\Delta_G F\})dS - [A]^T\int_V [B2]^T\{S\}\,dV\end{aligned} \tag{2.30}$$

where the stress in (2.29) has been written as a column vector. (The change in surface tractions due to a change in geometry will be derived later for the quadrilateral element.) The first two terms on the right are the generalized forces; their form is set by the choice of generalized displacements.

In forming the stiffness matrix and the equilibrium correction term (the first and last terms of (2.30), respectively), it is noted from (2.26) and (2.29) that the increment of displacement that occurs in going from the intermediate deformed configuration to the current configuration is required. Again, these are the quantities denoted by $\Delta\bar{v}$. Since the increment of displacement is the fundamental unknown, some method is required to estimate the values to be used in forming each of the terms. This estimate is obtained by a linear extrapolation of the increment of displacements that occur in the previous increment. Thus, if the load steps are equal, for example, then the estimate of the displacements is set equal to those that occurred in the previous increment. An iteration is carried out at each load step to reach convergence (within a given tolerance); the details will be described later.

As noted previously, the stiffness matrix derived above is nonsymmetric. To circumvent the problem of having to solve a nonsymmetric set of equations after the elements are assembled into the common global system, the stiffness matrix is decomposed into a symmetric and skew symmetric part, that is,

$$K_{ij} = 1/2\,(K_{ij} + K_{ji}) + 1/2\,(K_{ij} - K_{ji}) \tag{2.31}$$

where the first term on the right is the symmetric part and the second is the antisymmetric part. Thus, simplifying the notation of equation (2.30) and putting the nonsymmetric part of the stiffness matrix on the right side, we may write

$$[K]_S\{\Delta\bar{v}\} = \{P\} + \{\Delta P\} + \{F\} + \{\Delta F\} + \{\Delta_G F\} - \{E\} - [K]_A\{\Delta\bar{v}_{est}\} \tag{2.32}$$

The subscripts S and A respectively indicate the symmetric and antisymmetric parts of the stiffness matrix. The symbol E stands for the equilibrium correction term and the remaining

terms are self-explanatory. The nonsymmetric part of the stiffness matrix is now taken as an equivalent set of forces by using the estimated displacements that occur in going from the intermediate configuration to the current configuration.

2.4 INITIAL STRESS PROBLEMS

We close this chapter with a brief account of how the above derivation stands with respect to previous derivations; the closest are those that evolve from considering the incremental problem as an initial stress problem.

The initial stress problem has a long history that dates back to Cauchy [42]. More recently, Green, Rivlin, and Shield [43] and Murnaghan [44] have studied the problem. The formulation is presented in the textbook by Washizu [38].

Finite element investigators who have used the initial stress approach include Felippa [45], Hofmeister, Greenbaum, and Evensen [9], Murray and Wilson [46], Bergan [47], and Yaghmai [48].

Briefly, the approach that seems to be common to all of the above, except that of Hofmeister et al. [9], is to write the virtual work equation for two successive configurations, take the difference in the two, and then linearize the result to obtain incremental stiffness equations. Various coordinate systems are used in the derivations.

The approach of Hofmeister et al. [9] is to use the intermediate deformed configuration shown in Figure 2.1 as the current reference frame and to consider this as the initial state with the body subject to initial stress. Thus, the method involves updating coordinates and also transforming stresses to a common system so that they may be added. The importance of this last point was brought out by Nemat-Nasser and Shatoff [49] who derived an incremental approach and implemented it with the finite difference method.

The two primary points to be said for the derivation presented here are, first, its simplicity and, second, the nontruncation of terms. A linearization process is imposed, as discussed in the previous section, but the equations are complete and answers can be obtained as accurately as desired by using iteration. Moreover, as will be shown later, even without iteration, the formulation seems to give better results than have been obtained by previous incremental formulations.

CHAPTER 3
CONSTITUTIVE LAWS OF PLASTICITY

This chapter reviews the basic theory of plasticity required for the stress-strain relationship. Many publications may be consulted for a more extensive treatment, e.g., the text by Hill [50], the work of Koiter [51], and the extensive review by Naghdi [52]. Here the description will consider only small strain problems which may be assumed to be independent of temperature and time.

3.1 BASIC ASSUMPTIONS – INITIAL YIELD CONDITION

The state of stress is discussed in terms of a general nine-dimensional stress space. In this space there is an envelope which defines the limit of elastic behavior of a point within a body. As load is slowly applied, the state of stress at a single point in the body is defined by a trajectory which moves in the stress space. There is such a trajectory for all points in the body. As long as the trace of the trajectory moves within the envelope and does not touch the surface, the material at the point under consideration does not undergo any plastic deformation. Only trajectories that are within and on the boundary of the envelope have any meaning.

The envelope is referred to as the initial yield surface; it can be shown to be convex and contains the origin of the stress space. On the basis of experimental data and the behavior of inelastic deformations, the shape of the surface is considered to be limited to several general configurations. The initial state of the material is usually assumed to be isotropic and shows no preferred direction with respect to stress. Further, it is known that the initial yield is primarily brought about by shearing stresses. Bridgman [53], among others, has shown experimentally that the yielding is primarily independent of hydrostatic pressure. It is therefore convenient to express the envelope or yield function in terms of the invariants of the deviatoric stress tensor

$$\sigma'_{ij} = \sigma_{ij} - 1/3\, \delta_{ij}\, \sigma_{kk} \tag{3.1}$$

where the invariants are

$$\begin{aligned} J_1 &= \sigma'_{ii} = 0 \\ J_2 &= 1/2\, \sigma'_{ij}\, \sigma'_{ij} \\ J_3 &= 1/3\, \sigma'_{ij}\, \sigma'_{jk}\, \sigma'_{ki} \end{aligned} \tag{3.2}$$

Thus, the initial yield function may then be expressed as

$$f = f(J_2, J_3) \tag{3.3}$$

Many functions have been proposed for the initial yield condition but two have become the most reasonable for simulating experimental data. The first is the Tresca function expressed in terms of maximum shearing stresses. It is assumed that plastic flow can occur at the point where the maximum shearing stress reaches the yield stress obtained in pure shear. The second yield function is that due to von Mises and is the one that has been applied in the work here. In formulating the function, von Mises ignored the effects of the invariant J_3 and expressed the condition by the equation

$$f(J_2) = J_2 - 1/3\,\sigma_o^2 = 1/2\,\sigma'_{ij}\,\sigma'_{ij} - 1/3\,\sigma_o^2 = 0 \tag{3.4}$$

where σ_o is the yield stress obtained in a simple tension test. A convenient geometrical interpretation of the function is obtained when it is plotted in principal stress space. It turns out that the yield surface, or envelope, is a circular cylinder with the axis equally inclined to the three principal stress axes. The cylinder has infinite length.

3.2 LOADING CRITERIA

Once the state of stress at a point is such that plastic flow can occur, a criterion must be established to determine whether it actually takes place. Assume now that the yield function for the general case becomes a function of the plastic strain e^P_{ij}, that is,

$$f = f(\sigma_{ij}, e^P_{ij}) = 0 \tag{3.5}$$

and the function no longer defines just initial yield but also includes additional information and is now called the loading function.

Consider the differential

$$df = \frac{\partial f}{\partial \sigma_{ij}}\, d\sigma_{ij} + \frac{\partial f}{\partial e^P_{ij}}\, de^P_{ij} \tag{3.6}$$

at a point where equation (3.5) is satisfied. Then $df<0$ implies that $f<0$ and is the condition for unloading from a plastic state to an elastic state. An additional requirement for unloading is that no change can occur in the plastic strain. The terms neutral loading and loading can be defined by using a similar argument. In summary,

During unloading: $$\frac{\partial f}{\partial \sigma_{ij}}\, d\sigma_{ij} < 0,\ f = 0 \tag{3.7}$$

During neutral loading: $$\frac{\partial f}{\partial \sigma_{ij}}\, d\sigma_{ij} = 0,\ f = 0 \tag{3.8}$$

During loading: $$\frac{\partial f}{\partial \sigma_{ij}}\, d\sigma_{ij} > 0,\ f = 0 \tag{3.9}$$

A geometric interpretation can be associated with each of the above since the loading surface is closed. **For unloading, the stress increment vector is directed inward; during neutral loading,** it is tangent to the surface, and during loading, it is pointed outward.

3.3 WORK HARDENING – THE DRUCKER POSTULATE

When a uniaxial test specimen exhibits work hardening, the stress is a monotonically increasing function of increasing strain. A generalization to combined stress states is required. This generalization is attributed to Drucker and is fundamental in the theory of plasticity since all of the information required for the stress-strain relationships can be derived by using the concept. Drucker stated that if a body in equilibrium has its stress state changed continuously by an external agency such that the final stress state coincides with the original one (i.e., a closed cycle), then the work done by the external agency is not negative.

Assume that a body is in an equilibrium state of stress σ_{ij} and strain e_{ij}. Then, if small surface tractions are applied to the body, small increments in stress, $d\sigma_{ij}$, and strain, de_{ij}, will occur. Once the loading is removed, all of the elastic strains, de^e_{ij}, will be recovered. Then the body has experienced work hardening if the following two conditions are true: during loading;

$$d\sigma_{ij}\, de_{ij} > 0 \tag{3.10}$$

and on completion of the cycle,

$$d\sigma_{ij}\,(de_{ij} - de^e_{ij}) \geq 0 \tag{3.11}$$

The quantity in parentheses is the nonrecoverable plastic strain de^P_{ij} and thus the second equation can be rewritten

$$d\sigma_{ij}\, de^P_{ij} \geq 0 \tag{3.12}$$

3.4 FLOW RULE FOR WORK-HARDENING MATERIALS

As a consequence of the Drucker postulate, the following three properties of the loading function and inelastic deformations can be obtained.

a. The initial yield surface and all following loading surfaces are convex.

b. At a regular (smooth) point on the loading surface, the strain increment vector must be directed normal to the surface.

c. An increment of plastic strain must be a linear function of an increment of stress.

Statement a can be shown to be true by considering equation (3.12). If each of the increments of stress and strain is associated with a respective vector, then equation (3.12) states that the dot product of the two vectors must be equal to, or greater than, zero. This means that the angle between the two vectors is less than, or equal to, 90 degrees. In careful consideration of this, it may be simply stated that there can be no inward dents on the loading surface and thus must be convex at all points.

Statement b may be verified by using an argument similar to that given above. The additional conclusion can be reached that the direction of the strain increment vector is independent of the direction of the stress increment vector. Statement b may be expressed mathematically by

$$de_{ij}^{P} = \Lambda \frac{\partial f}{\partial \sigma_{ij}} \tag{3.13}$$

where Λ is a positive function dependent on stress, strain, and strain history. It is noted that the function f may be viewed as a plastic potential.

The meaning of statement c can be shown by considering the following. The loading function must remain zero during loading, i.e., in passing from one plastic state to another plastic state. This is expressed by

$$f(\sigma_{ij}, e_{ij}^{P}) = 0 \tag{3.14}$$

and is what Prager [54] called the consistency condition. Thus, we must have

$$df = \frac{\partial f}{\partial \sigma_{ij}} d\sigma_{ij} + \frac{\partial f}{\partial e_{ij}^{P}} de_{ij}^{P} = 0 \tag{3.15}$$

Now, substituting (3.13) into (3.15) and solving for Λ, we obtain

$$\Lambda = - \frac{\dfrac{\partial f}{\partial \sigma_{k\ell}} d\sigma_{k\ell}}{\dfrac{\partial f}{\partial e_{ij}^{P}} \dfrac{\partial f}{\partial \sigma_{ij}}} \tag{3.16}$$

Next the linear relationship between an increment of stress and an increment of strain is obtained by substituting (3.16) into (3.13):

$$de_{mn}^{P} = - \frac{\dfrac{\partial f}{\partial \sigma_{k\ell}} \dfrac{\partial f}{\partial \sigma_{mn}}}{\dfrac{\partial f}{\partial e_{ij}^{P}} \dfrac{\partial f}{\partial \sigma_{ij}}} d\sigma_{k\ell} \tag{3.17}$$

The relationship is linear since the fractional quantity does not contain the stress increment vector. This characteristic will be shown subsequently in an evaluation of the factor.

All of the above could be derived by the more general theory developed by Koiter [51] for loading surfaces with singular points, i.e., pointed surfaces. This generalization is not required here since the von Mises expression is used for the initial yield surface and subsequent loading surfaces.

3.5 SUBSEQUENT LOADING SURFACES – HARDENING RULES

It is necessary to know how the loading surface changes as load is continuously applied to the structure. Two principal theories have been used to determine this change, the isotropic rule and the kinematic hardening rule first suggested by Prager [55].

The basic concept behind the isotropic rule is that there is a continuous growth of the loading surface as plastic loading occurs at a point in the body under study. This is in sharp contrast to experimental evidence since the theory predicts a negative Baushinger effect. That is, as a point in a uniaxial test specimen is loaded, say into the inelastic compression range, and then unloaded and then carried into the tension range, the point at which plastic flow starts to occur is at a greater tensile stress than if the specimen were first loaded into the tension range. The equivalent concept is shown in Figure 3.1 in principal stress space. The important point to note is that the origin of the loading surface remains fixed and the surface grows with increasing loading.

The kinematic rule is more reasonable since it is in better agreement with experimental data. The principal idea behind this concept is shown in Figure 3.2. Both stresses and strains are associated with a displacement (reason for term - kinematic) such that the origin of the loading surface is allowed to translate while the size and shape of the surface is not allowed to change. The motion of the surface must be considered in a general stress space with constraints being applied for special conditions, for an example, no motion would be allowed in the third zero principal stress direction for plane stress.

3.6 EQUIVALENT STRESS AND EQUIVALENT STRAIN

The hardening rules for combined stress are related to the simple uniaxial test specimen. Some measure of stress and strain must be used to make the relationship meaningful. In other words, given a state of complex stress and strain at a point, what is the relationship between this state and our experimental data for a uniaxial test specimen?

A definition for equivalent stress is obtained from equation (3.4). This is the requirement for first yielding to occur under a condition of combined stress. Thus the effective stress is

$$\sigma_e = [3/2\ \sigma'_{ij}\ \sigma'_{ij}]^{1/2} \tag{3.18}$$

and reduces to the stress in a uniaxial specimen when the right side of the equation is written for that condition.

A definition of equivalent plastic strain is not quite as simple. One approach has been to define the equivalent strain increment, de_e^P, in terms of an increment of plastic work, i.e.,

$$dW_P = \sigma_e de_e^P \tag{3.19}$$

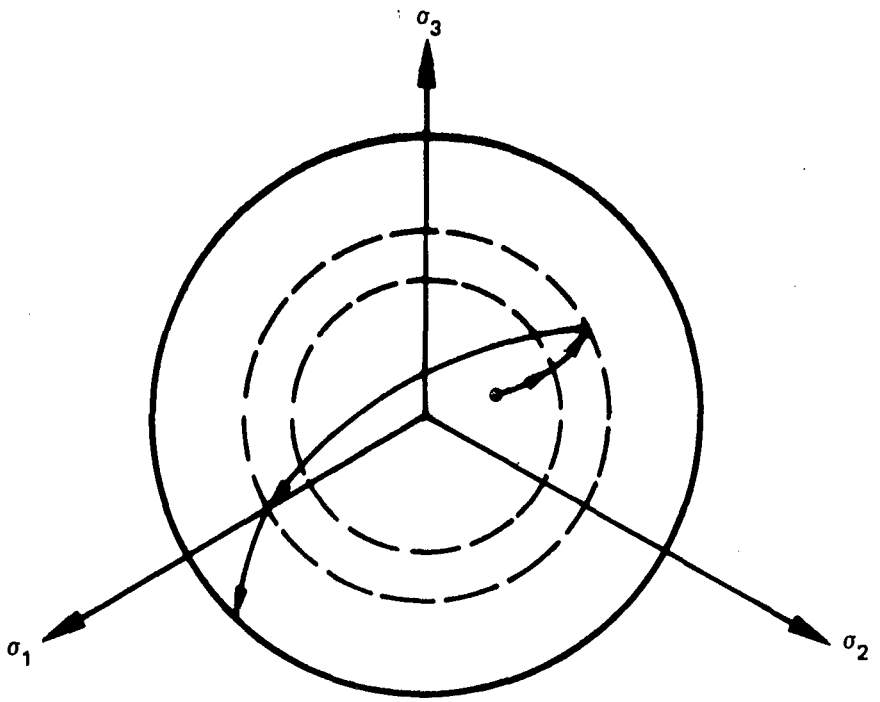

Figure 3.1 – Isotropic Hardening

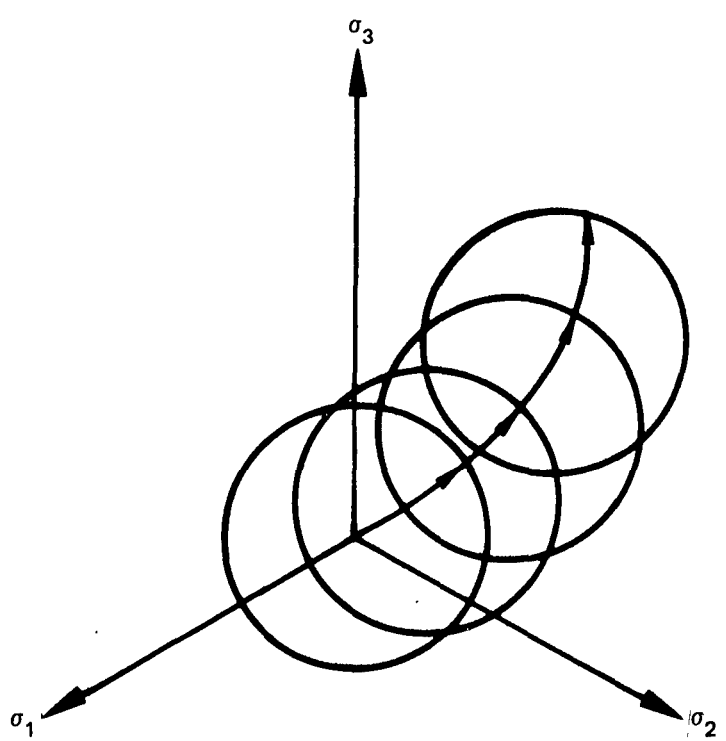

Figure 3.2 – Kinematic Hardening

Also, we must have

$$dW_P = \sigma_{ij}\, de_{ij}^P \tag{3.20}$$

which gives

$$de_e^P = 1/\sigma_e\, \sigma_{ij}\, de_{ij}^P \tag{3.21}$$

It was stated previously that hydrostatic pressure has no appreciable effect on inelastic deformation and thus that there is no change in volume as plastic flow occurs. Expressed mathematically, this means that the trace of the strain tensor vanishes, that is,

$$e_{ii} = 0 \tag{3.22}$$

and the deviatoric stress tensor may be substituted for the stress tensor in equation (3.21):

$$de_e^P = 1/\sigma_e\, \sigma'_{ij}\, de_{ij}^P \tag{3.23}$$

An explicit expression for the equivalent plastic strain may now be obtained by taking the scalar product of equation (3.23) with itself obtaining

$$de_e^P\, de_e^P = 1/\sigma_e^2\, \sigma'_{ij}\, \sigma'_{ij}\, de_{ij}^P\, de_{ij}^P \tag{3.24}$$

By using equation (3.18), the expression for the equivalent plastic strain now becomes

$$de_e^P = (2/3\, de_{ij}^P\, de_{ij}^P)^{1/2} \tag{3.25}$$

3.7 STRESS-TO-STRAIN TRANSFORMATION

With the above expressions for equivalent stress and strain, we may now look at the details of each of the hardening rules that we will be considering. In the isotropic-hardening rule, the change in the loading surface is reflected through a change in effective stress which is a function of the effective strain, that is, we now have

$$f = J_2\,(\sigma_{ij}) - 1/3\, \sigma_e\, (e_e^P)^2 \tag{3.26}$$

as the expression for the loading function.

At a material point where an increment of plastic strain occurs, equations (3.14), (3.15), and (3.17) must be true. The derivatives of the loading function with respect to stress and plastic strain are needed in order to determine the explicit expression for equation (3.17) for isotropic hardening. Thus, we can obtain the following

$$\frac{\partial f}{\partial \sigma_{ij}} = \frac{\partial f}{\partial J_2}\, \frac{\partial J_2}{\partial \sigma_{ij}} = \sigma'_{ij} \tag{3.27}$$

$$\frac{\partial f}{\partial e^P_{ij}} = \frac{\partial f}{\partial \sigma_e}\frac{\partial \sigma_e}{\partial e^P_e}\frac{\partial e^P_e}{\partial e^P_{ij}} = -2/3\,\sigma_e \frac{\partial \sigma_e}{\partial e^P_e}\frac{\partial e^P_e}{\partial e^P_{ij}} \tag{3.28}$$

The derivative of the loading function with respect to plastic strain is then obtained by substituting equation (3.21) into (3.28):

$$\frac{\partial f}{\partial e^P_{ij}} = -2/3\,\frac{\partial \sigma_e}{\partial e^P_e}\,\sigma'_{ij} \tag{3.29}$$

Thus, by using equation (3.18), the following becomes the linear relationship for an increment of plastic strain in terms of an increment of stress:

$$de^P_{mn} = \frac{\sigma'_{mn}\,\sigma'_{k\ell}}{2/3\,\dfrac{\partial \sigma_e}{\partial e^P_e}\,\sigma'_{ij}\,\sigma'_{ij}}\,d\sigma_{k\ell} = \frac{\sigma'_{mn}\,\sigma'_{k\ell}}{4/9\,\dfrac{\partial \sigma_e}{\partial e^P_e}\,\sigma_e^2}\,d\sigma_{k\ell} \tag{3.30}$$

The linearity of the factor on $d\sigma_{k\ell}$ is now evident since it is a function of only the current deviatoric stress, the current effective stress, and the current slope of the effective stress–effective plastic strain curve.

The loading function for the kinematic-hardening rule must be different from equation (3.26) since the loading surface is now allowed to shift but not to grow in size. Incorporating these two requirements, the loading function becomes

$$f = J_2\,(\sigma_{ij} - a_{ij}) - 1/3\,\sigma_o^2 \tag{3.31}$$

The array a_{ij} is the shift of the center of the loading surface with changing plastic strain, that is,

$$da_{ij} = C\,de^P_{ij} \tag{3.32}$$

where C is a constant factor dependent on the effective stress-effective plastic strain curve. As before, σ_o is the yield strength of the material which is obtained in a uniaxial test. The above form of the kinematic hardening is that proposed by Shield and Ziegler [56].

To reemphasize the difference between equations (3.26) and 3.31), the dependence of the loading function on the plastic strain for isotropic hardening comes through the change in effective stress which is a function of the effective plastic strain whereas for kinematic hardening, the change in plastic strain causes the center of the loading surface to shift by the amount specified by equation (3.32).

Equations (3.14), (3.15), and (3.17) must be satisfied for kinematic hardening as they were for the isotropic hardening, Instead of equations (3.27) and (3.28), we obtain the following two expressions

$$\frac{\partial f}{\partial \sigma_{ij}} = \sigma'_{ij} - a'_{ij} \tag{3.33}$$

$$\frac{\partial f}{\partial e^P_{ij}} = -C \frac{\partial f}{\partial \sigma_{ij}} \tag{3.34}$$

where

$$a'_{ij} = a_{ij} - 1/3\, \delta_{ij}\, a_{kk} \tag{3.35}$$

Substituting equations (3.33) and (3.34) into equation (3.17), we obtain

$$de^P_{mn} = \frac{(\sigma'_{ij} - a'_{ij})(\sigma'_{mn} - a'_{mn})}{C(\sigma'_{k\ell} - a'_{k\ell})(\sigma'_{k\ell} - a'_{k\ell})} d\sigma_{ij} \tag{3.36}$$

The denominator in the above expression may be simplified since as already stated, the size of the loading surface does not change and thus we may write

$$(\sigma'_{k\ell} - a'_{k\ell})(\sigma'_{k\ell} - a'_{k\ell}) = 2/3\, \sigma_o^2 \tag{3.37}$$

Thus, equation (3.36) may be written as

$$de^P_{mn} = \frac{(\sigma'_{ij} - a'_{ij})(\sigma'_{mn} - a'_{mn})}{2/3\, C\, \sigma_o^2} d\sigma_{ij} \tag{3.38}$$

The problem now is to determine the value of C in the above equation. This can be done by examining the form of the equation for a uniaxial loading test specimen. Equation (3.38) becomes

$$de^P_{11} = \frac{(2/3\, \sigma_{11} - a'_{11})(2/3\, \sigma_{11} - a'_{11})}{2/3\, C\, \sigma_o^2} d\sigma_{11} = \frac{d\sigma_{11}}{\frac{\partial \sigma_e}{\partial e^P_e}} \tag{3.39}$$

Written for this case, equation (3.37) becomes

$$\begin{aligned}(2/3\, \sigma_{11} - a'_{11})(2/3\, \sigma_{11} - a'_{11}) + (-1/3\, \sigma_{11} - a'_{22})(-1/3\, \sigma_{11} - a'_{22}) \\ + (-1/3\, \sigma_{11} - a'_{33})(-1/3\, \sigma_{11} - a'_{33}) = 2/3\, \sigma_o^2\end{aligned} \tag{3.40}$$

The incompressibility of plastic deformations requires that

$$a'_{22} = a'_{33} = -1/2\, a'_{11} \tag{3.41}$$

which can be substituted into equation (3.40) to obtain

$$3/2\, (2/3\, \sigma_{11} - a'_{11})^2 = 2/3\, \sigma_o^2 \tag{3.42}$$

Finally, combining equation (3.42) with equation (3.39), we obtain

$$C = 2/3 \frac{\partial \sigma_e}{\partial e_e^P} \tag{3.43}$$

As proposed by Shield and Ziegler [56] and formulated by equations (3.31) and (3.32), the form of kinematic hardening was intended for linear hardening where the slope of the equivalent stress-equivalent plastic strain curve is a constant. Nothing in the above derivation prohibits modeling the equivalent stress-equivalent plastic strain curve as a series of straight lines where the slope would be constant for each segment. This idealization is shown in Figure 3.3. Thus, we may assume that the above derivation is applicable in each one of the straight line segments of the idealized curve.

Now substituting equation (3.43) into equation (3.38), we obtain the desired relationship for kinematic hardening:

$$de_{mn}^P = \frac{(\sigma'_{ij} - a'_{ij})(\sigma'_{mn} - a'_{mn})}{4/9 \frac{\partial \sigma_e}{\partial e_e^P} \sigma_o^2} d\sigma_{ij} \tag{3.44}$$

The similarity is quite interesting when the above equation is compared with the equivalent one for isotropic hardening, equation (3.30). The kinematic-hardening relationship can be obtained from that for isotropic hardening by simply substituting the shifted, i.e., the corrected deviatoric stress tensor, for the usual deviatoric stress tensor and using the intial proportional limit of the material instead of the current value of effective stress.

3.8 STRAIN-TO-STRESS TRANSFORMATION

We now proceed to derive the stress-strain relationships which will be required for the finite element method. Equations (3.30) for isotropic hardening and equation (3.44) for kinematic hardening transform an increment of stress to an increment of plastic strain. An inverse relationship which transforms total strain to stress is required. The derivation will be carried out in terms of isotropic hardening; the transition to kinematic hardening is easily performed as described in the previous paragraph.

The assumption is first made that strain may be decomposed as follows

$$de_{ij}^T = de_{ij}^E + de_{ij}^P \tag{3.45}$$

where de_{ij}^T and de_{ij}^E are the total and elastic strains, respectively. We can then write

$$d\sigma_{ij} = C_{ijk\ell}(de_{k\ell}^T - \sigma'_{k\ell}\Lambda) \tag{3.46}$$

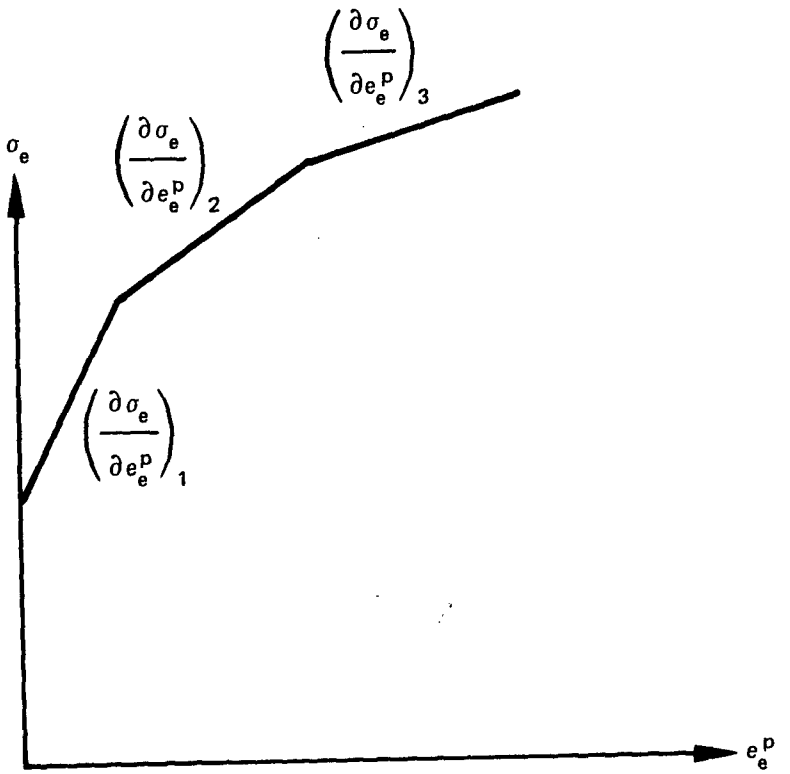

Figure 3.3 – Idealization of Plastic Stress-Strain Curve

where $C_{ijk\ell}$ is the elastic constitutive tensor which contains Young's modulus and Poisson's ratio. Equation (3.13) has been used in writing the above equation.

From equation (3.30), an explicit expression for Λ may be written:

$$\Lambda = \frac{\sigma'_{ij}}{4/9 \dfrac{\partial \sigma_e}{\partial e_e^P} \sigma_e^2} d\sigma_{ij} \tag{3.47}$$

Now multiplying equation (3.46) by σ'_{ij} and combining with equation (3.47), we may find an expression for Λ which is a function of strain and the current state:

$$\Lambda = \frac{\sigma'_{ij} C_{ijk\ell} de^T_{k\ell}}{4/9 \dfrac{\partial \sigma_e}{\partial e_P} \bar{\sigma}_e^2 + \sigma'_{ij} C_{ijk\ell} \sigma'_{k\ell}} \tag{3.48}$$

Equation (3.48) is now substituted into equation (3.46) to obtain the desired result:

$$d\sigma_{ij} = \left[C_{ijrs} - \frac{C_{ijk\ell} \sigma'_{k\ell} \sigma'_{pq} C_{pqrs}}{4/9 \dfrac{\partial \sigma_e}{\partial e_e^P} \sigma_e^2 + \sigma'_{pq} C_{pqrs} \sigma'_{rs}} \right] de^T_{rs} \tag{3.49}$$

The implementation of the above equation will be given later.

In addition to equation (3.49), an explicit expression for the differential of the equivalent plastic strain will be required during the solution of problems. This can be written as

$$de_e^P = \frac{2/3\, \sigma_e \sigma'_{ij} C_{ijrs}}{4/9 \dfrac{\partial \sigma_e}{\partial e_e^P} \sigma_e^2 + \sigma'_{ij} C_{ijk\ell} \sigma'_{k\ell}} de^T_{rs} \tag{3.50}$$

CHAPTER 4
GEOMETRIC DETAILS

The development of an adequate shell element requires that considerable attention be given to how the geometry of the shell surface is used in the formation and implementation of the element. As pointed out in the first chapter, Gallagher [15] has indicated that this has been one of the most difficult hurdles to overcome in developing shell elements.

4.1 SURFACE DEFINITION

The formation of the stiffness matrix for the quadrilateral, the determination of the loading on the element, and the transformation of the stiffness matrix, the displacements, and the loads require detailed information on shell geometry.

The theory for the element has been developed for application to surfaces that can be represented by a quadratic form. Referring to Figure 4.1, the surface must be able to be expressed by the function f where according to McConnell [57],

$$f(x') = Q_{ij}\, x'_i\, x'_j + b_k\, x'_k + C = 0 \tag{4.1}$$

Here x'_i is the auxiliary coordinate system of the surface and Q_{ij} and b_k are constants. Cartesian coordinate systems shown in the figure are the local element coordinate system and the global coordinate system. Each element will have its own coordinate system as will each surface.

It will also be necessary to represent the surface by a vector function

$$\underset{\sim}{r} = x'_1(\beta_1,\beta_2)\hat{i}'_1 + x'_2(\beta_1,\beta_2)\hat{i}'_2 + x'_3(\beta_1,\beta_2)\hat{i}'_3 \tag{4.2}$$

where β_1 and β_2 are the Gaussian coordinates on the surface, not necessarily orthogonal. The above is a parametric representation of the surface in terms of the coordinates β_1 and β_2.

The quadratic form equation (4.1), and the parametric representation, equation (4.2), are given in the appendix for the surfaces that are treated by the theory developed here.

4.2 ELEMENT DEFINITION AND BOUNDARY

The element corners are given by nodal points 1, 2, 3, and 4 shown in Figure 4.2. The local element coordinate system, x_i, is established by the first three nodes. In other words, these nodes set the X-Y plane and the fourth node is generally not in the plane. The element sides must be defined in a unique way so that there will be no overlapping or gaps between adjacent elements. This is done by letting the side of the element be along a line which is represented by a linear relationship between the (β_1,β_2) coordinates, that is, each of the sides is given by the equation

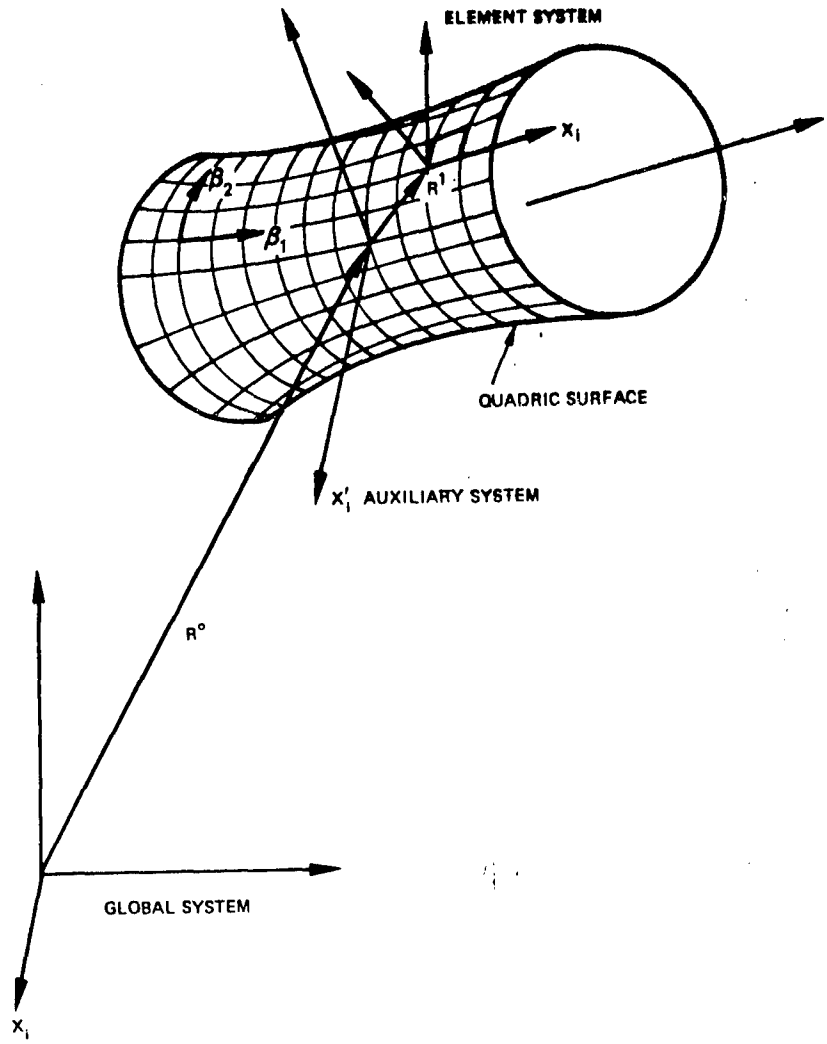

Figure 4.1 – Coordinate Systems

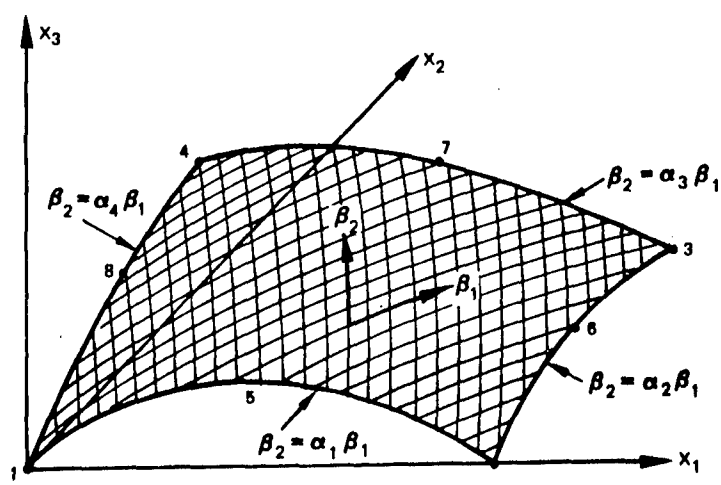

Figure 4.2 – Element in Local System

$$\beta_2 = \alpha_i \beta_1$$

where α_i is a constant and i assumes the values from one to four.

The midside nodes lie on the above-defined lines. The (β_1, β_2) coordinates of the nodes on each side are the mean of the (β_1, β_2) coordinates of the two nodes which define the side.

4.3 SLOPE OF SURFACE IN ELEMENT SYSTEM

During the computation of the element stiffness and the distributed loading on the element, the slope of the surface is required in the local element system. This is obtained by expressing the quadratic form of equation (4.1) in terms of the local element system. We use the transformation relationship between the element system and the coordinate system of the quadratic surface. This is written as

$$x'_i = a_{ik}\, x_k + \overset{1}{x}'_i \tag{4.3}$$

where the origin of the element system, nodal point 1, is given by the vector

$$\underset{\sim}{\overset{1}{R}}' = \overset{1}{x}'_i \hat{i}'_i \tag{4.4}$$

The transformation array, a_{ik}, is determined by using the first three nodal point coordinates as described above.

Now substituting (4.3) into (4.1), we obtain an expression for the surface in terms of the element system:

$$\begin{aligned} f(x) = {} & Q_{ij}\, a_{ik}\, a_{jk}\, x_k\, x_\ell + Q_{ij}\, a_{ik}\, x_k\, \overset{1}{x}'_j + Q_{ij}\, a_{j\ell}\, x_\ell\, \overset{1}{x}'_i \\ & + Q_{ij}\, \overset{1}{x}'_i\, \overset{1}{x}'_j + b_m\, a_{mn}\, x_n + b_m\, \overset{1}{x}_m + C = 0 \end{aligned} \tag{4.5}$$

The desired slopes are the derivatives of z with respect to x and with respect to y. Since it would be extremely tedious to solve for an explicit expression for z in terms of x and y (one would have to be derived for each surface), we choose to use implicit differentiation and tensor calculus to obtain the required slopes. As an example, to compute the derivative of z with respect to x, we can first write the derivative of f with respect to x

$$\frac{\partial f}{\partial x} + \frac{\partial f}{\partial z}\frac{\partial z}{\partial x} = 0 \tag{4.6}$$

Thus solving for the slope, we obtain

$$\frac{\partial z}{\partial x} = -\frac{\dfrac{\partial f}{\partial x}}{\dfrac{\partial f}{\partial z}} \tag{4.7}$$

Thus the derivatives of the function that expresses the surface in the element system are required. Differentiating equation (4.5), we obtain

$$\frac{\partial f}{\partial x_o} = Q_{ij}\, a_{ik}\, a_{j\ell}\, \delta_{ko}\, x_\ell + Q_{ij}\, a_{ik}\, a_{j\ell}\, x_k\, \delta_{\ell o} + Q_{ij}\, a_{ik}\, \delta_{ko}\, \overset{1}{x}{}'_j + Q_{ij}\, a_{j\ell}\, \delta_{\ell o}\, \overset{1}{x}{}'_i + b_m\, a_{mn}\, \delta_{no} \tag{4.8}$$

$$\frac{\partial f}{\partial x_m} = 2Q_{ij}\, a_{im}\, a_{j\ell}\, x_\ell + 2Q_{ij}\, a_{im}\, \overset{1}{x}{}'_j + b_p\, a_{pm}$$

Now substituting (4.8) into (4.7), we obtain the slope in the x-direction as

$$\frac{\partial z}{\partial x} = -\frac{2Q_{ij}\, a_{i1}\, a_{j\ell}\, x_\ell + 2Q_{ij}\, a_{i1}\, \overset{1}{x}{}'_j + b_p\, a_{p1}}{2Q_{ij}\, a_{i3}\, a_{j\ell}\, x_\ell + 2Q_{ij}\, a_{i3}\, \overset{1}{x}{}'_j + b_p\, a_{p3}} \tag{4.9}$$

and, similarly, the slope in the y-direction as

$$\frac{\partial z}{\partial y} = -\frac{2Q_{ij}\, a_{i2}\, a_{j\ell}\, x_\ell + 2Q_{ij}\, a_{i2}\, \overset{1}{x}{}'_j + b_p\, a_{p2}}{2Q_{ij}\, a_{i3}\, a_{j\ell}\, x_\ell + 2Q_{ij}\, a_{i3}\, \overset{1}{x}{}'_j + b_p a_{p3}} \tag{4.10}$$

Thus equations (4.9) and (4.10) are evaluated at each of the integration points in the element and then used to form the stiffness of the element and to compute the consistent nodal forces that are equivalent to the distributed loading. It should be noted that at a particular integration point in the x-y plane, everything is known that is required in the equations except the value of z, the distance of the element above or below the x-y plane. The value of z can be obtained by using the x-y coordinates of the integration point in equation (4.5), which can then be reduced to a quadratic equation in z. The correct value of z will be the one which has the least absolute value.

Although all of the above may seem to be somewhat involved, the only other alternative would be to assume that the height of the surface above the x-y plane can be represented adequately by a polynomial, a cubic for example. Thus since there are then ten free parameters in a cubic polynomial, ten values of the height would have to be computed and then ten equations would have to be written of the type

$$z^\circ = a_1 + a_2 x^\circ + a_3 y^\circ + a_4 x^{\circ 2} + a_5 x^\circ y^\circ + a_6 y^{\circ 2} + a_7 x^{\circ 3} + a_8 x^{\circ 2} y^\circ + a_9 x^\circ y^{\circ 2} + a_{10} y^{\circ 3} \tag{4.11}$$

Here (x°, y°) are the coordinates of the point where the height z° is evaluated. The equations would then have to be solved for the coefficients a_i. Finally, the value of the slopes at each of the integration points could then be calculated.

It is not clear that the cubic fit method is more efficient than the previous devised method that is used in the quadrilateral element. However, it is certain that the previous method is more accurate than the cubic fit since it is exact. The derivatives of functions that are represented by polynomial fits are notoriously poor. Thus one would not expect the slopes obtained from the cubic approximation to be very accurate.

4.4 SURFACE VECTORS

For the calculation of the element stiffness and the transformations required in implementing the element, it will be convenient to be able to compute vectors on a line on the surface. We will assume that the line can be represented by a linear function of β_1 and β_2. Thus the previously described element boundary fits this description. Moreover, we will further assume that the surface boundary can be adequately represented by a series of these linear curves. The convenience of having the capability to compute these vectors will become apparent later when we describe the computation of the element stiffness and the transformations.

Consider a portion of a surface shown in Figure 4.3 which has been modeled by a number of the quadrilateral finite elements. The line S1 is a linear curve between two elements and the line S2 is a portion of the boundary. Both lines are linear in the sense described above.

The vectors $\hat{b}$, $\hat{t}$, and $\hat{n}$ are unit vectors at the particular points J and L. The vector $\hat{n}$ is normal to the surface and is computed by first taking the cross product

$$\frac{\partial \underset{\sim}{r}}{\partial \beta_1} \times \frac{\partial \underset{\sim}{r}}{\partial \beta_2} = \underset{\sim}{n} \tag{4.12}$$

where $\underset{\sim}{r}$ is the vector function that defines the surface and is given in equation (4.2). The unit normal is then obtained by dividing the normal vector by its magnitude, i.e.,

$$\hat{n} = \frac{\underset{\sim}{n}}{|\underset{\sim}{n}|} \tag{4.13}$$

To compute the tangent vector, we must first express the line as a vector function. We do this by using the equation of the line which is a linear function of β_1 and β_2. Thus solving, say, for β_2 in terms of β_1 and substituting into equation (4.2), we obtain

$$\underset{\sim}{r}(\beta_1, \beta_2(\beta_1)) = \underset{\sim}{\rho}(\beta_1) = F(\beta_1)\hat{i}'_1 + G(\beta_1)\hat{i}'_2 + H(\beta_1)\hat{i}'_3 \tag{4.14}$$

where $\underset{\sim}{\rho}$ is now the vector equation of the line between the elements or of the segment of the boundary. This depends on the particular situation or case for which the computation is being performed. We now obtain the tangent vector to the line by computing the derivative of $\underset{\sim}{\rho}$ with respect to β_1 to obtain

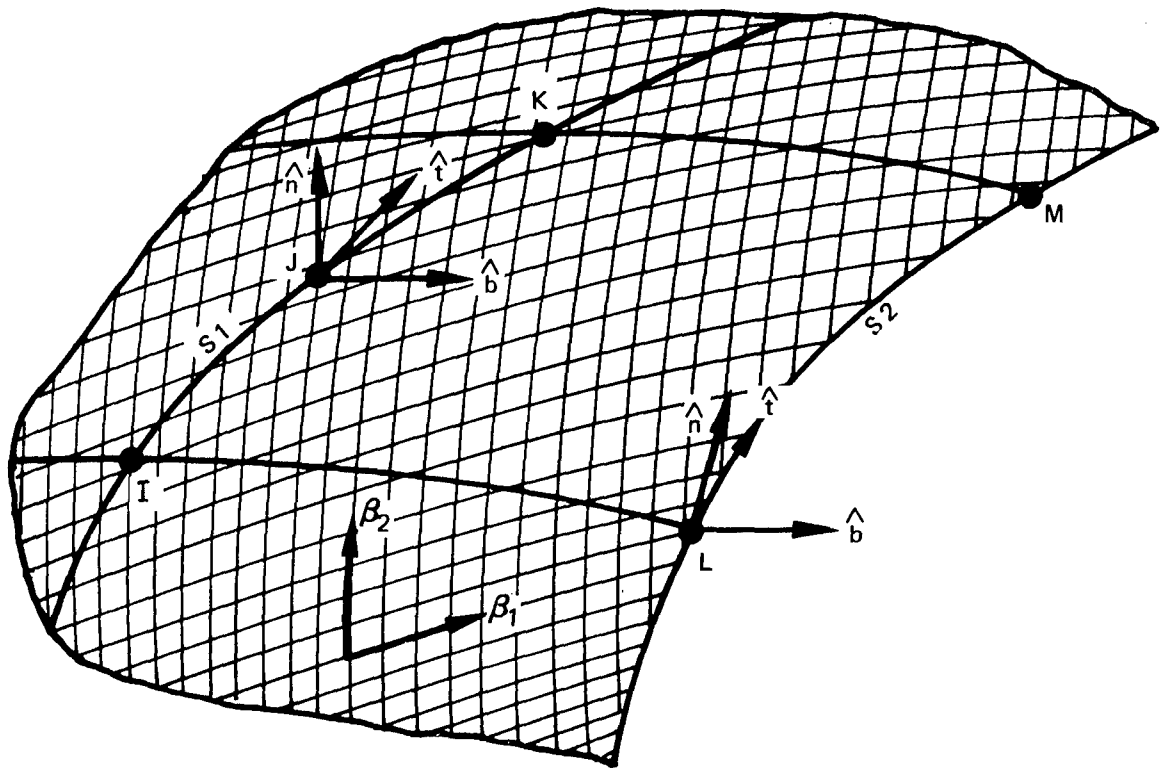

Figure 4.3 – Surface Vectors

$$\frac{\partial \underset{\sim}{\rho}}{\partial \beta_1} = \frac{\partial F}{\partial \beta_1} \hat{i}_1' + \frac{\partial G}{\partial \beta_1} \hat{i}_2' + \frac{\partial H}{\partial \beta_1} \hat{i}_3' \tag{4.15}$$

The unit tangent vector is now obtained by dividing the above vector by its length, as was done for the normal vector. The positive sense of the tangent vector is taken in the direction of increasing β_1. If the line happens to be on a constant β_1 line, the above process for computing the tangent vector is performed by using β_2 as the parameter.

The final vector $\hat{b}$ is obtained by performing the cross product

$$\hat{b} = \hat{t} \times \hat{n} \tag{4.16}$$

This vector is a unit vector since the two vectors used in the cross product are unit vectors. However, the $\hat{b}$ vector is not necessarily the binormal to the curve between two elements or the curve along the boundary, but it is a unique vector which is sufficient for our purpose, namely, to compute the element stiffness and perform transformations. If it so happened that the linear line on the surface was also a geodesic line, then the normal to the curve would coincide with the normal to the surface and then the vector would be the binormal to the curve at the point in question.

CHAPTER 5
QUADRILATERAL SHELL FINITE ELEMENT

The derivation of the shell quadrilateral finite element will be obtained by showing the particular form of the basic formulation presented in Chapter 2. At particular points in the derivation, we will draw on the geometric information given in Chapter 4.

5.1 STRAIN DISPLACEMENT RELATIONSHIP

The strain displacement relationship for the quadrilateral element is that due to Marguerre [58] and also presented in Washizu [38]. It is assumed that the strain is represented adequately by letting the element be a segment of a shell that does not differ greatly from a segment of a flat plate which has an initial deformation. This approximation will not limit the application of the element and falls within the well-known shallow shell theory. Thus the only limitation imposed is that each individual element is a shallow shell. The specifics and source of this limitation will be brought out in the derivation.

Referring to Figure 5.1., the undeformed shell element is assumed to be represented by the mapping

$$\begin{aligned} x &= X \\ y &= Y \\ z &= \bar{w} \end{aligned} \tag{5.1}$$

where $\bar{w}$ is the distance from the (X, Y) plane to the midfiber of the shell. After load-induced deformation, the midfiber mapping becomes

$$\begin{aligned} x &= X + u \\ y &= Y + v \\ z &= \bar{w} + w \end{aligned} \tag{5.2}$$

where we consider u, v, w, and $\bar{w}$ to be functions of X and Y only.

Prior to load-induced deformation, a point on the midfiber can be represented by the vector

$$\underset{\sim}{r}_o^{(o)} = X\hat{i}_1 + Y\hat{i}_2 + \bar{w}\hat{i}_3 \tag{5.3}$$

and a point distance ξ above or below the midfiber by

$$\underset{\sim}{r}^{(o)} = \underset{\sim}{r}_o^{(o)} + \xi\,\hat{n}^{(o)} \tag{5.5}$$

where $\hat{n}^{(o)}$ is the normal to the surface before deformation. This normal is computed by taking the cross product

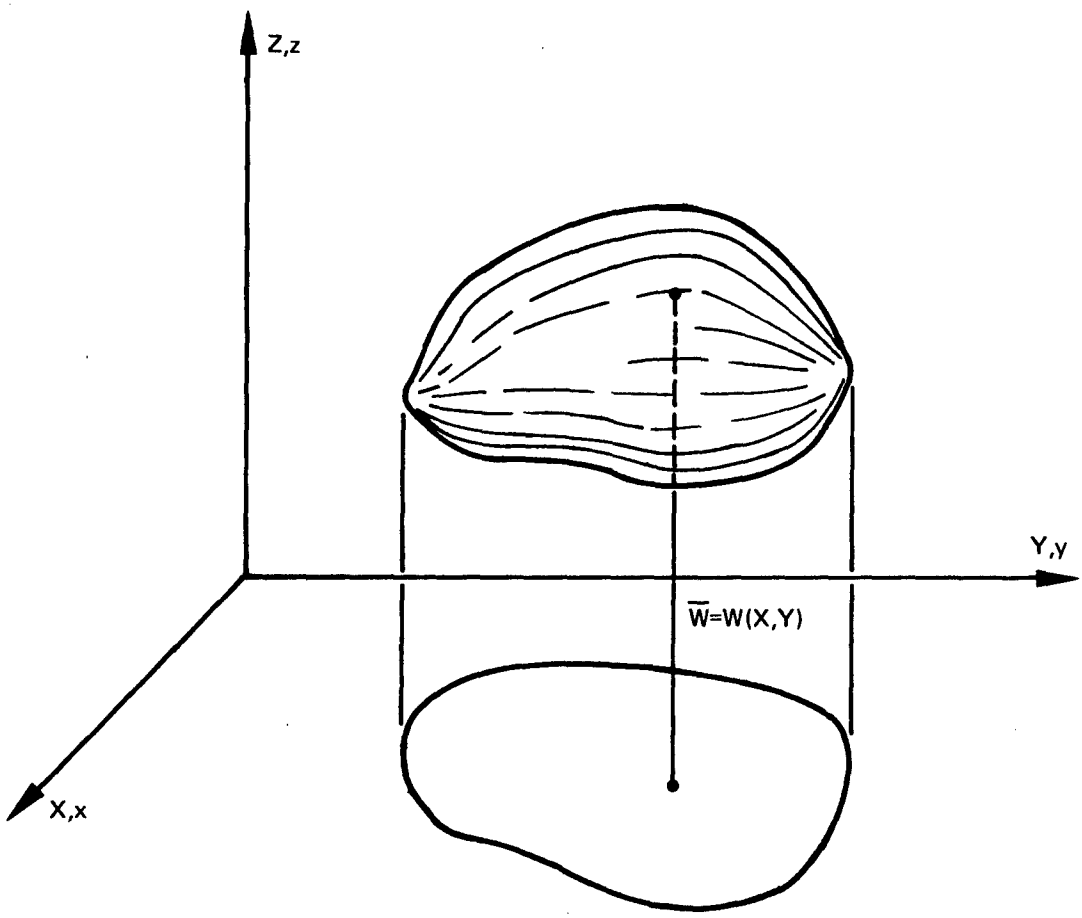

Figure 5.1 – Mapping of Shell Surface

$$\hat{n}^{(o)} = \frac{\dfrac{\partial \underset{\sim}{r}_o^{(o)}}{\partial X} \times \dfrac{\partial \underset{\sim}{r}_o^{(o)}}{\partial Y}}{\left| \dfrac{\partial r_o^{(o)}}{\partial X} \times \dfrac{\partial r_o^{(o)}}{\partial Y} \right|} \tag{5.5}$$

After load is applied to the element, a point on the midsurface assumes the position

$$\underset{\sim}{r}_o = (X+u)\hat{i}_1 + (Y+v)\hat{i}_2 + (\bar{w}+w)\hat{i}_3 \tag{5.6}$$

The normal to the new position is now computed by

$$\hat{n} = \frac{\dfrac{\partial \underset{\sim}{r}_o}{\partial X} \times \dfrac{\partial \underset{\sim}{r}_o}{\partial Y}}{\left| \dfrac{\partial \underset{\sim}{r}_o}{\partial X} \times \dfrac{\partial \underset{\sim}{r}_o}{\partial Y} \right|} \tag{5.7}$$

The approximation of the shallow shell theory in Cartesian coordinates is now introduced through the assumption that

$$\left(\frac{\partial \bar{w}}{\partial X}\right)^2, \left(\frac{\partial \bar{w}}{\partial Y}\right)^2, \left|\frac{\partial \bar{w}}{\partial X}\ \frac{\partial \bar{w}}{\partial Y}\right| << 1 \tag{5.8}$$

and thus sets the limitations on how "deep" the shell element can be without degrading the results of the computations.

We will further assume that the shell element is thin and the curvature is not very large, such that

$$\left|\xi \frac{\partial^2 \bar{w}}{\partial X^2}\right|, \left|\xi \frac{\partial^2 \bar{w}}{\partial Y^2}\right|, \left|\xi \frac{\partial^2 \bar{w}}{\partial X \partial Y}\right| << 1 \tag{5.9}$$

and that multiples of ξ cause lower order magnitude terms. Also, since we will be using the approximation that the stretching terms are small, we may assume that

$$\frac{\partial u}{\partial X}, \frac{\partial u}{\partial Y}, \frac{\partial v}{\partial X}, \frac{\partial v}{\partial Y}, << 1 \tag{5.10}$$

Imposing (5.8), the normal to the element surface before loading may be computed by (5.5) to obtain

$$\hat{n}^{(o)} = -\frac{\partial \bar{w}}{\partial X}\hat{i}_1 - \frac{\partial \bar{w}}{\partial Y}\hat{i}_2 + \hat{i}_3 \tag{5.11}$$

After deformation, the normal to the midsurface is obtained from (5.6)

$$\hat{n} = -\left(\frac{\partial \bar{w}}{\partial X} + \frac{\partial w}{\partial X}\right)\hat{i}_1 - \left(\frac{\partial \bar{w}}{\partial Y} + \frac{\partial w}{\partial Y}\right)\hat{i}_2 + \hat{i}_3 \tag{5.12}$$

where (5.10) has been used along with the assumption that the square of the derivative of w may be ignored in computing the unit vector.

The additional constraint of the Kirchoff hypothesis will be imposed by the equation

$$\underset{\sim}{r} = \underset{\sim}{r}_o + \xi \hat{n} \tag{5.13}$$

which is the position vector of any point through the thickness after deformation.

We may now compute the strain tensor by using (2.3). Before proceeding, it is important to note that equation (2.3) is based on the assumption that the line segment before deformation can be written directly in terms of the increment of the Lagrangian coordinates. This is not true for the case here where the actual load-induced deformation starts out from a deformed configuration, i.e., the element shell surface. We may still use a Lagrangian description as long as all quantities are referenced to the basic configuration in the (X, Y) plane. Thus, using (5.4) and (5.13), we may write (2.3) in the form

$$\begin{aligned} ds^2 - dS^2 &= \left(\frac{\partial \underset{\sim}{r}}{\partial X_i} dX_i\right) \cdot \left(\frac{\partial \underset{\sim}{r}}{\partial X_j} dX_j\right) - \left(\frac{\partial \underset{\sim}{r}^{(o)}}{\partial X_i} dX_i\right) \cdot \left(\frac{\partial \underset{\sim}{r}^{(o)}}{\partial X_j} dX_j\right) \\ &= 2E_{ij}\, dX_i\, dX_j \end{aligned} \tag{5.14}$$

The final expressions for the strain quantities are now obtained by substituting the previous expressions into (5.14) and dropping all terms which are assumed to be small for the reasons stated previously. For any position through the thickness of the shell, the three strain terms become

$$E_{XX} = \frac{\partial u}{\partial X} + \frac{\partial w}{\partial X}\frac{\partial \bar{w}}{\partial X} + 1/2\left(\frac{\partial w}{\partial X}\right)^2 - \xi \frac{\partial^2 w}{\partial X^2} \tag{5.15}$$

$$E_{YY} = \frac{\partial v}{\partial Y} + \frac{\partial \bar{w}}{\partial Y}\frac{\partial w}{\partial Y} + 1/2\left(\frac{\partial w}{\partial Y}\right)^2 - \xi \frac{\partial^2 w}{\partial Y^2} \tag{5.16}$$

$$2E_{XY} = \frac{\partial u}{\partial Y} + \frac{\partial v}{\partial X} + \frac{\partial \bar{w}}{\partial X}\frac{\partial w}{\partial Y} + \frac{\partial \bar{w}}{\partial Y}\frac{\partial w}{\partial X} + \frac{\partial w}{\partial X}\frac{\partial w}{\partial Y} - 2\xi \frac{\partial^2 w}{\partial X \partial Y} \tag{5.17}$$

The above equations are appropriate for small direct strains and moderate rotations.

5.2 ASSUMED DISPLACEMENTS

The quadrilateral element on the surface of the shell was shown in Figure 4.2. We must now examine the region that is the projection of the element onto the local (X, Y) plane. In the Lagrangian sense, this region contains the material coordinates in which we will assume that a certain displacement exists and over which we will have to express the loading and perform the integration for the stiffness equation.

On the shell surface, the element is quadrilateral in shape but the projected region in the (X, Y) plane is not. Nodal points 1-3 establish the (X, Y) plane and thus the local element coordinate system. The remaining nodes are projected onto the plane to establish the eight-sided polygon shown in Figure 5.2. The true region is curvilinear in shape for the general application, but the above approach should be sufficient to represent the area.

Following the work of Fraeijs de Veubeke [59], we use patching-type bicubic functions for the assumed displacement pattern. This approach was used originally for studying plate problems, but one of the requirements to maintain compatibility between shell elements is that the same order (here bicubic) polynomial must be used for each of the three u, v, and w displacements. We refer here only to the displacements of the midfiber of the shell element and consider only the u displacement first.

Referring to Figure 5.2, the complete ten-term cubic polynomial is used over the entire region, that is,

$$u_c = a_1 + a_2 X + a_3 Y + a_4 X^2 + a_5 XY + a_6 Y^2 + a_7 X^3 + a_8 X^2 Y + a_9 XY^2 + a_{10} Y^3 \qquad (5.18)$$

Next, the two auxiliary coordinate systems shown in the figure are introduced. An additional function

$$u' = a_{11} Y'^2 + a_{12} Y'^3 + a_{13} X' Y'^2 \qquad (5.19)$$

is defined to be acting in the region where Y' is greater than zero. Also, a third function

$$u'' = a_{14} Y''^2 + a_{15} Y''^3 + a_{16} X'' Y''^2 \qquad (5.20)$$

is defined to be acting in the region where Y'' is greater than zero. Each of the functions is written with unknown coefficients which are to be determined. Thus, the u displacement at any point within the region can be expressed by

$$u = u_c + u' + u'' \qquad (5.21)$$

with the prime and double-prime functions being defined as above. All three displacements on the right side of (5.21) are directed parallel to the positive X axis.

Similar to the u displacement, the v and w displacements are defined by

$$v = v_c + v' + v'' \qquad (5.22)$$

and

$$w = w_c + w' + w'' \qquad (5.23)$$

where the prime and double-prime terms have the same meaning, only now the range on the coefficient subscripts is 17 to 32 on v and 33 to 48 on w. We may express this in matrix form, which is the equivalent of equation (2.18):

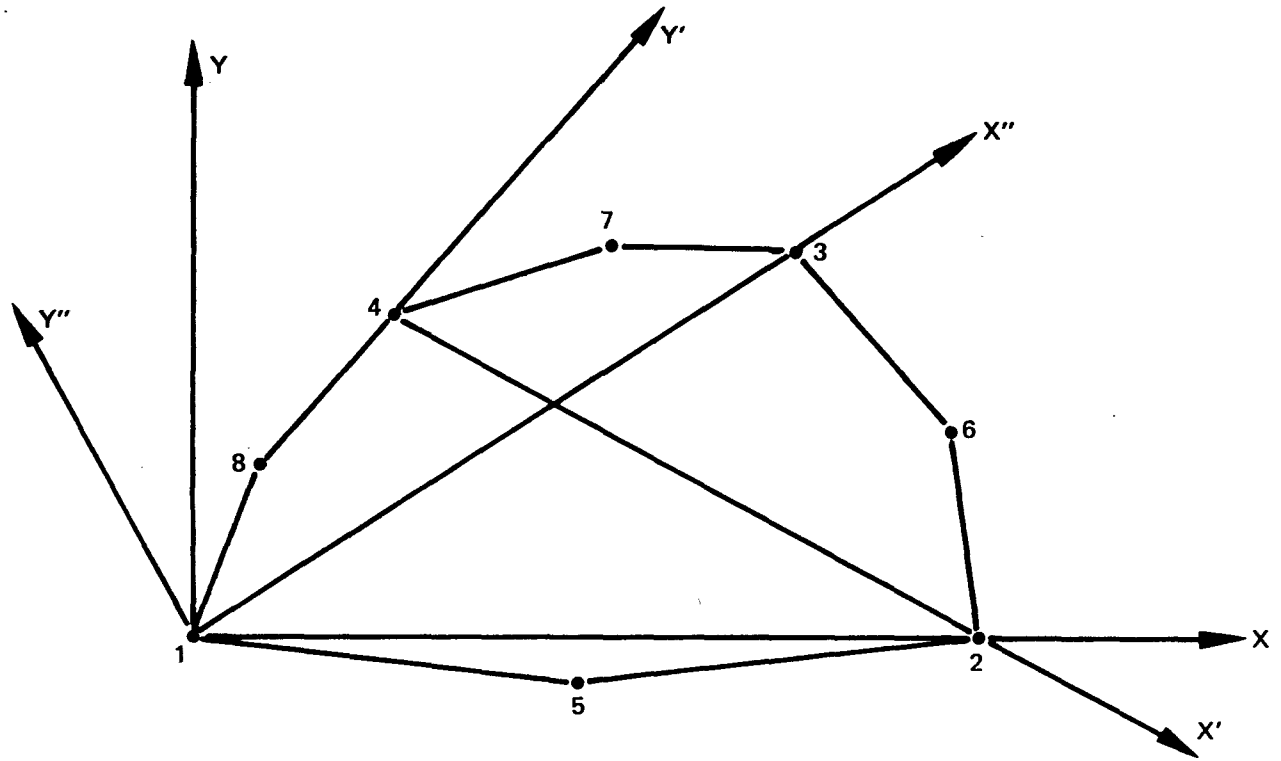

Figure 5.2 – Auxiliary Coordinate Systems

$$\begin{Bmatrix} u \\ v \\ w \end{Bmatrix} = \left[\begin{array}{c|c|c} r & 0 & 0 \\ \hline 0 & r & 0 \\ \hline 0 & 0 & r \end{array}\right] \begin{Bmatrix} a_1 \\ \vdots \\ a_{16} \\ \hline a_{17} \\ \vdots \\ a_{32} \\ \hline a_{33} \\ \vdots \\ a_{48} \end{Bmatrix} \tag{5.24}$$

where

$$\lfloor r \rfloor = \lfloor 1 \; X \; Y \; X^2 \; XY \; Y^2 \; X^3 \; X^2Y \; XY^2 \; Y^3 \; Y'^2 \; Y'^3 \; X'Y'^2 \; Y''^2 \; Y''^3 \; X''Y''^2 \rfloor \tag{5.25}$$

The above displacements are only for the midfiber of the shell element where equation (2.18) was written for the general case for any point in the body. The displacement for any point through the thickness of the element will come from the constraints of the Kirchoff hypothesis, equation (5.13).

5.3 GENERALIZED DISPLACEMENTS

The concept of generalized displacements was introduced in Chapter 2 through equation (2.20) and the characteristics of these displacements were stated. One characteristic was that the number of generalized displacements is equal to the number of undetermined coefficients. Thus for the quadrilateral, we will introduce 48 generalized displacements in accordance with equation (5.24). Our eventual goal here is to express the displacements of the midsurface of the element, equation (5.24), in terms of the generalized displacements.

The nine generalized displacements

$$\lfloor \bar{v} \rfloor = \left\lfloor u \; v \; w \; \frac{\partial u}{\partial X} \; \frac{\partial u}{\partial Y} \; \frac{\partial v}{\partial X} \; \frac{\partial v}{\partial Y} \; \frac{\partial w}{\partial X} \; \frac{\partial w}{\partial Y} \right\rfloor \tag{5.26}$$

will be used at nodes 1, 2, 3, and 4, and the three generalized displacements

$$\lfloor \phi \rfloor = \left\lfloor \frac{\partial u}{\partial b} \; \frac{\partial v}{\partial b} \; \frac{\partial w}{\partial b} \right\rfloor \tag{5.27}$$

will be used at each of the midside nodes 5, 6, 7, and 8, giving the required total of 48. The b direction in equation (5.27) is the direction defined by equation (4.16) and shown at point J in Figure 4.3.

It was pointed out in Chapter 4 that the direction and positive sense of b in equation (4.16) is unique and is referenced to the coordinate system on the shell surface. Thus the derivative of the displacements with respect to b in two adjacent elements will have a positive

sense in the outward direction in one and an inward positive sense in the other. This is important for maintaining compatibility between the two adjacent elements since the displacements along their common boundary line are expressed in terms of the generalized displacements at the nodes on the line.

Expressions for the generalized displacements, equation (5.26) and (5.27), can be determined by using equations (5.24) and (5.25). The first three displacements of (5.26) are the same as (5.24). The remaining generalized displacements can be determined by the chain rule. As an example, from (5.21), we have

$$\frac{\partial u}{\partial X_i} = \frac{\partial u_c}{\partial X_i} + a_{ji} \frac{\partial u'}{\partial X'_j} + C_{ji} \frac{\partial u''}{\partial X''_j} \tag{5.28}$$

where

$$a_{ji} = \frac{\partial X'_j}{\partial X_i} \tag{5.29}$$

and

$$C_{ji} = \frac{\partial X''_j}{\partial X_i} \tag{5.30}$$

and thus the derivatives of the total u function with respect to X and Y can be determined. The second order tensors of (5.29) and (5.30) are arrays of direction cosines which relate the two additional coordinate systems to the basic element coordinate system. Also, the derivative of u at midside node m with respect to the direction b can be determined from

$$\frac{\partial u}{\partial b^m} = d_i^m \frac{\partial u_c}{\partial X_i} + d_k^m a_{jk} \frac{\partial u'}{\partial X'_j} + d_k^m C_{jk} \frac{\partial u''}{\partial X''_j} \tag{5.31}$$

where

$$d_i^m = \frac{\partial X_i}{\partial b^m} \tag{5.32}$$

Expression (5.32) is a shorthand notation for the two direction cosines which relate the X and Y axes to direction b at midside node m.

We may now write the 48 equations in the generalized displacements so that each is evaluated at its respective nodal point in accordance with equation (2.20), but since the same polynomial form is used for each of the u, v, and w displacements, only 16 equations have to be formed. Thus, considering only the generalized displacements in u, we may write

$$[\bar{v}] = \left[u_1 \cdots u_4 \,\middle|\, \frac{\partial u}{\partial X_1} \cdots \frac{\partial u}{\partial X_4} \; \frac{\partial u}{\partial Y_1} \cdots \frac{\partial u}{\partial Y_4} \,\middle|\, \frac{\partial u}{\partial b_5} \cdots \frac{\partial u}{\partial b_8} \right] = [\delta \,|\, \epsilon \,|\, \gamma] \tag{5.33}$$

where the numerals indicate nodal point numbers. The Greek alphabet symbols are introduced for future reference. Now, writing (2.20) for the u displacement

$$\begin{Bmatrix} \delta \\ \epsilon \\ \gamma \end{Bmatrix} = [\bar{R}] \begin{Bmatrix} a_1 \\ \vdots \\ a_{16} \end{Bmatrix} \tag{5.34}$$

and inverting, we obtain equation (2.21) for the quadrilateral element

$$\begin{Bmatrix} a_1 \\ \vdots \\ a_{16} \end{Bmatrix} = [\bar{R}]^{-1} \begin{Bmatrix} \delta \\ \epsilon \\ \gamma \end{Bmatrix} = [\bar{A}] \begin{Bmatrix} \delta \\ \epsilon \\ \gamma \end{Bmatrix} \tag{5.35}$$

where the bar has been written over the A matrix to indicate that only the u displacement has been considered.

Equation (5.35) expresses the unknown coefficients of the u displacement within the element in terms of the u generalized displacements at the corner and midside nodes. The A bar matrix is identical for the v and w displacements and does not have to be computed.

The midside nodes in (5.35) are undesirable and are difficult to implement in a finite element computer program. In the present application, they are eliminated by assuming a linear variation of u, v, and w along the side of the element in the b direction. Thus, considering only the u displacement, the derivative of u in the b direction at the midside node is assumed to be the mean of the combination of the derivative of u with respect to X and Y at each of the nodes which define the side of the element. This may be shown by first rewriting (5.35) in the form

$$\begin{Bmatrix} a_1 \\ \vdots \\ a_{16} \end{Bmatrix} = \left[[\bar{A}]^{\delta} \,\vdots\, [\bar{A}]^{\epsilon} \,\vdots\, [\bar{A}]^{\gamma} \right] \begin{Bmatrix} \delta \\ \epsilon \\ \gamma \end{Bmatrix} \tag{5.36}$$

The linear variation may be expressed by

$$\{\gamma\} = [G] \{\epsilon\} \tag{5.37}$$

where the terms of G are factors of one-half and direction cosines. Thus as an example, using the notation of (5.32), we may write

$$\frac{\partial u}{\partial b_6} = 1/2 \left(d_1^6 \frac{\partial u}{\partial X_2} + d_1^6 \frac{\partial u}{\partial X_3} + d_2^6 \frac{\partial u}{\partial Y_2} + d_2^6 \frac{\partial u}{\partial Y_3} \right) \tag{5.38}$$

The other three equations are obtained similarly. Substituting (5.37) into (5.36),

$$\begin{Bmatrix} a_1 \\ \vdots \\ a_{16} \end{Bmatrix} = \left[[\bar{A}]^{\delta} \mid [\bar{A}]^{\epsilon} + [\bar{A}]^{\gamma}[G] \right] \begin{Bmatrix} \delta \\ \hline \epsilon \end{Bmatrix} \tag{5.39}$$

we obtain an equation for the coefficients in terms of the generalized displacements at only the corner nodes.

Equation (2.22) may now be formed for all the coefficients and the generalized displacements at each of the four corner nodes by using the transformation matrix formed in equation (5.39). Before doing this, it is necessary to introduce additional generalized displacements which are the derivatives of u, v, and w with respect to the Z coordinate. These additional generalized displacements do not describe the deformation of the element, but they will facilitate the transformations in going to and from various coordinate systems that will have to be performed later. Thus, the set of generalized displacements at each of the four corner nodes is now

$$[\bar{v}]_i = \left[u\ v\ w\ \frac{\partial u}{\partial X}\ \frac{\partial u}{\partial Y}\ \frac{\partial u}{\partial Z}\ \frac{\partial v}{\partial X}\ \frac{\partial v}{\partial Y}\ \frac{\partial v}{\partial Z}\ \frac{\partial w}{\partial X}\ \frac{\partial w}{\partial Y}\ \frac{\partial w}{\partial Z} \right]_i \tag{5.40}$$

The equivalent of equation (2.21) for the quadrilateral element can now be written as

$$\begin{Bmatrix} a_1 \\ \vdots \\ a_{48} \end{Bmatrix} = [A] \begin{Bmatrix} \bar{v}_1 \\ \hline \bar{v}_2 \\ \hline \bar{v}_3 \\ \hline \bar{v}_4 \end{Bmatrix} = [A] \{\bar{v}\} \tag{5.41}$$

where the columns of the A matrix are obtained from equation (5.39) and are ordered in accordance with the ordering of the generalized displacement in (5.40). The columns which correspond to the derivatives with respect to Z are void.

The final equation which expresses the displacements within the element in terms of the generalized displacements at the four corner nodes may now be written by substituting (5.41) into (5.24) to obtain

$$\begin{Bmatrix} u \\ v \\ w \end{Bmatrix} = \left[\begin{array}{c|c|c} r & 0 & 0 \\ \hline 0 & r & 0 \\ \hline 0 & 0 & r \end{array} \right] [A] \{\bar{v}\} \tag{5.42}$$

5.4 GENERALIZED STRESSES AND STRAINS

The stiffness equation, equation (2.30), was derived for a general three-dimensional problem and must be specialized for plate and shell problems which are solved by using the Kirchoff hypothesis, equation (5.13). We begin by introducing the concept of generalized stresses and strains.

Equation (3.49) gives the constitutive relationship for an increment of stress in terms of an increment of total strain. Introducing the notation of Marçal [60], we may write

$$\{\Delta S\} = [p^-]\,\{\Delta E\} \tag{5.43}$$

where the stresses and strains have been put into vector form and the matrix p^- is the term in brackets in equation (3.49).

The generalized stresses are introduced through the equation

$$\begin{Bmatrix} \Delta N \\ \hline \Delta M \end{Bmatrix} = \int_{-\frac{h}{2}}^{\frac{h}{2}} \begin{Bmatrix} \Delta S \\ \hline Z\Delta S \end{Bmatrix} dZ \tag{5.44}$$

where the stresses are integrated through the thickness, h, of the element. The generalized stresses are now the thrust and moment per unit inch.

The expression for generalized strains can be obtained by first writing an increment of total strain as

$$\{\Delta E\} = \{\Delta \bar{E}\} + Z\{\Delta \kappa\} \tag{5.45}$$

where the first term is the strain at the midfiber and the second term is the additional strain due to bending. Using (2.15) and (5.15) through (5.17), the two components of strain for the quadrilateral element become

$$\{\Delta \bar{E}\} = \begin{Bmatrix} \Delta \bar{E}_{XX} \\ \Delta \bar{E}_{YY} \\ 2\Delta \bar{E}_{XY} \end{Bmatrix} = \begin{Bmatrix} \Delta \dfrac{\partial u}{\partial X} + \left(\dfrac{\partial \bar{w}}{\partial X} + \dfrac{\partial w}{\partial X}\right)\Delta \dfrac{\partial w}{\partial X} + 1/2\left(\Delta \dfrac{\partial w}{\partial X}\right)^2 \\ \Delta \dfrac{\partial v}{\partial Y} + \left(\dfrac{\partial \bar{w}}{\partial Y} + \dfrac{\partial w}{\partial Y}\right)\Delta \dfrac{\partial w}{\partial Y} + 1/2\left(\Delta \dfrac{\partial w}{\partial Y}\right)^2 \\ \Delta \dfrac{\partial u}{\partial Y} + \Delta \dfrac{\partial v}{\partial X} + \left(\dfrac{\partial \bar{w}}{\partial X} + \dfrac{\partial w}{\partial X}\right)\Delta \dfrac{\partial w}{\partial Y} + \left(\dfrac{\partial \bar{w}}{\partial Y} + \dfrac{\partial w}{\partial Y}\right)\Delta \dfrac{\partial w}{\partial X} + \Delta \dfrac{\partial w}{\partial X}\Delta \dfrac{\partial w}{\partial Y} \end{Bmatrix} \tag{5.46}$$

and

$$\{\Delta\kappa\} = \begin{Bmatrix} \Delta\kappa_{XX} \\ \Delta\kappa_{YY} \\ 2\Delta\kappa_{XY} \end{Bmatrix} = \begin{Bmatrix} -\Delta \dfrac{\partial^2 w}{\partial X^2} \\ -\Delta \dfrac{\partial^2 w}{\partial Y^2} \\ -2\Delta \dfrac{\partial^2 w}{\partial X \partial Y} \end{Bmatrix} \quad (5.47)$$

The engineering definition of shear strain has been used in (5.46) and (5.47). Substituting (5.43) into (5.44) and using (5.45), we obtain the relationship between the components of generalized strains and generalized stresses:

$$\begin{Bmatrix} \Delta N \\ \hline \Delta M \end{Bmatrix} = \int_{-\frac{h}{2}}^{\frac{h}{2}} \left[\begin{array}{c|c} [p^-] & Z[p^-] \\ \hline Z[p^-] & Z^2[p^-] \end{array}\right] dZ \begin{Bmatrix} \Delta\bar{E} \\ \hline \Delta\kappa \end{Bmatrix} \quad (5.48)$$

5.5 STIFFNESS MATRIX AND EQUILIBRIUM CORRECTION VECTOR

The previous definitions of generalized stresses and generalized strains set the form of the stiffness matrix and the equilibrium correction vector of equation (2.30). The D matrix of that equation is the matrix under the integral in (5.48). The B1 and B2 matrices of (2.30) are defined in Table 5.1. The B1 matrix is the increment in generalized strain and is thus identical to the combination of (5.46) and (5.47). The B2 matrix comes from the variation on the increment of strain. The specific evaluation of the two matrices required in the numerical integration is performed by using the expressions for the u, v, and w displacements given in (5.24). The numerical integration procedure is described in the next chapter.

5.6 LOADING

The distributed loading for the quadrilateral element depends on the relationship of the differential area on the shell surface to the projected differential area in the (X, Y) plane. The two differential areas are shown in Figure 5.3. An increment of distributed load expressed in terms of area on the shell surface must be corrected to the equivalent distributed load in the base plane since this is where the integration will be performed. Moreover, the change in the area on the shell due to a change in deformation must also be determined.

The vector differential area on the shell surface can be expressed as the cross product of the differential vectors on the surface

$$d\underset{\sim}{a} = d\underset{\sim}{r} \times \delta\underset{\sim}{r} \quad (5.49)$$

TABLE 5.1
B1 AND B2 MATRICES

$$[BI] = \left[\begin{array}{c|c|c} \frac{\partial}{\partial X}[r] & 0 & \left(\frac{\partial \bar{w}}{\partial X}+\frac{\partial w}{\partial X}+g\Delta\frac{\partial w}{\partial X}\right)\frac{\partial}{\partial X}[r] \\ \hline 0 & \frac{\partial}{\partial Y}[r] & \left(\frac{\partial \bar{w}}{\partial Y}+\frac{\partial w}{\partial Y}+g\Delta\frac{\partial w}{\partial Y}\right)\frac{\partial}{\partial Y}[r] \\ \hline \frac{\partial}{\partial Y}[r] & \frac{\partial}{\partial X}[r] & \left(\frac{\partial \bar{w}}{\partial X}+\frac{\partial w}{\partial X}\right)\frac{\partial}{\partial Y}[r]+\left(\frac{\partial \bar{w}}{\partial Y}+\frac{\partial w}{\partial Y}\right)\frac{\partial}{\partial Y}[r]+h\Delta\frac{\partial w}{\partial X}\frac{\partial}{\partial Y}[r] \\ \hline 0 & 0 & -\frac{\partial^2}{\partial X^2}[r] \\ \hline 0 & 0 & -\frac{\partial^2}{\partial Y^2}[r] \\ \hline 0 & 0 & -2\frac{\partial^2}{\partial X \partial Y}[r] \end{array}\right]$$

I = 1 g = 1/2 h = 1

I = 2 g = 1 h = 2

[r] is defined in equation (5.25)

or by the tensor equivalent

$$da_i = e_{ijk}\, dx_j\, \delta x_k = e_{ijk}\, x_{j,m}\, dX_m\, x_{k,n}\, \delta X_n \tag{5.50}$$

Thus, an expression for the shell surface area can be obtained in terms of the base plane area by using (5.1) in (5.50), i.e.,

$$\underset{\sim}{da} = \left(-\frac{\partial \bar{w}}{\partial X}\hat{i}_1 - \frac{\partial \bar{w}}{\partial Y}\hat{i}_2 + \hat{i}_3\right) dA \tag{5.51}$$

which will be used shortly to obtain the consistent loading vector. As expected, equation (5.51) is similar to the equation of the normal on the shell surface, (5.11).

We now turn to the problem of determining the change in the area due to the change in deformation that occurs in going from the intermediate configuration to the current configuration. We may write the incremental equivalent of (5.2) as

$$x_i + \Delta x_i = X_i + u_i + \Delta u_i \tag{5.52}$$

where it is understood that the initial warping, $\bar{w}$, is included in the component u_i on the right side for i equal to three. The change in the differential area can now be expressed by

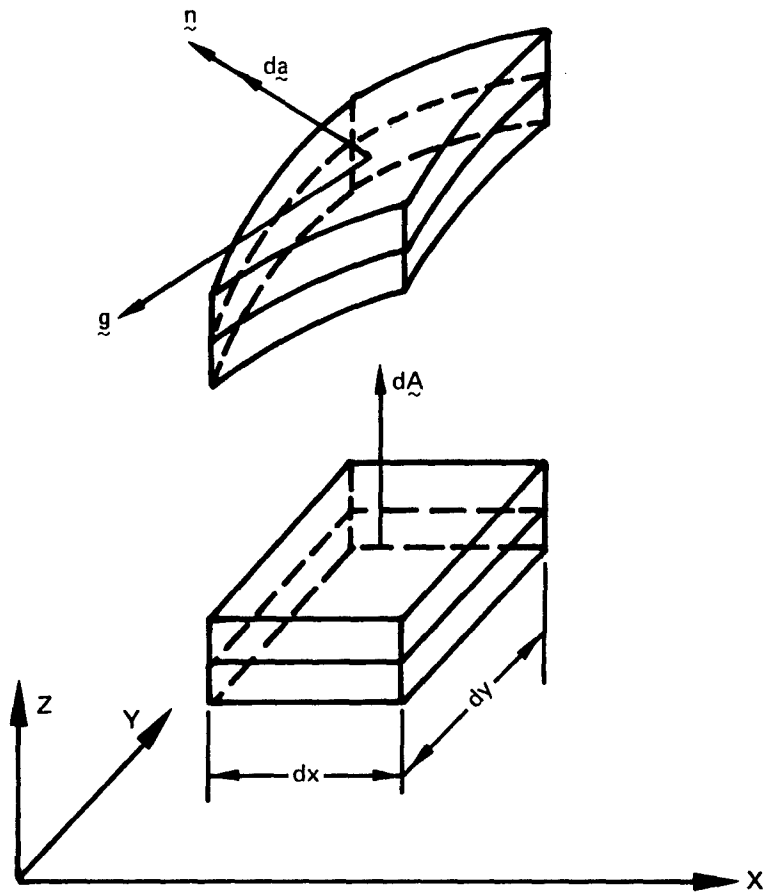

Figure 5.3 – Differential Area on Shell Surface and in Base Plane

$$\Delta da_i = e_{ijk}\, d(x_j + \Delta x_j)\, \delta(x_k + \Delta x_k) - e_{ijk}\, dx_j\, \delta x_k \tag{5.53}$$

Substituting (5.52) into (5.53), the change in area can be shown to be

$$\begin{aligned}\Delta da_i = e_{ijk} (&\delta_{jm}\, \Delta u_{k,n} + u_{j,m}\, \Delta u_{k,n} + \Delta u_{j,m}\, \delta_{kn} + \Delta u_{j,m}\, u_{k,n} \\ &+ \Delta u_{j,m}\, \Delta u_{k,n})\, dX_m\, \delta X_n\end{aligned} \tag{5.54}$$

Now imposing the assumptions of (5.8) and (5.10), the final expression for the change in area turns out to be

$$\begin{aligned}\Delta d\underset{\sim}{a} &= \left(-\Delta \frac{\partial w}{\partial X} \hat{i}_1 - \Delta \frac{\partial w}{\partial Y} \hat{i}_2 + 0\, \hat{i}_3\right) dA \\ \Delta d\underset{\sim}{a} &= \Delta m_j\, \hat{i}_j\, dA\end{aligned} \tag{5.55}$$

It is interesting to note that (5.55) is similar to the difference in equations (5.12) and (5.11), the difference between the surface normals after and before deformation. The m components are the estimated displacements within the element and their computation will be described subsequently.

The loading terms, (2.27) and (2.28), may be determined for the quadrilateral element by using equations (5.51) and (5.55). The relative first-order amplitude of the two differential areas before loading is

$$\frac{|d\underset{\sim}{a}|}{|d\underset{\sim}{A}|} = \left[1 + \left(\frac{\partial \bar{w}}{\partial X}\right)^2 + \left(\frac{\partial \bar{w}}{\partial Y}\right)^2\right]^{1/2} = C(X, Y) \tag{5.56}$$

The body force per unit volume of the shell surface is shown in Figure 5.3, which is expressed in terms of the local element system as

$$\underset{\sim}{g} = g_j\, \hat{i}_j \tag{5.57}$$

The incremental part of (2.27) may now be written in matrix form using (5.56) and the notation of (2.32)

$$\{\Delta P\} = h[A]^T \int_A [r]^T \{\Delta g\}\, C dA \tag{5.58}$$

where h is the thickness of the element and the scalar symbol A indicates integration over the (X, Y) plane. The total load P of (2.32) at the intermediate configuration is obtained by simply adding all the increments that have been computed previously.

The case of uniform normal pressure will now be considered for the distributed surface loading. The surface traction acting on the shell is given by the equation

$$\underset{\sim}{f} = -p\, d\underset{\sim}{a} \tag{5.59}$$

and the traction can be expressed in terms of unit area in the (X, Y) plane by using (5.51) and (5.56) to obtain

$$F_i = p_{\ell i} C(X, Y) dA \tag{5.60}$$

With (5.60), the incremental term of (2.27) due to surface loading is now

$$\{\Delta F\} = -\Delta p [A]^T \int_A [r]^T \{\ell\} C(X, Y) dA \tag{5.61}$$

where the components of the surface differential area have been put into column vector form.

The change in the surface traction due to the change in deformation may be written directly now as

$$\{\Delta F_G\} = -p [A]^T \int_A [r]^T \{\Delta m\} C(X, Y) dA \tag{5.62}$$

where the symbol m is defined in (5.55).

The ℓ components in (5.61) are dependent on the geometry of the shell whereas from (5.55), the m components are dependent on the increment of displacements that occur within the element. Using (5.42), we may write the m components as

$$\Delta m_i = \lfloor 0 \,|\, 0 \,|\, r \rfloor_{,i} [A] \{\Delta \bar{v}\} \tag{5.63}$$

where the comma is used to indicate partial differentiation with respect to the index i. The m components can now be put into vector form by writing

$$\{\Delta m\} = [q] [A] \{\Delta \bar{v}\} \tag{5.64}$$

where the last row of the matrix q is void in accordance with (5.55). Now substituting (5.64) into (5.62), we obtain the final form of the increment of load due to the change in deformation as

$$\{\Delta F_G\} = -p [A]^T \int_A [r]^T C(X, Y) [q] dA [A] \{\Delta \bar{v}\} \tag{5.65}$$

In forming the above vector, it was noted previously that we need the increment of displacement that occurs in going from the intermediate configuration to the current configuration. Since these are the fundamental unknowns, the same procedure applies here as was used for estimating the displacements described for equation (2.30).

Similar to the total body force loading, the total distributed loading, F in (2.32), is obtained by adding all of the contributions computed and using (5.61) and (5.65) for all previous increments.

The loading terms derived above are the generalized forces and are conjugate to the generalized displacements in the sense that the product of the two produces work which is a

scalar. Thus, the choice of a particular generalized displacements used and the application of the virtual work theorem produced the generalized forces.

5.7 TRANSFORMATIONS

It is important to develop a consistent and valid approach for transforming the generalized displacements and forces to and from various coordinate systems. The effectiveness of the element would be greatly reduced if its use were restricted to one system.

Consider first the transformation of the generalized displacements at a node given by (5.40). It is necessary to obtain a method that transforms the displacements between the global system and the local element system.

The transformation of global coordinates (barred) to local element coordinates will be taken as

$$X_i = a_{ij}\,\bar{X}_j \tag{5.66}$$

where

$$a_{ij} = \cos(X_i, \bar{X}_j) \tag{5.67}$$

The generalized displacements at nodal point i are partitioned as follows

$$\left\lfloor u\ v\ w \;\middle|\; \frac{\partial u}{\partial X}\ \frac{\partial u}{\partial Y}\ \frac{\partial u}{\partial Z}\ \frac{\partial v}{\partial X}\ \frac{\partial v}{\partial Y}\ \frac{\partial v}{\partial Z}\ \frac{\partial w}{\partial X}\ \frac{\partial w}{\partial Y}\ \frac{\partial w}{Z} \right\rfloor_i = \lfloor \bar{V}^1 \ \ \bar{V}^2 \rfloor_i \tag{5.68}$$

where, as before, the bar over the displacements indicates the values at the nodes. The transformation of the first type (superscript 1) is straightforward since they are vector components. Thus

$$\bar{v}_i^1 = a_{ij}\,\bar{V}_j^1 \tag{5.69}$$

where the capital letters indicate the generalized displacements in the global system.

To see how the second type of generalized displacement (superscript 2) will transform, consider an increment of the first type of generalized displacement in the local element coordinate system, i.e.,

$$d\bar{v}_i^1 = \frac{\partial v_i^1}{\partial X_j}\,dX_j \tag{5.70}$$

Using (5.69), we obtain

$$d\bar{v}_i^1 = \frac{\partial}{\partial X_j}(a_{ik}\,\bar{V}_k^1)\,dX_j \tag{5.71}$$

and expanding the above

$$d\bar{v}_i^1 = \frac{\partial}{\partial X_\ell}(a_{ik}\,\bar{V}_k^1)\,\frac{\partial \bar{x}_\ell}{\partial X_j}\,dX_j \tag{5.72}$$

Since the transformation is independent of the position in the coordinate system, we may write

$$d\bar{v}_i^1 = a_{ik}\,a_{j\ell}\,\frac{\partial \bar{V}_k^1}{\partial X_\ell}\,dX_j \tag{5.73}$$

where the inverse of (5.66) has been used. Comparing (5.70) and (5.73), we see that

$$\frac{\partial \bar{v}_i^1}{\partial X_j} = a_{ik}\,a_{j\ell}\,\frac{\partial \bar{V}_k^1}{\partial \bar{X}_\ell} \tag{5.74}$$

Thus the transformation of the second type of generalized displacement is

$$\bar{v}_{ij}^2 = a_{ik}\,a_{j\ell}\,\bar{V}_{k\ell}^2 \tag{5.75}$$

which is the transformation for second-order tensors.

The transformation of the first type of generalized force follows from (5.69) and the equality of work performed in the local element system and the global system [61]. Equating the work performed in the local system to that in the global system,

$$f_i^1\,\bar{v}_i^1 = F_i^1\,\bar{V}_i^1 \tag{5.76}$$

and substituting (5.69)

$$f_i^1\,(a_{ij}\,\bar{V}^1) = F_i^1\,\bar{V}_i^1 = F_j^1\,\bar{V}_j^1 \tag{5.77}$$

we obtain

$$f_i^1\,a_{ij} = F_j^1 \tag{5.78}$$

Now multiplying by the transformation tensor

$$f_i^1\,a_{kj}\,a_{ij} = f_i^1\,\delta_{ki} = a_{kj}\,F_j^1 \tag{5.79}$$

we obtain the transformation of the first type of generalized forces as

$$f_k^1 = a_{kj}\,F_j^1 \tag{5.80}$$

Since the second type of generalized displacements transform as second-order tensors, the generalized forces must also be elements of a second-order tensor in order to be conjugate to the displacements in the sense that the product of the generalized displacements and generalized forces produce work which is a scalar. Thus as was done for the first type of forces and displacements in (5.76), we may now equate the work in the local and global coordinate systems:

$$f^2_{ij}\,\bar{v}^2_{ij} = F^2_{ij}\,\bar{V}^2_{ij} \tag{5.81}$$

and the derivation follows similarly to that given for the first type. Substituting (5.75) into (5.81),

$$f^2_{ij}\,a_{im}\,a_{jn}\,\bar{v}^2_{mn} = F^2_{ij}\,\bar{V}^2_{ij} = F^2_{mn}\,\bar{V}^2_{mn} \tag{5.82}$$

and thus

$$f^2_{ij}\,a_{im}\,a_{jn} = F^2_{mn} \tag{5.83}$$

Now multiplying by the transformation tensors

$$f^2_{ij}\,a_{\ell m}\,a_{im}\,a_{pn}\,a_{jn} = f^2_{ij}\,\delta_{\ell i}\,\delta_{pj} = a_{\ell m}\,a_{pn}\,F^2_{mn} \tag{5.84}$$

we finally obtain

$$f^2_{\ell p} = a_{\ell m}\,a_{pn}\,F^2_{mn} \tag{5.85}$$

All of the above may now be put into matrix notation. Equation (5.69) may be expressed as

$$\{\bar{v}^1\} = [t^1]\,\{\bar{V}^1\} \tag{5.86}$$

where the notation is self-explanatory.

The second type of displacement transformation could be written as

$$\{\bar{v}^2\} = [t^2]\,[\bar{V}^2]\,[t^2]^T \tag{5.87}$$

but would cause problems in the implementation of the element. The element has been exercised in a program (to be described in the next chapter) which presently has provision only for the transformation of generalized displacements and forces which transform as vectors. The reason is that there has been no need for any other type of transformation since the degrees of freedom of most other elements have transformed as vectors. Cowper et al. [22] developed a shell element for shallow shell applications; some of its degrees of freedom are similar to the second type used here, but the transformations are performed in a two-dimensional space.

If (5.75) is expanded, then the second type of generalized displacements and forces could be transformed in one operation in the same sense as that required for the transformation of the first type of displacements and forces. If we write the transformation of the second type of generalized displacements as

$$\{\bar{v}^2\} = [t^2]\,\{\bar{V}^2\} \tag{5.88}$$

then the examination of the expansion of (5.75) reveals that the transformation matrix in (5.88) will be in the form

$$[t^2] = \left[\begin{array}{c|c|c} a_{11}[a] & a_{12}[a] & a_{13}[a] \\ \hline a_{21}[a] & a_{22}[a] & a_{23}[a] \\ \hline a_{31}[a] & a_{32}[a] & a_{33}[a] \end{array}\right] \tag{5.89}$$

where the matrix a is the array of the second-order transformation array of (5.66). Now combining (5.86) and (5.88), the transformation of all of the generalized displacements at nodal point i takes the form

$$\left\{\begin{array}{c} \bar{v}^1 \\ \hline \bar{v}^2 \end{array}\right\} = \left[\begin{array}{c|c} t^1 & 0 \\ \hline 0 & t^2 \end{array}\right] \left\{\begin{array}{c} \bar{V}^1 \\ \hline \bar{V}^2 \end{array}\right\} = [t]\{\bar{V}\}_i \tag{5.90}$$

Using (5.90), the transformation of all the generalized displacements, i.e., degrees of freedom, of the element can be obtained as

$$\left\{\begin{array}{c} \bar{v}_1 \\ \bar{v}_2 \\ \bar{v}_3 \\ \bar{v}_4 \end{array}\right\} = \left[\begin{array}{c|c|c|c} [t] & 0 & 0 & 0 \\ \hline 0 & [t] & 0 & 0 \\ \hline 0 & 0 & [t] & 0 \\ \hline 0 & 0 & 0 & [t] \end{array}\right] \left\{\begin{array}{c} \bar{V}_1 \\ \bar{V}_2 \\ \bar{V}_3 \\ \bar{V}_4 \end{array}\right\} \tag{5.91}$$

or

$$\{\bar{v}\} = [T]\{\bar{V}\} \tag{5.92}$$

Starting with equation (5.88), a parallel development of the matrix expressions could be given for the transformation of the generalized forces. The final equation, which has the same meaning as equation (5.92), will simply be written as

$$\{f\} = [T]\{F\} \tag{5.93}$$

where the transformation matrix is the same as in (5.92).

The transformation of the element stiffness matrix from the local element system to the global system follows directly using (5.92) and (5.93). The stiffness equation can be expressed as

$$[k]\{\bar{v}\} = \{f\} \tag{5.94}$$

where the matrix k is the element stiffness in local coordinates. Now substituting (5.92) and (5.93) into (5.94), we obtain

$$[k]\,[T]\,\{\bar{V}\} = [T]\,\{F\} \tag{5.95}$$

Then operating on both sides of the above equation by the inverse of the transformation matrix, we obtain (since orthogonal transformation)

$$[T]^{-1}\,[k]\,[T]\,\{\bar{V}\} = [T]^{T}\,[k]\,[T]\,\{\bar{V}\} \tag{5.96}$$

The stiffness in global coordinates can now be written as

$$[K] = [T]^{T}\,[k]\,[T] \tag{5.97}$$

and the stiffness equation in global coordinates can be expressed as

$$[K]\{\bar{V}\} = \{F\} \tag{5.98}$$

The stiffness equation in local coordinates given in (5.94) is equivalent to the incremental stiffness equation of (2.32). The notation has been simplified here to clarify the derivation of the transformations. Thus (5.98) is equivalent to the incremental equation (2.32) expressed in global coordinates.

5.8 CONVERGENCE REQUIREMENTS

In the development of any finite element, it is essential that particular attention be paid to satisfying convergence requirements. It is important that the convergence be monotonic so that the investigator will always know on which side of the correct solution his current solution lies.

During the early application of the finite element method, an unfortunate situation developed when it was found that better "convergence" rates were often obtained if the known correct requirements for convergence were relaxed. These practices are dangerous and should be discouraged, particularly when one starts to apply the same methods to nonlinear problems where the solutions are much more difficult than in linear problems. The use of such practices serves only to cloud the picture.

Irons and Draper [62] state three requirements as necessary to ensure convergence:

a. The assumed displacement functions must be continuous within the element and the displacements must be compatible between adjacent elements.

b. The displacement functions must include the rigid body displacements.

c. The displacement functions must include the constant strain states of the element.

The second requirement is actually a special case of the third under certain conditions. The first two of the above requirements were mentioned in Chapter 1 as two of the four primary difficulties that have impeded the derivation of curved shell elements [15].

The compatibility requirements for a particular element come from the geometrical boundary conditions obtained in the derivation when a variational principle, such as the principle of virtual work is used. The necessary boundary conditions for the shallow shell theory being used are compatibility of the u, v, and w displacements and the derivative of the normal displacement w in the direction normal to the edge [38]. These are boundary conditions that are imposed on an element by the surrounding elements.

The continuity of the u, v, and w displacements is ensured since we are using equal order bicubic functions for each of the three displacements. Continuity could not be guaranteed if we were using lesser order polynomials for u and v than for w.

The continuity of the rotational displacement is effected through the use of the three surface vectors. The normal rotation is computed through the use of equation (5.31) and was explained in Section 5.3. It is noted that the midside node in elements 1 and 2 in Figure 5.4 is actually two different material points in the X-Y plane of each of the two elements (not shown) which is mapped to the same spatial point J on the shell surface.

The intent of the second requirement for convergence is to induce no strain in the element when it undergoes a rigid body motion. This requirement on the assumed displacements is strictly in the context of the small displacement theory. Considering equation (5.14), we see that all of the terms of the strain tensor must be included to describe the unrestricted motion of a line segment undergoing a rigid body motion. Thus if we are to truncate the expressions for strain and retain only the linear terms, the concept of inducing strains by rigid body motion becomes a relative matter which is limited to the small displacement theory.

It is known that the inclusion of the rigid body modes in the assumed displacement pattern gives improved linear results [26]. The assumed displacements used here for the formulation, equations (5.24) and (5.25), do include rigid body translation and rotation (linear terms). In view of the above remarks on the truncation of the expression for strain, some additional information is needed on the adequacy of the formulation for application to linear problems.

Examination of the eigenvalues of the stiffness matrix is a convenient method to determine the adequacy of an element for satisfying the rigid body requirement. It is known that there will be zero eigenvalues equal in number to the number of rigid body degrees of freedom [63].

During the generation of the stiffness matrix for the quadrilateral element, it was found necessary to place a 1.0 on the diagonal for those degrees of freedom which are derivatives with respect to Z. There are a total of 12 of these degrees of freedom. Thus for an ascending ordering of the eigenvalues, the nineteenth is the first one that can be associated with the deformation of the element since the first six are attributed to the rigid body motion. We will subsequently examine the eigenvalues of the stiffness matrices of several elements in order to demonstrate the above characteristics.

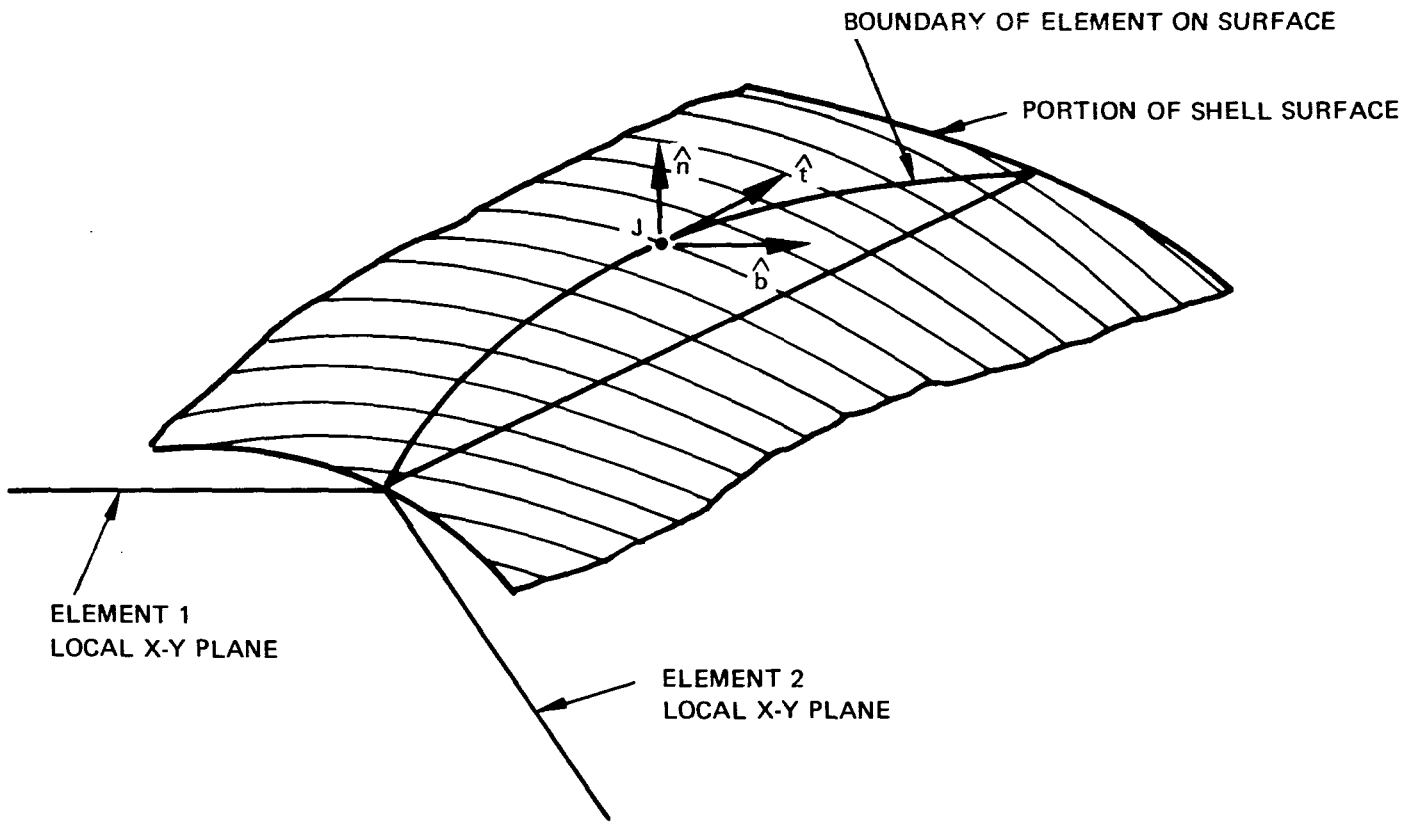

Figure 5.4 – Element Interface on Shell Surface

CHAPTER 6
IMPLEMENTATION OF THEORY

The previously described theory has been incorporated in an early version of the general purpose program developed by Marçal and his associates at Brown University. The methods of solution in the program have been described [64, 65] in a number of previous publications and the basic techniques used will be reviewed only briefly here. The description will be primarily limited to the implementation of the quadrilateral element and the previously described incremental formulation developed herein.

6.1 LINEAR ELASTIC LARGE DEFORMATION SOLUTIONS

The study of the large deflection of structures where the material remains elastic requires much less computational effort than when the material of the structure is carried into the inelastic range. The [D] matrix of equation (2.30) remains constant throughout the loading history.

Each of the component terms in equation (2.30) is integrated over the volume and surface of the element in the local coordinate system. The region of integration for the element is shown in Figure 6.1. Each of the integrals is computed by the approximate method whereby the region is subdivided into 16 subtriangles and the integrand is then evaluated at the centroid of the subtriangle. To integrate the function f over the element, the approximation is made that

$$\int f(x,y)\, dA \approx \sum_{i=1,16} f_i(x^c, y^c)\, \Delta A_i \tag{6.1}$$

where the superscript c indicates the function evaluated at the subtriangle centroid. Thus the product of the terms appearing in the integrand of each of the respective terms is evaluated at the centroid, multiplied by the contributing area, and then summed.

The evaluation of the B1 and B2 matrices given in Table 5.1 for the quadrilateral is required for the computation of the element stiffness matrix and the equilibrium correction vector in (2.30). In Table 5.1, the terms in parentheses shown with bars are the local slopes of the element surface derived in Chapter 4. The remaining terms in the parentheses are, first, the effect of initial displacements as termed by Marçal [6] and, second, the estimate of the displacement that will occur in going from the intermediate configuration to the current configuration. The latter are prefixed by the del symbol. The initial displacements are the total displacements that have occurred up through the intermediate configuration. The determination of the estimated displacements, i.e., the displacements that are to be computed for the current increment, was described following the derivation of equation (2.30) but additional detail will be given subsequently.

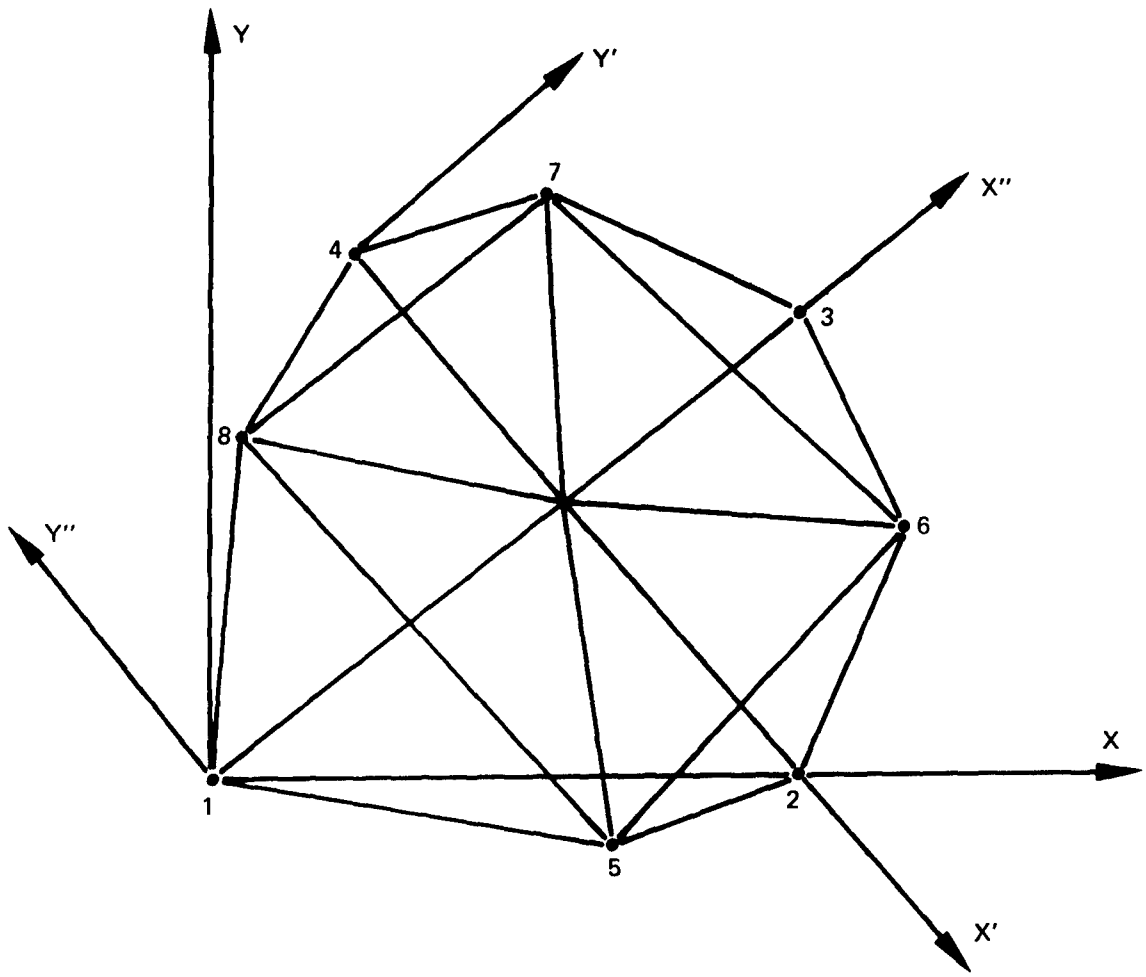

Figure 6.1 – Region of Integration

Thus, it is relatively straightforward to form the stiffness matrix and the equilibrium load correction vector of equation (2.30). The explicit evaluation of the B1 and B2 matrices at each of the integration points is obtained first by computing the derivatives of the r matrix, defined in equation (5.25), through the use of equation (5.28). The initial displacements and the estimated displacements at the integration points within the element are dependent on the initial and estimated generalized displacements at the element nodal points. For the quadrilateral, the initial and estimated displacements are in the w component only. Their relationship to the generalized displacements at the nodes is

$$\frac{\partial w}{\partial X_\alpha} = \frac{\partial}{\partial X_\alpha}_{\alpha=1,2} \left[\, 0 \,\middle|\, 0 \,\middle|\, r \,\right] [A] \{\bar{v}\} \tag{6.2}$$

which is written in the local element coordinate system. Thus the initial and estimated displacements are computed for the integration point and added to the local slope of the shell at the point. This sum is then used in forming the B1 and B2 matrices.

The analysis is started by applying a small portion of the total load and computing the linear elastic response. For this part of the analysis, the initial displacements are zero and the estimated displacements are not used because (a) it is assumed that the load is applied to the undeformed structure and (b) the applied load is so small that the response is linear. At this point the B1 and B2 matrices are identical and the computed stiffness matrix is symmetric. The stiffness matrices are assembled into the global, i.e., the total stiffness matrix, and the resulting equations are solved for the generalized displacements at the nodes resulting from the application of the first loading. The computation of the consistent loading vectors for distributed loading is straightforward and was described in Chapter 5.

The nonlinear analysis begins at this point. The previously computed generalized displacements at the nodes are first used to compute the estimated generalized nodal point displacements that will occur in the next increment of loading. This estimate is obtained by a simple linear extrapolation. Thus by using the previous notation for the generalized nodal displacements in the global system, we may write the estimated displacements for the next increment of loading as

$$\{\Delta\bar{V}_{i+1}\}_e = f\{\Delta\bar{V}_i\} \tag{6.3}$$

where f is the ratio of the applied loading in the next increment to the applied loading in the increment just computed.

The element stiffness matrices are now recomputed to incorporate the nonlinear effects. The generalized nodal displacements and the estimated nodal displacements that will occur in the current increment, obtained through equation (6.3), are first transformed to the local element coordinate system by equation (5.92). The element internal initial displacements and estimated displacements are now computed for each integration point by using equation (6.2). These values are then used in forming the B1 and B2 matrices required for the element stiffness

matrix and the equilibrium load correction vector of equation (2.30). The generalized stresses computed at the conclusion of the initial linear analysis are also used in forming the equilibrium load correction vector.

The newly computed stiffness matrices are now transformed and assembled again into the global system. The total load vector is augmented first by the increment of direct loading and then by the equilibrium load correction vector and the estimated change in surface loading due to a change in geometry - if this effect is being included in the analysis. These, too, are transformed to the global system. The estimated displacements within the element for use in equation (5.65) for computing the load due to a change in geometry are computed identically to those that were computed to form the B1 and B2 matrices. The solution of the stiffness equations now yields the increment of generalized displacements at the nodes resulting from the application of the increment of load.

The incremental displacements of the nodes that are computed will not be exact since the estimated incremental displacements that were used in forming the stiffness equations were not exact. This is true in general since a linear extrapolation is used to obtain the displacements and we know from the outset that the load-deflection curve is nonlinear.

An important advantage of the method being described is that we know that the solution technique could give the exact answer if we were able to use the exact increment of displacements in forming the stiffness equation; this, of course, is impossible since it is what we are after in the first place. The word "exact" is used in the context that we are working with the full equilibrium equations and use no linearization approximation (except for estimating displacement) during their derivation. Barring divergence, we know that the increment of displacements that we have just computed will give a better estimate of the true incremental displacement than will the linearly extrapolated values used at the beginning of the increment Thus the computed incremental displacements may now be used to form the revised element stiffness matrices, the equilibrium load correction vector, and the loading vector due to the change in geometry. This is done all within the current increment of loading, that is, without changing the load. The process is repeated until the desired accuracy is reached.

The decision to stop the iteration in any one increment of loading is based on the computed displacement at a preselected nodal point. If the newly computed displacement divided by the estimated displacement or the displacement computed in the previous iteration is less than a chosen ratio, then the process is stopped for the current increment and the analysis goes on to the next increment of loading. Typical values of the ratio and the strategy used in performing an analysis will be described later when we consider particular case studies.

6.2 INELASTIC LARGE DEFORMATION SOLUTIONS

The analytical process used when the material in the structures becomes nonlinear and path dependent is somewhat similar to that just described, but it is more involved. We must now consider the changing D matrix in equation (2.30), which is written there for the general

continuum case. For the specialized case of the quadrilateral shell finite element, where the equilibrium equations have been redefined in terms of the generalized stresses and strains convenient for plate and shell problems, the D matrix takes the form of the integral in equation (5.48). At any point through the shell, the stress and strain must satisfy equation (3.49) so we must show how this equation is implemented for the quadrilateral to form the relationship between generalized stress and strain.

Figure 6.2 shows a section through the thickness of the element and the 11 stations used to perform the numerical integration. These 11 stations are used at each of the 16 integration points shown in Figure 6.1

Equation (5.48) is rewritten here for convenience

$$\begin{Bmatrix} \Delta N \\ \Delta M \end{Bmatrix} = \int_{-\frac{h}{2}}^{\frac{h}{2}} \left[\begin{array}{c|c} [p^-] & Z[p^-] \\ \hline Z[p^-] & Z^2[p^-] \end{array}\right] dZ \begin{Bmatrix} \Delta \bar{E} \\ \Delta \kappa \end{Bmatrix}$$

and the nomenclature is as defined previously. The submatrix p is the stress-strain relationship given in parentheses in equation (3.49). For the present case, it is three by three for plane stress in conformance with the Kirchoff assumptions. To simplify the description, the equation will be rewritten as

$$\begin{Bmatrix} \Delta N \\ \Delta M \end{Bmatrix} = \int_{-\frac{h}{2}}^{\frac{h}{2}} \left[\begin{array}{c|c} DD & DB \\ \hline DB & BB \end{array}\right] dZ \begin{Bmatrix} \Delta \bar{E} \\ \Delta \kappa \end{Bmatrix} \tag{6.4}$$

The components of each of the submatrices are computed approximately as follows:

$$DD_{ij} \approx \sum_{k=1,11} (p_{ij})_k \Delta Z \tag{6.5}$$

$$DB_{ij} \approx \sum_{k=1,11} (p_{ij})_k Z_k \Delta Z \tag{6.6}$$

$$BB_{ij} \approx \sum_{k=1,11} (p_{ij})_k Z_k^2 \Delta Z \tag{6.7}$$

where the components of p are determined at each step of the loading. The integral is evaluated by using the Simpson rule for approximation.

The total numerical integration scheme for computing the element stiffness matrix may now be written as

$$[K]_{SYM} = \left[[A]^T \left(\sum_{\ell=1,16} [B2]_\ell \left(\sum_{k=1,11} \left[\begin{array}{c|c} [p] & [p]Z \\ \hline [p]Z & [p]Z^2 \end{array}\right]_k \Delta Z \right)_\ell [B1]_\ell \Delta A \right) [A] \right]_{SYM} \tag{6.8}$$

where the symmetric part is taken as the stiffness and the nonsymmetric part is treated as an equivalent force as described in Chapter 2.

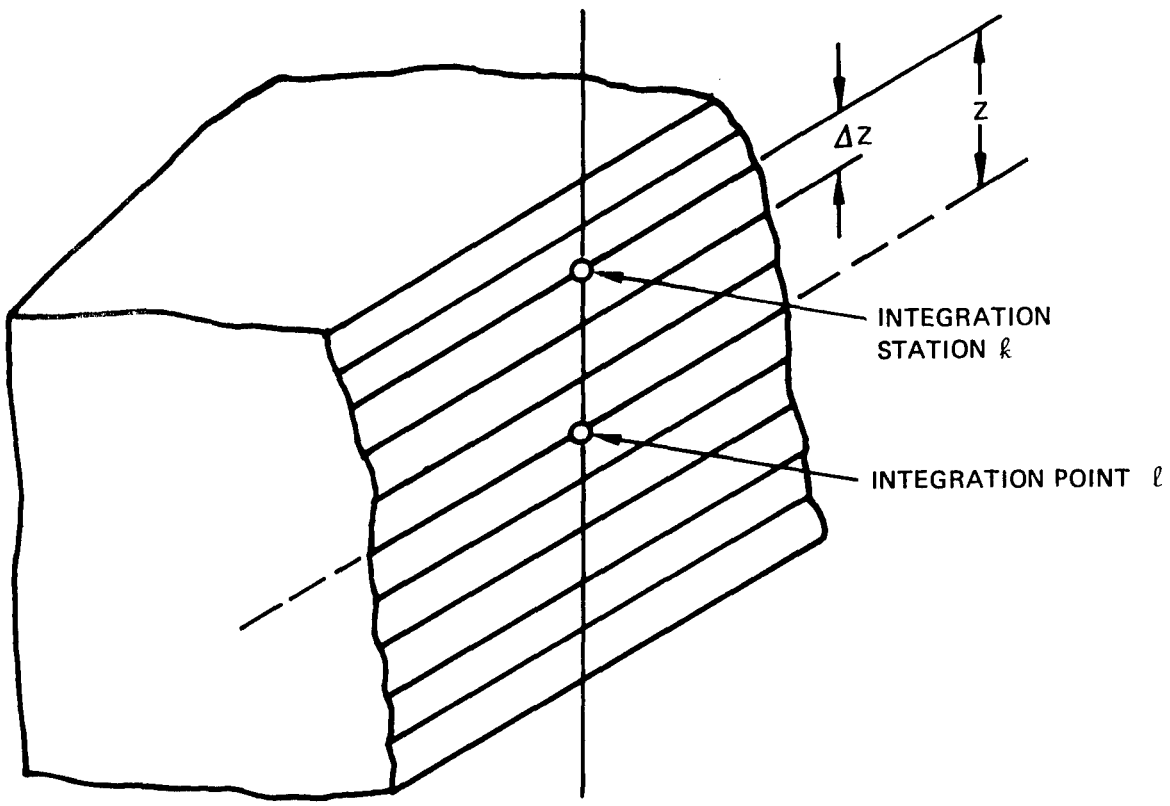

Figure 6.2 -- Section Through Element

The varying nonconservative behavior of inelastic materials requires recording the trace of each material point in the stress and strain space. Thus for each of the 11 stations through the thickness at each of the 16 integration points of the element, sufficient information has to be recorded to allow determination of the current incremental relationship between stress and strain. The three current stresses, two direct and one in-plane shear, and the current equivalent plastic strain must be stored for each point for both the isotropic and kinematic hardening rules. Additionally, the isotropic rule uses the current equivalent yield stress whereas the kinematic rule uses the center of the current yield surface to determine the appropriate incremental relationship. The following description applies primarily to the isotropic hardening rule.

The program allows the option of scaling the linear solution to the load which causes yielding at the highest stressed point within one of the elements or the option of incrementing the load (as described in the previous section) with elastic material properties before the plasticity analysis started. This second option is important for structures in which the effects of nonlinear geometry may be important, e.g., shells.

After each increment of load is applied and a solution is obtained, each point in each element is tested to determine whether it will go into the plastic range on application of the next increment of load. This is found from the estimated generalized nodal point displacements described in the previous section. Thus, using the relationship between incremental generalized strain and incremental generalized nodal point displacement in local element coordinates as

$$\begin{Bmatrix} \Delta\bar{E} \\ \Delta\bar{K} \end{Bmatrix} = [B2]\,[A] \left\{\Delta\bar{v}\right\}_e \tag{6.9}$$

we may obtain the strain at any point through the thickness by using equation (5.45). Once the estimated strain is computed, the estimated increment of stress that will occur is computed in accordance with equation (5.43) where only elastic material properties are used in the equation. This estimate of stress is then added to the stress that exists at the point. If on the basis of the von Mises criterion it is determined that the point will remain elastic, then computation of the stiffness can continue. If not, the material at the point will be in the transition region and the estimated reduction in stiffness will have to be determined.

The approach introduced by Marçal and King [66] for determining the incremental relationship between stress and strain is briefly outlined as follows:

a. For simplification here, it is assumed that the increment of load will allow the point to remain elastic during part of the increment, say the ratio m, and that the remaining part will be inelastic, (1-m). McNamara [67] described the use of this method for determining the value of m in connection with problems of transient vibration. Figure 6.3 gives a representation of the method. The value of m is obtained by writing the von Mises yeild condition

$$J_2\,(S^o + m\,\Delta S) = 1/3\,\sigma_o^2 \tag{6.10}$$

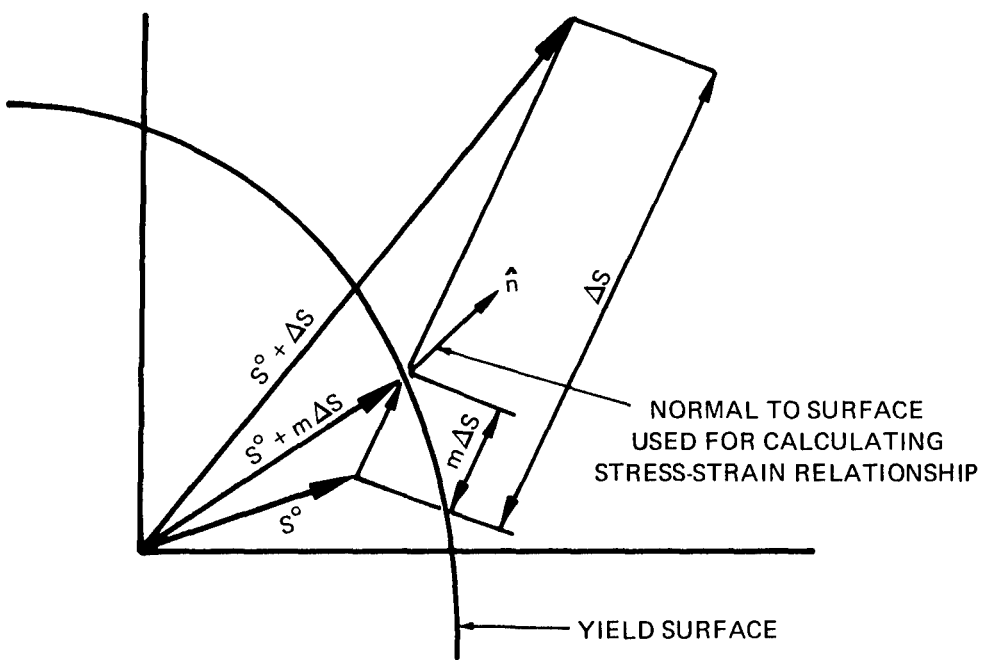

Figure 6.3 – Calculation of Ratio m and Normal to Yield Surface

where S^o is the stress state at the intermediate configuration and ΔS is the increment of stress that results if the increment of load allows the material to remain elastic. A quadratic equation in m results and the root is taken that causes the stress vector to be pointed outward from the loading surface.

b. With the value of m, the estimated increment of stress occurring up to yield is added to the current stress. The deviatoric part of these stresses is then computed.

c. Now by using the estimated deviatoric stresses, the total estimated strains (from the estimated nodal point generalized displacements and equation (6.9)), the slope of the equivalent stress-equivalent plastic strain curve, and the equivalent stress in equation (3.50), the estimated increment of equivalent plastic strain can be computed. If this is the first plastic loading of the point, the initial slope of the equivalent stress-equivalent plastic strain curve is used in the computation. The strain is then reduced by the value of m. Writing the estimated plastic strain in finite increment form, we have

$$\Delta e_e^p = (1-m)\frac{2/3\,\sigma_e\,\sigma'_{ij}\,C_{ijrs}}{4/9\,\dfrac{d\sigma_e}{de_p^e}\,\sigma_e^2 + \sigma'_{ij}\,C_{ijk\ell}\,\sigma'_{k\ell}}\,\Delta e_{rs}^T \tag{6.11}$$

d. The above-computed equivalent plastic strain allows determination of the estimated slope of the material curve at the end of the increment. This slope is used to determine a weighted mean slope that is assumed to be acting over the increment.

e. The final incremental stress-total strain relationship is computed to be

$$\Delta\sigma_{ij} = \left(mC_{ijrs} - (1-m)\frac{C_{ijk\ell}\,\sigma'_{k\ell}\,\sigma'_{pq}\,C_{pqrs}}{4/9\,\dfrac{d\sigma_e}{de_p^e}\,\sigma_e^2 + \sigma'_{pq}\,C_{pqrs}\,\sigma'_{rs}}\right)\Delta e_{rs}^T \tag{6.12}$$

f. If this is the last iteration of a particular load increment, the equivalent plastic strain and total stress are now updated and stored by using equations (6.11) and 6.12), respectively. If more iterations are needed to meet the desired accuracy, the quantity in parentheses in equation (6.12), which corresponds to the p matrix in equations (6.5) through (6.7), is used to form the D matrix for the next iteration.

The description of the implementation of the kinematic hardening rule is essentially the same as given above except that the loading surface translates; this requires tracking and storing the surface origin. Special attention has to be taken to ensure that the surface translates along the normal to the surface for the plane stress case under consideration here. Hibbitt [11] satisfied this requirement by recognizing the incompressibility of plastic deformations. Thus the trace of the translation tensor in equation (3.32) must be equal to zero. This is satisfied by adding to the two direct stress translation components the negative of their sum.

CHAPTER 7
NUMERICAL EXAMPLES

The accuracy of the previously derived shell element and nonlinear formulation will now be examined. We will first consider the linear applications of the element, then study a very simple, highly nonlinear rod and spring problem, and finally consider nonlinear applications of the shell element.

7.1 RIGID BODY MODES

Our method for studying the rigid body modes of the quadrilateral shell element was introduced in Section 5.8. It was stated there that the linear stiffness matrix should have six zero eigenvalues, corresponding to each of the rigid body modes; since we are using a numerical approach, the six eigenvalues will not be exactly zero. We also pointed out that the eigenvalue would be considered in ascending order and that the nineteenth would be the first one associated with the deformation of the element.

The results of the study of the eigenvalues are given in Figure 7.1. The stiffness matrix of an element that represents the 10-inch sector of a spherical shell is analyzed. Four different radii of the sphere are considered. The matrix subroutine package of the Argonne National Laboratory [69] was used to compute the values.

The results shown in the figure clearly demonstrate the characteristics stated in Section 5.8. It is also seen that as the element becomes more and more shallow, i.e., as the ratio of element side length to radius of shell decreases, the results become closer to what is expected. The first six eigenvalues were very small compared to the seventh. Moreover, there was a big difference between the eighteenth and nineteenth eigenvalues.

The dependency of the computed eigenvalues on the shallowness of the element indicates that for application to small displacement problems, the adequacy of shell fininte elements to satisfy the rigid body requirement is highly dependent on the strain-displacement relationships that are used in the element. In other words, as the element becomes flatter, the shell terms become less significant and the computed values approach the ideal values.

7.2 MEMBRANE CYLINDER - STRESSES

Examination of the need for an equilibrium correction term in the incremental formulation (Section 2.2) showed that it arose from the fact that the stresses did not satisfy the equilibrium equation at each point within the element and on the boundary. Thus, the equilibrium equations are satisfied only in an integral or average sense. The question arises then as to how to interpret the stresses that can be computed at each one of the integration points shown in Figure 6.1. In other words, how can physically meaningful stresses be obtained? One way would be to make the elements very small, smaller than required for an accurate displacement solution. Of course, this is undesirable because the additional elements increase computing costs.

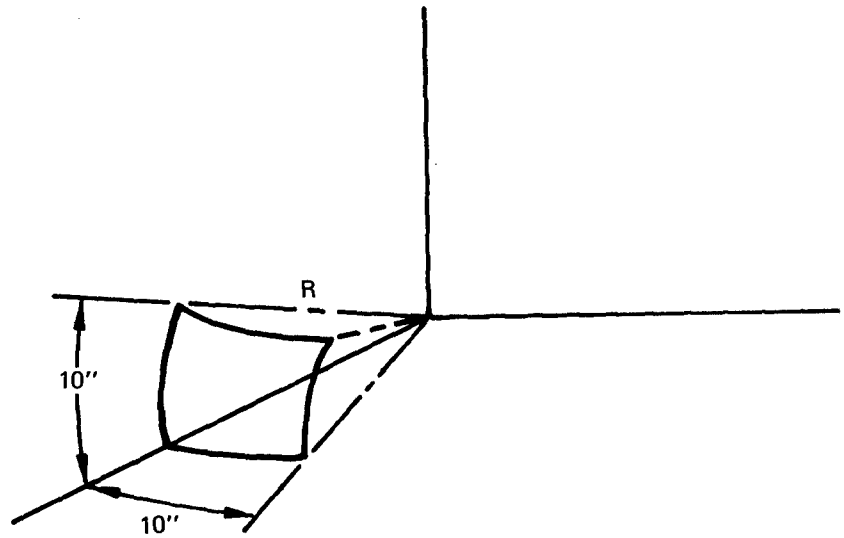

EIGENVALUES

R	1	2	3	4	5
25	$-0.85(10)^{-6}$	$-0.22(10)^{-6}$	$0.16(10)^{-6}$	$0.16(10)^{-5}$	1.0
50	$-0.19(10)^{-5}$	$-0.10(10)^{-5}$	$-0.39(10)^{-7}$	$0.25(10)^{-6}$	0.42
100	$-0.16(10)^{-5}$	$-0.17(10)^{-6}$	$0.78(10)^{-8}$	$0.29(10)^{-6}$	$0.69(10)^{-2}$
1000	$-0.12(10)^{-5}$	$-0.27(10)^{-7}$	$0.18(10)^{-6}$	$0.50(10)^{-6}$	$0.94(10)^{-6}$

R	6	7	18	19	48
25	1.0	1.0	$0.45(10)^{2}$	$0.15(10)^{6}$	$0.29(10)^{9}$
50	0.84	1.0	1.0	$0.14(10)^{6}$	$0.29(10)^{9}$
100	$0.14(10)^{-1}$	1.0	1.0	$0.14(10)^{6}$	$0.29(10)^{9}$
1000	$0.18(10)^{-5}$	1.0	1.0	$0.14(10)^{6}$	$0.29(10)^{9}$

Figure 7.1 – Eigenvalues of Stiffness Matrix of Quadrilateral Element for Sector of Sphere

When applying the quadrilateral element, the use of average strains to compute the stresses has been found a very convenient approach. Thus, by using the notation of Chapters 5 and 6, the average strain may be written as

$$\begin{Bmatrix} \Delta\bar{E} \\ \Delta\bar{\kappa} \end{Bmatrix} = [B2]_{avg}[A] \{\Delta\bar{v}\} \tag{7.1}$$

where

$$[B2]_{avg} = \frac{1}{\sum_{i=1,16} \Delta S_i} \left(\sum_{i=1,16} [B2]_i \Delta S_i \right) \tag{7.2}$$

and ΔS_i is the area of the subtriangle i in Figure 6.1. Thus equation (7.2) is an expression for a weighted B2 matrix with which the average strain can be computed.

The analysis of the membrane cylinder shown in Figure 7.2 demonstrates the argument for using the average strain concept. The cylinder is loaded externally with hydrostatic pressure. It is restrained from moving in the longitudinal direction and thus is in a state of plane strain. The cylinder is idealized with three elements all of the same size.

The radial displacement computed by using the quadrilateral element agreed within 2 percent of the exact value. However, the membrane stresses computed at the 16 integration points ranged from 25 percent over to 15 percent under the exact values. The average membrane stresses computed by using equation (7.1) were 4.5 percent over the exact values. This is much better than obtainable by the usual practice of taking the stress at the centroid of the element (approximately 15 percent under the correct value).

7.3 GRAVITY-LOADED CYLINDER

The quadrilateral element was evaluated with reference to the cylindrical shell roof shown in Figure 7.3. The shell was loaded by its own dead load; it was supported by diaphragms (simple support) at each end and was free along both sides.

The roof problem has been studied by many developers of finite elements for shells and has become a bench mark for comparing the accuracy of the elements reported. In a paper comparing the finite difference and finite element methods, Forsberg [70] pointed out the difference in deflections that can be obtained with the finite element method in application to this problem. He reported that these differences can be attributed to the shell equations used in formulating the various elements. By first programming the shallow shell and then the deep shell equations into a very accurate finite difference program, he was able to explain the differences that had previously been reported in the literature. Forsberg also indicated [70] that the analysis which uses flat plate elements converges to the results obtained by the deep shell equations implemented in the finite difference program.

The convergence of solutions to the displacement obtained at the center of the free edge is plotted in Figure 7.4 for several of the most recent elements published and for the

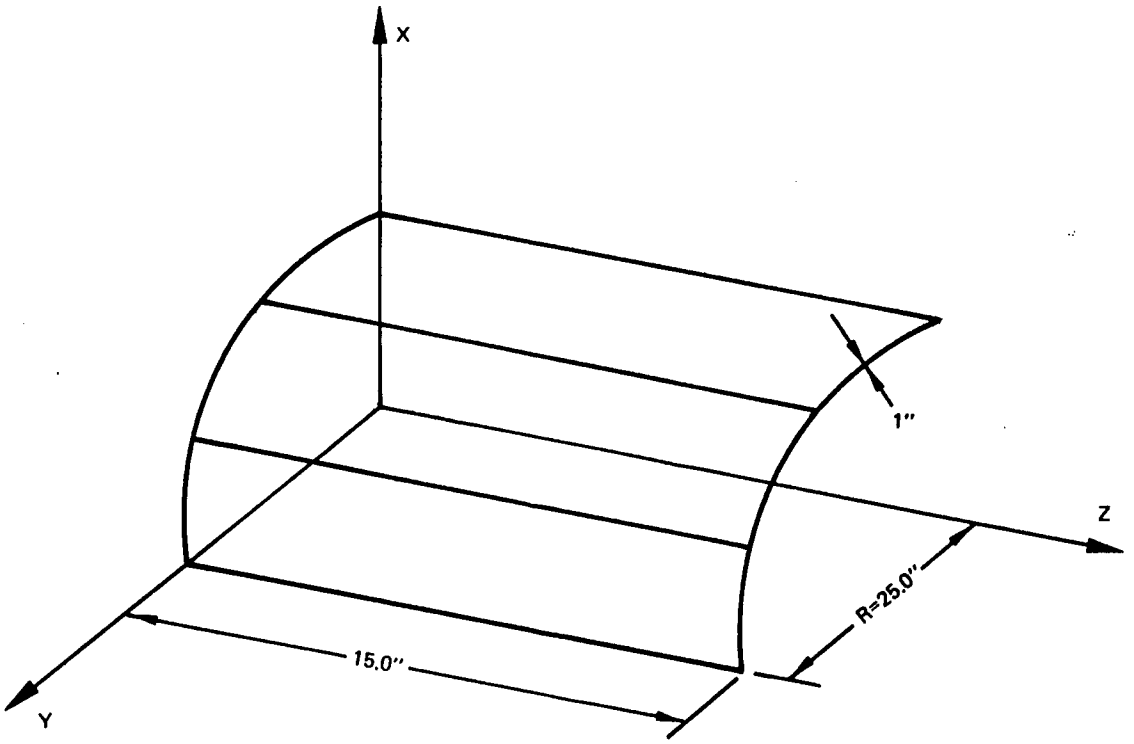

YOUNG'S MODULUS = $3(10)^7$
POISSON'S RATIO = 0.3
LOADING = UNIFORM EXTERNAL PRESSURE

Figure 7.2 – Membrane Cylinder

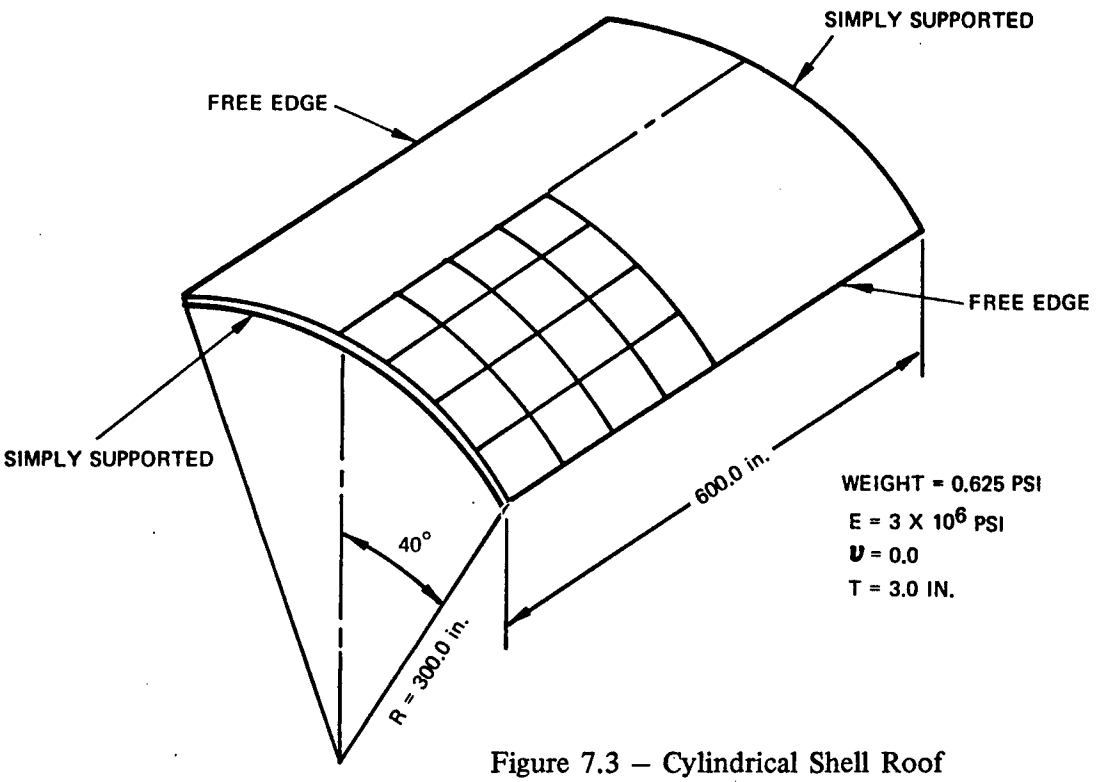

Figure 7.3 – Cylindrical Shell Roof

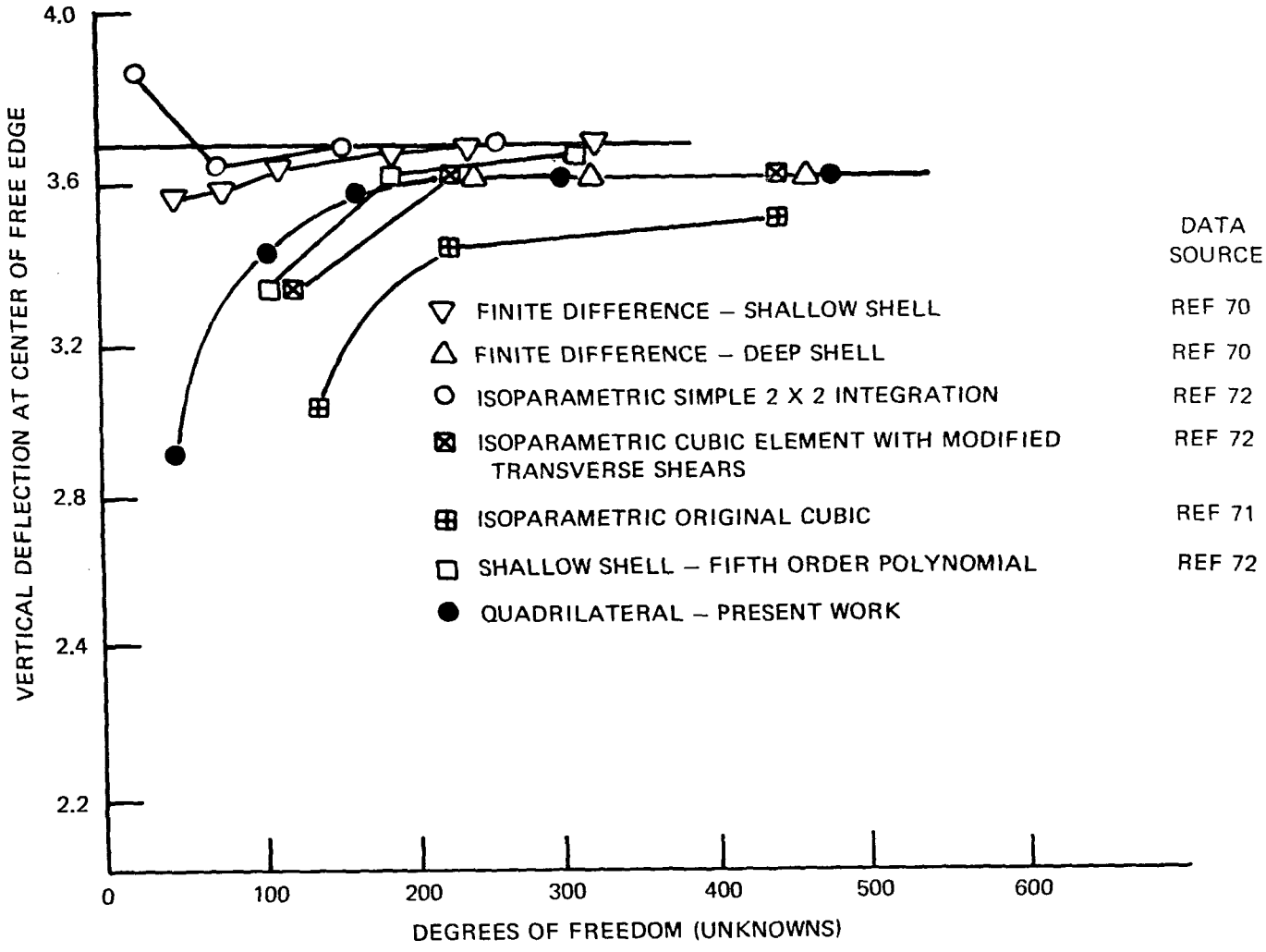

Figure 7.4 – Total Number of Degrees of Freedom (Unknowns)

quadrilateral element reported here. The two results obtained by the finite difference shallow shell and deep shell study of Forsberg [70] are also shown. The abscissa is the total number of unknowns.

Ahmed et al. [71] extended to shell problems the isoparametric concept used for the development of a broad class of finite elements. These results are shown in Figure 7.4. Specializations were recently added to make the original formulation more effective with reference to thin shells [72]. Several schemes were studied, and two of the more rapidly converging ones are included in Figure 7.4. The first is the case where a simple 2 x 2 Gauss point integration was used with the parabolic element, and the second is the application of a cubic element with modified transverse shears. It is interesting to note that the first converges to the shallow shell results and the second to the deep shell results obtained by Forsberg [70].

The result obtained by the rapidly converging element of Cowper et al. [22] is also plotted in Figure 7.4. This element is a conforming type and uses fifth order polynomials for displacements, which explains its good behavior. Its convergence to the shallow shell displacement of Forsberg [70] is as expected since it is this type of strain displacement equation which is used in global coordinates to derive the element.

Finally, the displacements obtained from the quadrilateral element reported here are given in Figure 7.4 for increasing grid refinement. Meshes of 2 x 2, 3 x 3, 4 x 4, 4 x 5, and 4 x 7 were used in the study. The five and seven subdivisions were in the longitudinal direction. Since the Marguerre shallow shell theory [58] is applied in local element coordinates and not in global coordinates, the displacements converge to the deep shell displacement. Computing time for the 3 x 3 case on the CDC 6400 was 2.6 minutes, approximately three times that required on a CDC 6600 computer.

7.4 RING-STIFFENED CYLINDER

In Section 5.3, the generalized displacements were increased to 12 per node to include the derivative of u, v, and w with respect to z. This was done to facilitate the transformation of the element so that it could be applied to branched and stiffened shells.

The portion of the ring-stiffened cylinder shown in Figure 7.5 was analyzed to demonstrate this capability. It is assumed that the cylinder is infinite in length with periodic spacing of the stiffening rings. Node A is a midbay between two rings. Since the behavior is periodic, the idealization shown may be used to analyze the shell.

At points where the shell is not intersected by another shell or stiffening reinforcement, such as nodal point B, a local nodal point coordinate system is established as described in Section 4.4 and the degrees of freedom that are derivatives with respect to the shell normal are set equal to zero. This is generally true in applying the element. Since these degrees of freedom are not associated with the stiffness of the element, they are eliminated. This is not done at points such as C since the derivatives with respect to the normal on the shell surface are degrees of freedom that are associated with the stiffness of the elements in the web of

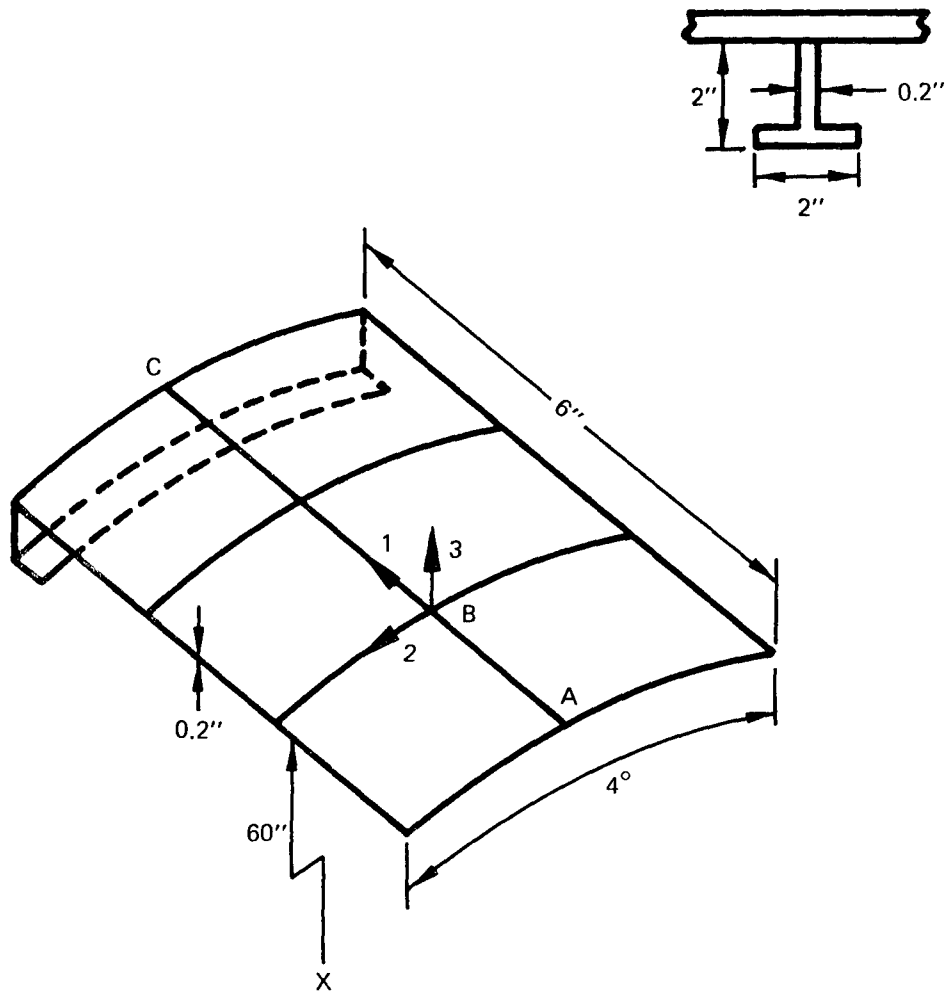

RADIAL DISPLACEMENTS		
POINT	COMPUTED	REFERENCE 73
A	$6.00\ (10)^{-4}$	$6.29\ (10)^{-4}$
C	$2.62\ (10)^{-4}$	$2.66\ (10)^{-4}$

Figure 7.5 – 10-Element Idealization of Ring-Stiffened Cylinder

the stiffener. Thus there is a maximum of nine degrees of freedom at points such as B, and a maximum of twelve degrees of freedom at points such as C.

The results obtained by using the quadrilateral element in the ten-element idealization are tabulated in the figure. The displacements obtained by using the theory presented by Pulos and Salerno [73] are also shown. The maximum difference is seen to be approximately 4.5 percent. It is noted that the study could just as well have been done with five elements since there is no variation in the circumferential direction.

7.5 BAR-SPRING PROBLEM

The previously derived incremental formulation is applicable to all nonlinear static structural problems which include the effects of large deformations. Figure 7.6 presents a very simple, but highly nonlinear, problem that is good for purposes of evaluation and comparison.

The bar problem has been studied by a number of investigators, most recently by Hibbitt [11] who uses the example to demonstrate the error that occurs in summing stresses in an incremental solution to nonlinear problems. Previous incremental formulations linearized the nonlinear equation in order to obtain a solution; this caused an error in the accumulated stresses since the strain, and hence the stresses, change quadratically in an increment. The results of the linearized formulation are plotted in Figure 7.6 along with the results obtained by the incremental formulation derived herein. The finite element results are plotted against the exact solution. Note that the formulation derived in the present study noticeably improves the computed displacements.

Since the formulation that was derived in Chapter 2 is complete, an iteration process should lead to very accurate answers for the bar-spring case. This was found to be true.

The results of the study are given in Table 7.1. The linear result was obtained first with a 1/10-pound load. The displacement was then computed at load levels that were multiples of 3 pounds up to 30 pounds. The tolerance ratio referred to in the table is described in the last paragraph of Section 6.1. The integers shown in the table are the number of iterations required to go from one load level to the next in order to obtain the indicated accuracy.

The entries in the table indicate that very accurate results can be obtained with the formulation if one is willing to pay the price for computing. There may be cases where extreme accuracy is desired, but for most practical problems, the high number of iterations shown for the tighter tolerances is not warranted. The important point is that the accuracy is there if it is needed.

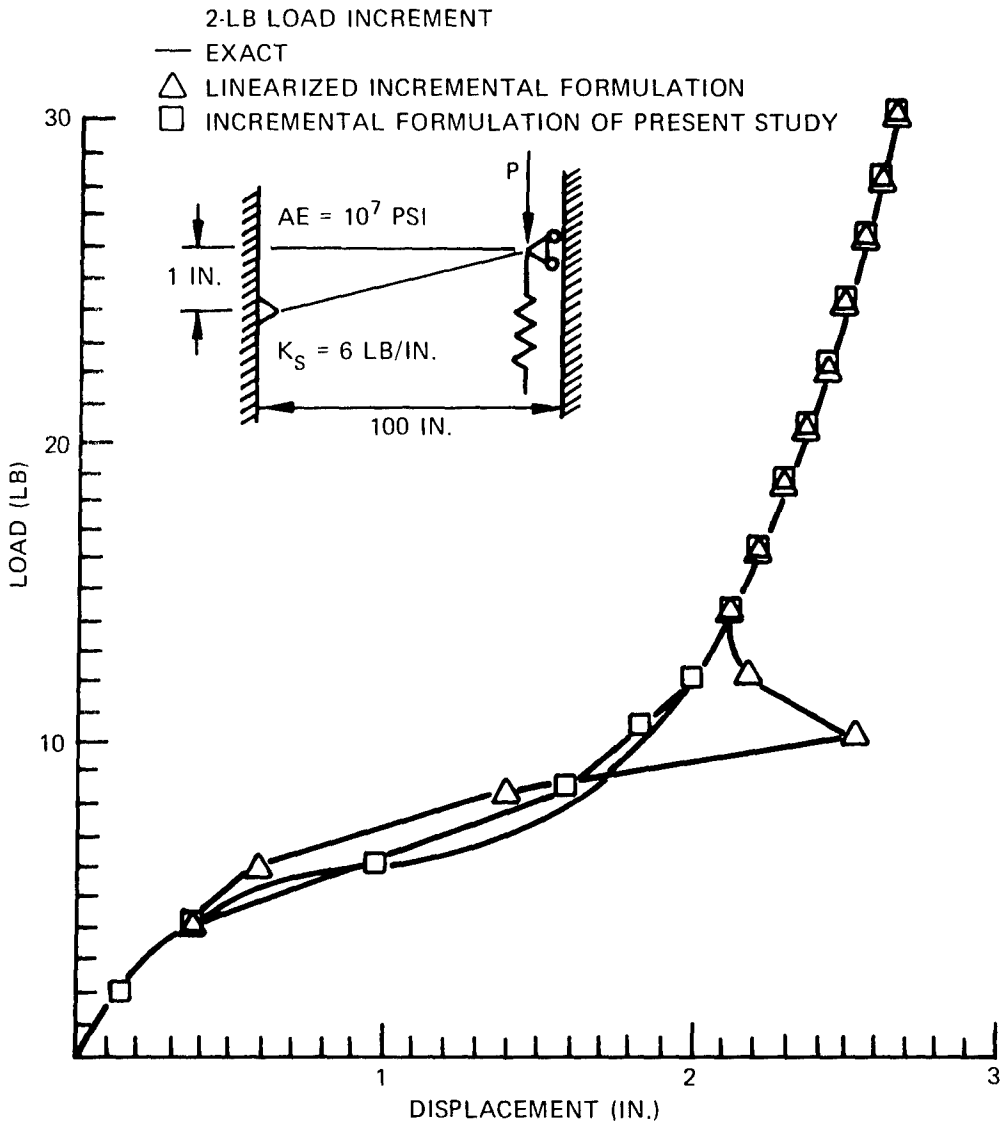

Figure 7.6 – One-Dimensional Bar-Spring Problem

TABLE 7.1

BAR-SPRING PROBLEM

DISPLACEMENT VERSUS TOLERANCE RATIO

Load lb	Exact Solution	Tolerance Ratio							
		2.0	1.75	1.5	1.25	1.1	1.05	1.01	1.001
0.1		0.00625059							
3.0	0.235363	^{0}0.22458	^{0}0.22458	^{0}0.22458	^{0}0.22458	^{1}0.232882	^{1}0.232882	^{2}0.234794	^{5}0.235340
6.0	1.0000	^{0}0.593575	^{0}0.593575	^{1}0.681971	^{1}0.681971	^{3}0.794509	^{5}0.858871	^{13}0.966944	^{26}0.997661
9.0	1.76462	^{1}1.79608	^{1}1.79608	^{1}1.79130	^{1}1.79130	^{1}1.76925	^{1}1.76409	^{1}1.76428	^{1}1.76488
12.0	2.0000	^{0}1.94017	^{1}2.00431	^{1}2.00418	^{2}1.99996	^{2}1.99991	^{3}1.99992	^{3}2.00026	^{4}2.00024
15.0	2.16169	^{0}2.17539	^{0}2.15485	^{0}2.15424	^{1}2.16286	^{1}2.16329	^{2}2.16168	^{3}2.16193	^{4}2.16189
18.0	2.28913	^{0}2.26873	^{0}2.28626	^{0}2.28646	^{1}2.29059	^{1}2.29062	^{2}2.28908	^{3}2.28936	^{4}2.28930
21.0	2.39610	^{0}2.40428	^{0}2.39155	^{0}2.39134	^{0}2.39144	^{1}2.39731	^{2}2.39604	^{3}2.39630	^{4}2.39624
24.0	2.48921	^{0}2.47746	^{0}2.48749	^{0}2.48765	^{0}2.48861	^{1}2.49023	^{1}2.49017	^{3}2.48939	^{4}2.48933
27.0	2.57222	^{0}2.57828	^{0}2.56939	^{0}2.56925	^{0}2.56878	^{1}2.57309	^{2}2.57210	^{3}2.57238	^{4}2.57231
30.0	2.64747	^{0}2.63890	^{0}2.64651	^{0}2.64663	^{0}2.64717	^{1}2.64823	^{1}2.64808	^{3}2.64761	^{4}2.64755

7.6 SIMPLY SUPPORTED SQUARE PLATE

The next example gives a further comparison between the linearized formulation and the formulation developed in this study. The structure is a simply supported square plate (Figure 7.7) subjected to uniform pressure loading. The plate is restrained against in-plane motion and thus causes the buildup of membrane forces. The thickness is 0.1 in., Young's modulus is 30 million psi, and Poisson's ratio is 0.316.

Levy [74] solved this problem by a trigonometric series expansion. Bergan [47] used 16 elements for a finite element solution to the problem and performed a Newton-type iteration at each load level to improve the results. Their results are shown in Figure 7.7 along with the Hibbitt results [11] for the linearized formulation and the formulation developed in the present study. Both runs with each of Hibbitt and present formulations were performed with the tolerance ratio set equal to 2.0 in order to compare running times. Since the formulation presented in Chapter 2 does not require the computation of the initial stress, i.e., geometric stiffness matrix, one would expect the running time to be less for this theory. The formulation of this study took 57 percent of the time required for the theory presented by Hibbitt [11]. One would not expect this same reduction in all cases since as size the problem gets larger, the computation of stiffness matrices becomes a smaller part of the total computing

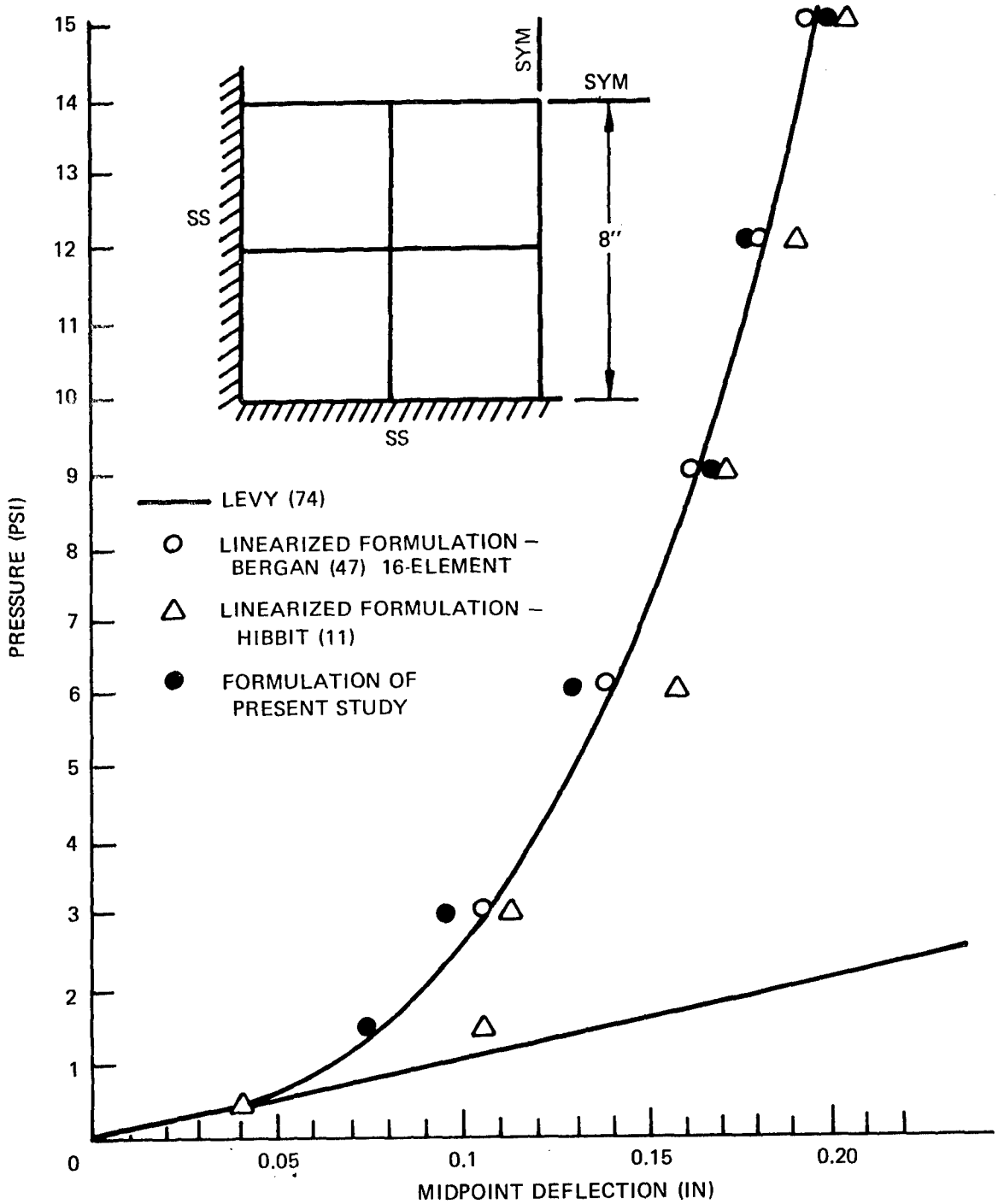

Figure 7.7 – Load Deflection Curve for Square Plate

time. Note that again that the present formulation gives improved results over the linearized formulation for the same idealization and iterative scheme.

7.7 CENTRALLY LOADED SPHERICAL CAP

The centrally loaded aluminum cap shown in Figure 7.8 was analyzed to give an example of inelastic material behavior. A 90-deg segment of the cap was idealized with seven elements. This case and the experimental results are from Penning and Thurston [75]. The shell was fixed at the boundary, Young's modulus was equal to 1×10^7, and Poisson's ratio was 0.33. The proportional limit of the effective stress-effective strain curve was 37,000 psi. To model the strain-hardening portion of the curve, three linear segments with the following properties were used: 0.5×10^7, 0.0; 0.15×10^7, 0.9×10^{-3}; and 0.44×10^6, 0.28×10^{-2}. The first number in each pair gives the slope and the second number the starting equivalent plastic strain of the segment.

The comparison between experimental results and the computed results obtained here is shown in Figure 7.9. Two different loading cases are studied, concentrated load and the case where the load is distributed over an area of 0.5-in. radius at the apex. The experimental result for the first case is for a loaded area with a radius equal to 0.0625. It was felt that having the load concentrated at a point would be sufficient to model the physical behavior.

The considerable difference in the displacements for the two cases shown in Figure 7.9 can be explained by the early yielding that occurred in the point-loaded case. Only this case was run by both the linearized formulation and the formulation presented in this study. The tolerance ratio used in all runs was 1.2. The present formulation required 63 percent of the computing time required for the linearized formulation.

7.8 PEAR-SHAPED CYLINDER

The next problem, shown in Figure 7.10, poses a good exercise for both the quadrilateral element and the nonlinear incremental formulation presented herein. This example is taken from Hartung [76] whose results were obtained with the finite difference method. The structure is similar to a proposed configuration for a space shuttle fuselage.

The load was applied to the end of the cylinder by a uniform end shortening. The cylinder was modeled by eight of the quadrilateral shell elements. Only one-fourth of the total area of the cylinder had to be modeled because of the double symmetry. The tolerance ratio used in the analysis was 1.05. Again, this is the ratio described in the last paragraph of Section 6.1. The integers in parentheses next to the data points indicate the number of iterations required to go from one load step to the next. Thus in the first increment of loading after the linear solution, i.e., in going from 100 to 200 lb of loading, the equations were formed the one required time plus five additional times. In the upper limits of the loading, the equations were merely assembled and solved one additional time.

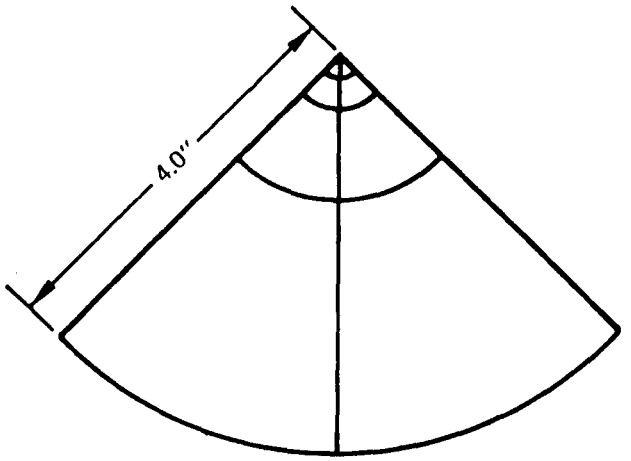

IDEALIZATION – SEVEN ELEMENTS

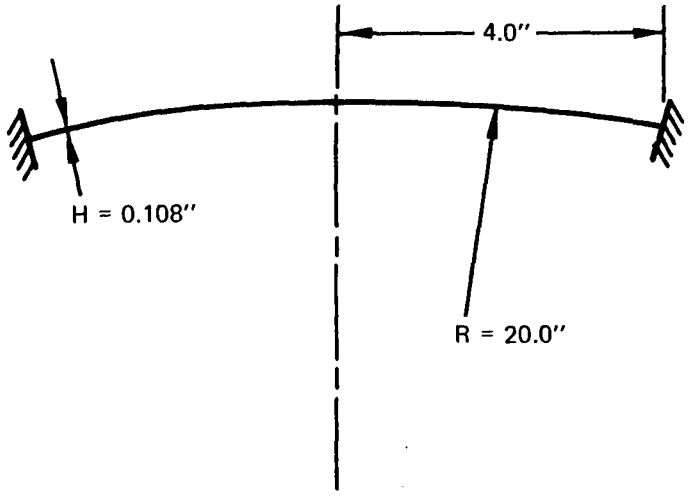

Figure 7.8 – Centrally Loaded Spherical Cap

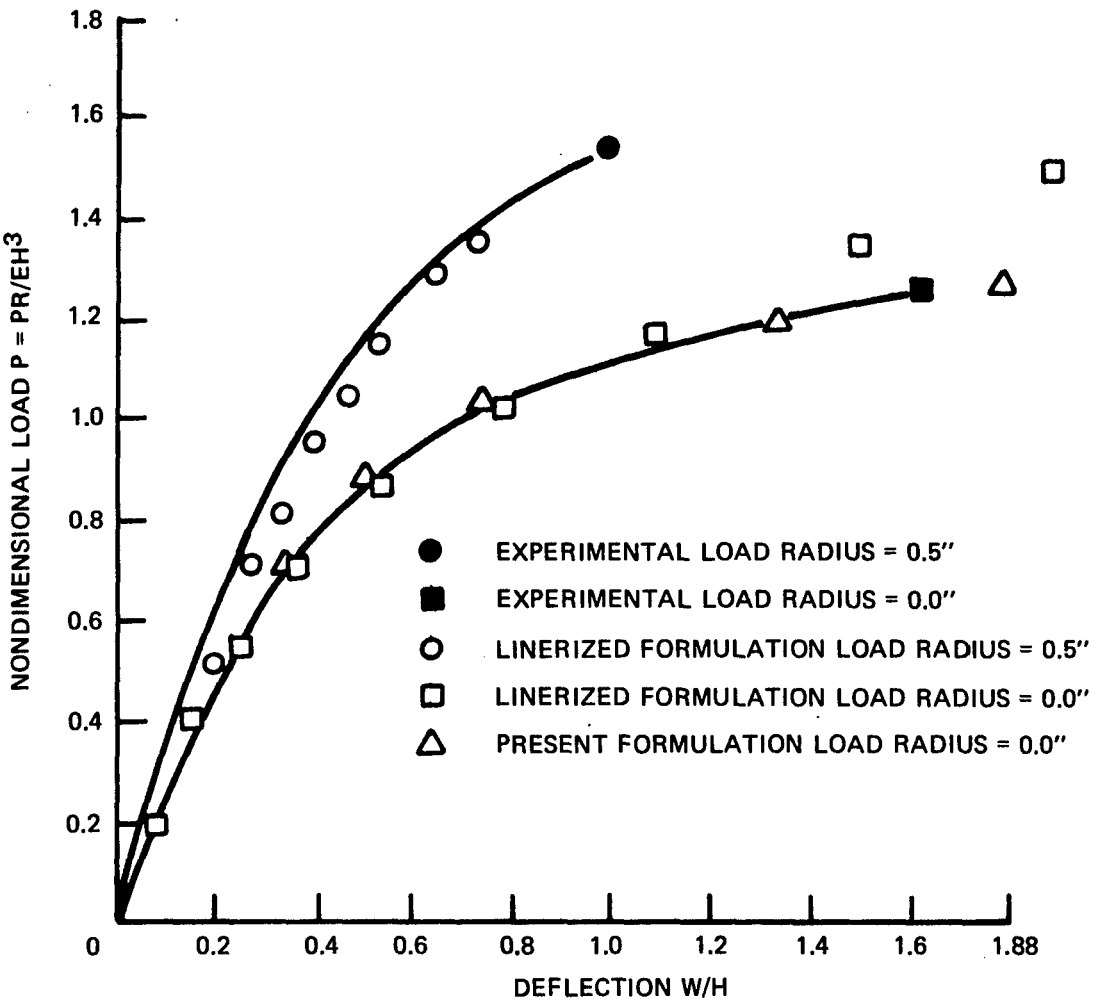

Figure 7.9 – Comparison of Computed and Experimental Results for Centrally Loaded Spherical Cap

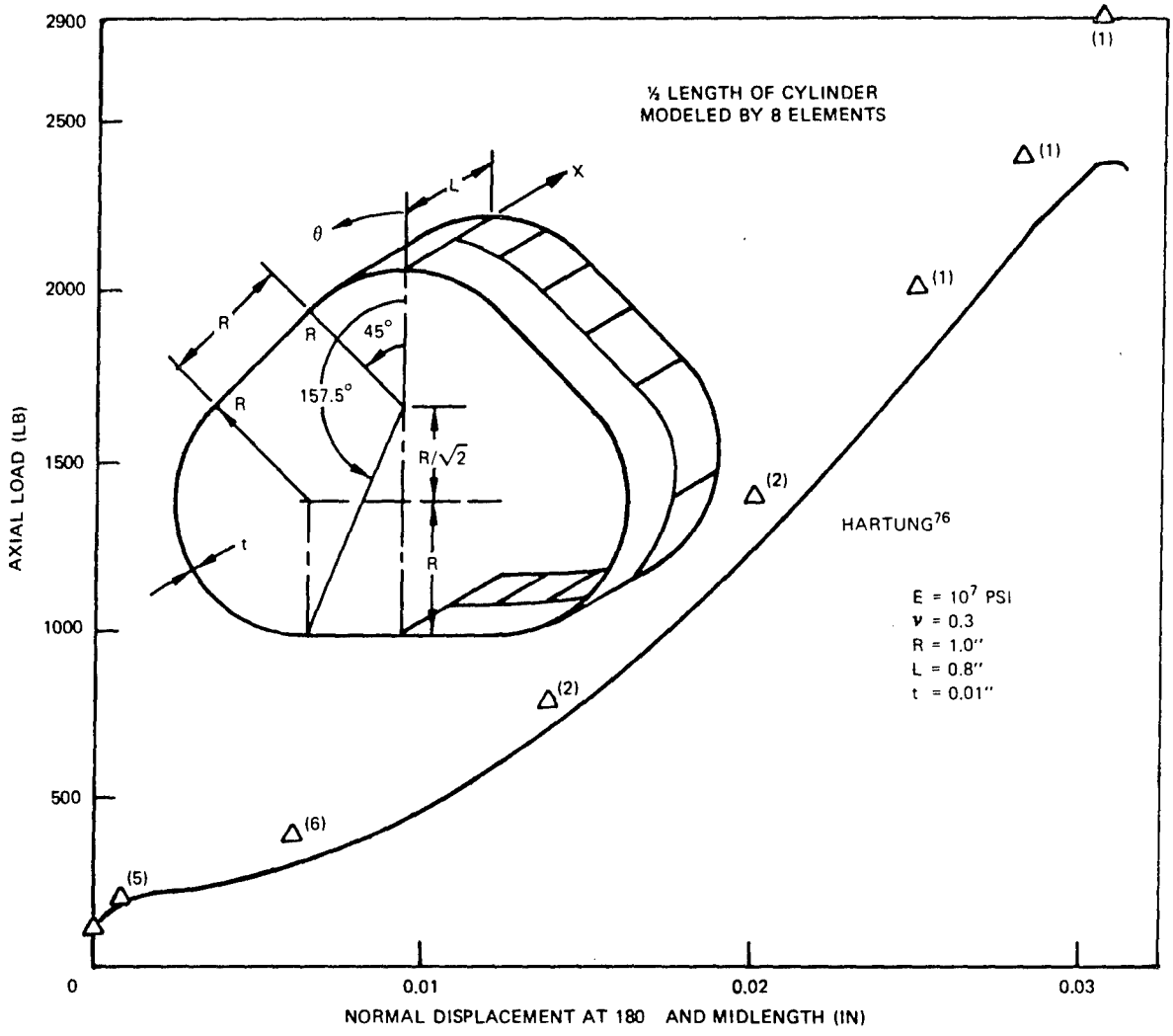

Figure 7.10 – Load-Displacement for Pear-Shaped Cylinder

The Hartung analysis [76] predicted a collapse at about 2400 lb whereas the present analysis was able to determine an equilibrium position at 2800 lb, the load at which the computation was stopped. The results given here for the finite element analysis cannot be regarded as conclusive until the same result is obtained in another analysis performed with a greater number of elements. This additional run would have to be made if the present analysis were being done for production or design work. At this point we note only that it is very encouraging that a reasonable analysis is obtainable with only eight elements and that the maximum load is reached in eight increments of loading.

CHAPTER 8
SUMMARY AND RECOMMENDATIONS FOR FURTHER WORK

8.1 SUMMARY

The first part of this dissertation presented a derivation for an incremental solution procedure for general structural mechanics problems. It was shown that the contribution of the sum of all previous increments had to be included in the solution for each load increment. The resulting nonlinear equilibrium equations were then manipulated and put into a form which allowed a combined incremental-iterative approach to their solution. The finite element formulation was then used to put the equilibrium equations into a form for their numerical solution. Since the resulting set of equations in the displacements turned out to be nonlinear and nonsymmetric in the coefficients, a solution procedure was introduced which uses present linear-symmetric equation solvers. The result of all the above was a direct solution procedure whereby the nonlinear incremental equations can be solved by using existing solution procedures without the need to first linearize the equations.

Next, the basic theory of plasticity required for the stress-strain relationships was reviewed. The description considered only small strain problems which may be assumed to be independent of temperature and time. Although this was not a primary part of this dissertation, its inclusion demonstrated the versatility of the previously derived formulation of the incremental equilibrium equations and solution procedure. The inclusion of the plastic material behavior was possible because a linear stress relationship was obtained between an increment of total stress in terms of an increment of total strain, and this is what was needed in the derivation of the incremental formulation.

The geometry of a general quadratic surface was considered next in preparation for the derivation of the quadrilateral shell element. The development work done here provides the necessary tools for performing an analysis of a structure which may be made up of several different quadratic surfaces. The slopes of the surface in terms of the local system can be computed by using a coordinate transformation in which the quadratic form of the surface is expressed in terms of the variables of each individual element coordinate system. This then enables the exact shell geometry to be used for computing the element stiffness matrices and for correcting the load to the base plane projected reference system. The work on geometry was concluded with emphasis on the surface vectors which were to be used later in satisfying the element convergence requirements and in performing transformations.

The derivation of the quadrilateral shell element was performed using the Marguerre shallow shell strain-displacement relationships [58]. The assumed displacement distribution used in the element is the same as that first proposed by Fraeijs de Veubeke [59] except that a linearization of the derivative degrees of freedom was imposed along the boundary to eliminate the midside nodes. The previous incremental formulation of the equilibrium equations was then specialized for the quadrilateral element in terms of the generalized stresses and strains; this resulted in expressions for the matrices used in computing the stiffness matrix and the

equilibrium correction vector. The form of the load vectors due to pressure loading, the change in loading due to a change in geometry, and the body force loading were derived. Transformations required for the element stiffness matrix and its degrees of freedom were then developed. These consistent transformations eventually facilitated the study of branched and stiffened shells. The derivation of the quadrilateral element was concluded with an explanation of the work done to ensure that the element satisfied the necessary convergence requirements.

The vehicle used for implementing all of the above and without which the work would have been practically impossible is the general purpose nonlinear finite element computer program developed by Marçal and his associates at Brown University. The format of the program is such that it is a very valuable research tool, and it is this capability that was exploited in performing the present work.

The primary work on the dissertation was concluded with the application of the quadrilateral element and the nonlinear incremental formulation. Examination of the adequacy of the shell element to satisfy the rigid body displacement requirement indicated that as the element became shallower, it had an increased ability to undergo rigid body motion without induced strains. The examination of the stresses in the element strengthened past experiences with higher order finite elements which had indicated that a weighted mean or average of the stresses provides far better values that have more physical meaning. The linear application of the shell element appears to work well for the cases studied, e.g., in application to a gravity-loaded cylinder, it gave very good results compared with previously published elements. Its application to a simple bar-spring problem proved to be very interesting and on the basis of agreement achieved with exact values, the formulation appears to have the capability to produce very accurate results. The use of the quadrilateral element in conjunction with the incremental formulation introduced here gives improved behavior over the previous linearized formulation. The application of the element and the formulation to a pear-shaped cylinder provided very encouraging results. This is the only known finite element solution to this problem.

8.2 RECOMMENDATIONS FOR FURTHER WORK

There are a number of possible extensions to the work reported in this dissertation. The most rewarding would be efforts to reduce the inordinate amount of computing time required for the nonlinear analysis of structures.

The nonlinear incremental formulation introduced herein uses a linear extrapolation method for estimating the amount of displacement that will occur in going from the intermediate configuration to the current configuration. Some higher order scheme should be investigated to determine whether it is possible to reduce the number of iterations required to reach convergence.

Another variation on the present incremental formulation that warrants investigation is the treatment of all nonlinearities as pseudo forces. As noted in the introduction, the nonlinearity due to inelastic material behavior is treated this way in the initial strain approach. There is a particular advantage in doing this, particularly for large problems, since the system of stiffness equations has to be solved only once during the solution process. (The evaluation of earlier formulations indicated that the equations had to be solved for each iteration.) Thus, if a method could be perfected to treat all of the nonlinearities as pseudo forces, the equivalent forces could be computed and then back-substituted to obtain the displacements. However, efforts to treat geometric nonlinearities as pseudo forces have not been too successful.

A pilot study was conducted to determine whether the formulation developed herein was sufficiently accurate and stable to permit all of the geometric nonlinearities to be transposed the right side and to treat them as equivalent forces. Using similar symbols as given in equation (2.32), we may write the resulting equation as

$$[K]^L \{\Delta\bar{V}\} = \{P\} + \{\Delta P\} + \{F\} + \{\Delta F\} + \{\Delta_G F\} - \{E\} - [K]^N \{\Delta\bar{V}_{est}\} \tag{8.1}$$

where now the superscripts on the K matrix indicate the linear and nonlinear parts.

Equation (8.1) was applied first to the bar-spring problem studied previously (Section 7.5). A tolerance ratio of 1.001 was used in the computation. The results obtained by using equation (8.1) are compared in Figure 8.1 with experimental values and with the results of a linearized formulation by Haisler et al.[77] for load increments of 0.2 and 0.05 pounds. The results agreed within two or three significant digits for the similar case given in Table 7.1 up to a certain level.

Loads were applied at the same levels in the bar-spring problem as given in Table 7.1, but the computation would not settle down for the 24-lb load level and simply oscillated about the correct displacement. It is believed, however, that this problem could be overcome by improving the controls used for determining convergence.

Equation (8.1) was also utilized to analyze the pear-shaped cylinder studied previously (Section 7.8). The tolerance ratio of 1.05 was again used. The solution process of equation (8.1) behaved very well and results obtained were identical to those given in Figure 7.10, including the number of iterations to reach convergence.

Finally, it is recommended that the incremental formulation presented in this dissertation be extended to dynamic problems by including inertia effects. This area of research may prove fruitful inasmuch as the solution of nonlinear dynamic problems is extremely difficult.

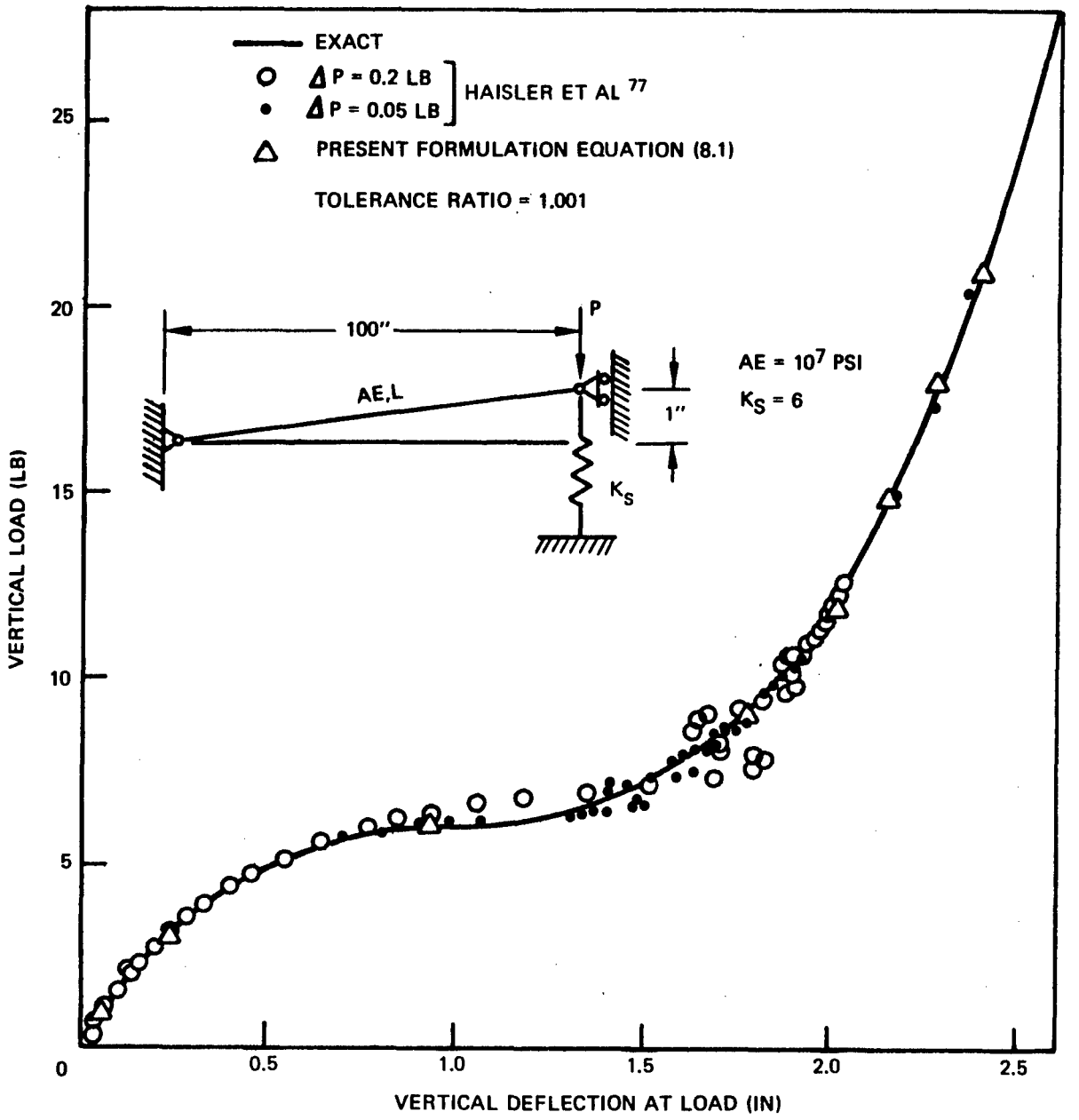

Figure 8.1 – Nonlinear Geometric Pseudo-Force Solution

ACKNOWLEDGMENTS

The author is grateful for the guidance received from his dissertation Director, Professor Nicholas Perrone, and the patience he displayed during the period when it seemed that the work would never be completed. The author also thanks Professors R.N. Vaishnav and J.H. Baltrukonis for their useful comments on the dissertation.

Special appreciation is due Professor Pedro V. Marçal of Brown University not only for his useful discussions on the work but also for the author's association with him over the past several years. The author's discussions with Dr. H.D. Hibbitt of the MARC Analysis Research Corporation of Providence, Rhode Island, are also gratefully acknowledged.

The author sincerely appreciates the benefit gained from his association with Mr. Martin Krenzke while employed at NSRDC over the past 9 years. The work in this dissertation was, in large part, a result of this experience.

Miss Nita Hight typed the manuscript and Mr. Fred Breiter prepared the figures. Both of these were done from very rough notes and required more than their usual fine efforts. Thanks also go to Mr. Peter Roth for programming the surface subroutines required for the quadrilateral element.

Finally, the author is deeply indebted to those marvelous people, his two daughters, Kathleen and Suzanne, and his wife, Diane, for the many hours they have given to him during the time required for the preparation and writing of this dissertation. Without their understanding and encouragement, this work would have been impossible.

APPENDIX
QUADRATIC SURFACES

	QUADRATIC FORM	PARAMETRIC FORM
CYLINDER	$\frac{X_1'^2}{A^2}+\frac{X_2'^2}{B^2}=1$	$X_1'=A\cos\beta_1$ $X_2'=B\sin\beta_1$ $X_3'=\beta_2$
CONE	$\frac{X_1'^2}{A^2}+\frac{X_2'^2}{B^2}-\frac{X_3'^2}{C^2}=0$	$X_1'=A\beta_2\cos\beta_1$ $X_2'=B\beta_2\sin\beta_1$ $X_3'=C\beta_2$
ELLIPSOID	$\frac{X_1'^2}{A^2}+\frac{X_2'^2}{B^2}+\frac{X_3'^2}{C^2}=1$	$X_1'=A\cos\beta_1\cos\beta_2$ $X_2'=B\sin\beta_1\cos\beta_2$ $X_3'=C\sin\beta_2$
HYPERBOLOID OF ONE SHEET	$\frac{X_1'^2}{A^2}+\frac{X_2'^2}{B^2}-\frac{X_3'^2}{C^2}=1$	$X_1'=A\cosh\beta_2\cos\beta_1$ $X_2'=B\cosh\beta_2\sin\beta_1$ $X_3'=C\sinh\beta_2$
HYPERBOLOID OF TWO SHEETS	$\frac{X_1'^2}{A^2}+\frac{X_2'^2}{B^2}-\frac{X_3'^2}{C^2}=-1$	$X_1'=A\sinh\beta_2\cos\beta_1$ $X_2'=B\sinh\beta_2\sin\beta_1$ $X_3'=C\cosh\beta_2$
ELLIPTIC PARABOLOID	$\frac{X_1'^2}{A^2}+\frac{X_2'^2}{B^2}-2CX_3'=0$	$X_1'=A\beta_1\cos\beta_2$ $X_2'=B\beta_1\sin\beta_2$ $X_3'\ \frac{\beta_1^2}{2C}$
HYPERBOLIC PARABOLID	$\frac{X_1'^2}{A^2}-\frac{X_2'^2}{B^2}+2CX_3'=0$	$X_1'=A(\beta_1-\beta_2)$ $X_2'=B(\beta_1+\beta_2)$ $X_2'=\frac{2\beta_1\beta_2}{C}$

REFERENCES

1. Ilyushin, *"Some Problems in the Theory of Plastic Deformations,"* (in Russian), Prikl. Mat. Mekh. Vol. 7, pp. 245-272, 1943; English translation, BMB-12, Grad. Div. Appl. Math., Brown Univ., for David W. Taylor Model Basin, 1946.

2. Armen, H., Pifko, A. and Levine, H.S., *"Finite Element Analysis of Structures in the Plastic Range,"* NASA CR-1649, February 1971.

3. Argyris, J.H., *"Elasto-Plastic Matrix Displacement Analysis of Three-Dimensional Continua,"* Journal of the Royal Aeronautical Society, Vol. 69, September 1965, pp. 633-636.

4. Mallett, R.H., and Marçal, P.V., *"Finite Element Analysis of Nonlinear Structures,"* Journal of the Structures Division, American Society of Civil Engineers, Vol. 94, No. ST9, September 1968, pp. 2081-2105.

5. Martin, H.C., *"Derivation of Stiffness Matrices for the Analysis of Large Deflection and Stability Problems,"* Proc. 1st Conference on Matrix Methods in Structural Mechanics, AFFDL-TR-66-80, 1966, pp. 697-715.

6. Marçal, P.V., *"The Effect of Initial Displacements on Problems of Large Deflection and Stability,"* Brown University, Division of Engineering, ARPA E54, November 1967.

7. Hibbitt, H.D., Marçal, P.V., and Rice, J.R., *"A Finite Element Formulation for Problems of Large Strain and Large Displacement,"* Brown University Report No. 2, ONR N00014-67-A-0191-0007, June 1969.

8. Oden, J.T., and Keys, J.E., *"Numerical Analysis of Finite Axisymmetric Deformation of Incompressible Elastic Solids of Revolution,"* Int. J. Solids Struct., 1970, Vol. 6, pp. 497-518.

9. Hofmeister, L.D., Greenbaum, G.A., and Evensen, D.A., *"Large Strain, Elasto-Plastic Finite Element Analysis,"* Proceedings of the AIAA/ASME 11th Structures, Structural Dynamics and Material Conference, Denver, Colorado, April 22-24, 1970, pp. 250-259.

10. Stricklin, J.A., Haisler, W.E., and Von Riesemann, W.A., *"Geometrically Nonlinear Analysis by the Direct Stiffness Method,"* Texas A&M University, Aerospace Engineering Department, Report 70-16, August 1970.

11. Hibbitt, H.D., *"A Numerical Thermo-Mechanical Model for the Welding and Subsequent Loading of a Fabricated Structure,"* Ph.D. Thesis, Division of Engineering, Brown University, June 1972.

12. Greene, B.E., Strome, D.R., and Weikel, R.D., *"Application of the Stiffness Method to the Analysis of Shell Structures,"* Proc. Aviation Conference, ASME, Los Angeles, March 1961.

13. Clough, R.W., and Tocher, J.L., *"Analysis of Thin Arch Dams by the Finite Element Method,"* Proc. of Symposium on Theory of Arch Dams, Southhampton Univ. 1964 (Pergamon Press, 1965).

14. Zienkiewicz, O.C., and Cheung, Y.K., *"Finite Element Method of Analysis for Arch Dam Shells and Comparison with Finite Difference Procedures,"* Proc. of Symposium on Theory of Arch Dams, Southhampton Univ. 1964 (Pergamon Press, 1965).

15. Gallagher, R.H., *"Analysis of Plate and Shell Structures,"* Proc. of Symposium on Application of Finite Element Methods in Civil Engineering, Vanderbilt University, 1969.

16. Key, S.W., and Beisinger, Z., *"The Analysis of Thin Shells with Transverse Shear Strains by the Finite Element Method,"* Proc. of Second Air Force Conference on Matrix Methods in Struct. Mech., Ohio, 1968.

17. Argyris, J.H., and Scharph, D.W., *"The Sheba Family of Shell Elements for the Matrix Displacement Method,"* J. Royal Aeronautical Society, 72, pp. 873-883, 1968.

18. Dupuis, G.A., *"Application of Ritz's Method to Thin Elastic Shell Analysis,"* Brown University, Division of Engineering, Naval Ship Research and Development Center, Technical Report 1, 1970.

19. Dupuis, G.A., and Goel, J.J., *"A Curved Finite Element for Thin Elastic Shells,"* Brown University, Division of Engineering, Office of Naval Research, Technical Report 4, 1969.

20. Zienkiewicz, O.C., Irons, B.M., Ergatoudis, J., Ahmad, S., and Scott, F.C., *"Iso-Parametric and Associated Element Families for Two- and Three-Dimensional Analysis,"* **Finite Element Methods in Stress Analysis**, pp. 383-432, The Technical University of Norway, Trondheim, Norway, 1969.

21. Zienkiewicz, O.C., **The Finite Element Method in Engineering Science, McGraw-Hill, London, 1971.**

22. Cowper, G.R., Lindberg, G.M., and Olson, M.D., *"A Shallow Shell Finite Element of Triangular Shape,"* International Journal of Solids and Structures, pp. 1133-1155, August 1970.

23. Cowper, G.R., Lindberg, G.M., and Olson, M.D., *"Comparison of Two High-Precision Triangular Finite Elements for Arbitrary Deep Shells,"* Proc. of Third Air Force Conference on Matrix Methods in Struct. Mech., Ohio, 1970.

24. Strickland, G.E., and Loden, W.A., *"A Doubly-Curved Triangular Shell Element,"* Proc. of Second Air Force Conference on Matrix Methods in Struct. Mech., Ohio, 1968.

25. Connor, J., and Brebbia, C., *"Stiffness Matrix for Shallow Rectangular Shell Element,"* Proc. ASCE, Journal of the Eng. Mech. Div., No. EM 2, April 1968.

26. Cantin, R., and Clough, R., *"A Curved Cylindrical Shell Discrete Element,"* AIAA Journal, Vol. 6, No. 5, May 1968.

27. Bogner, F., Fox, R., and Schmit, L., *"A Cylindrical Shell Discrete Element,"* AIAA Journal, Vol. 5, No. 4, April 1967.

28. Gallagher, R.H., and Yang, H., *"Elastic Instability Predictions for Doubly-Curved Shells,"* Proc. of Second Air Force Conference on Matrix Methods in Struct. Mech., Wright-Patterson AFB, Ohio, 1968.

29. Wempner, G., Oden, J.T., and Kross, D., *"Finite-Element Analysis of Thin Shells,"* Proc. ASCE, Journal of the Eng. Mech. Div., No. EM 6, December 1968.

30. Bonnes, G., Dhatt, G., Giroux, Y., and Robichaud, L., *"Curved Triangular Elements for the Analysis of Shells,"* Proc. of Second Air Force Conference on Matrix Methods in Struct. Mech., Ohio, 1968.

31. Greene, B., Jones, R., and Strome, D., *Dynamic Analysis of Shells Using Doubly-Curved Finite Elements,"* Proc. Second Air Force Conference on Matrix Methods in Struct. Mech., Ohio, 1968.

32. Utku, S., *"Stiffness Matrices for Thin Triangular Elements of Nonzero Gaussian Curvature,"* AIAA Journal, Vol. 5, No. 9, September 1967.

33. Deak, C., *"Analysis of Shallow Shells by the Displacement Method,"* Univ. of Wash., College of Eng., Report 77-4, June 1967.

34. Dhatt, G., *"Numerical Analysis of Thin Shells by Curved Triangular Elements Based on Discrete-Kirchoff Hypothesis,"* Proc. of Symposium on Application of Finite Element Methods in Civil Engineering, Vanderbilt Univ., November 13-14, 1969.

35. Olson, M., and Lindberg, G., *"Vibration Analysis of Cantilevered Curved Plates Using a New Cylindrical Shell Finite Element,"* Proc. of the Second Air Force Conference on Matrix Methods in Structural Mechanics, Wright-Patterson AFB, Ohio, October 1968.

36. Koiter, W.T., *"A Consistent First Approximation in the General Theory of Thin Elastic Shells,"* **The Theory of Thin Elastic Shells**,pp. 12-33, Proc. Symp. IUTAM, Delft 1959, North-Holland Publishing Co., Amsterdam, 1960.

37. Budiansky, B., and Sanders, J.L., *"On the Best First-Order Linear Shell Theory,"* **Progress in Applied Mechanics**, pp. 129-140, The Macmillan Co., New York, 1963.

38. Washizu, K., **Variational Methods in Elasticity and Plasticity**, Pergamon Press, 1968.

39. Novozhilov, V.V., **The Theory of Thin Shells**, P. Noordhoff Ltd., The Netherlands, 1959.

40. Fung, Y.C., **Foundations of Solid Mechanics**, Prentice Hall, Englewood Cliffs, New Jersey, 1965.

41. Fraeijs de Veubeke, B., *"Displacement and Equilibrium Models in the Finite Element Method,"* **Stress Analysis**, edited by O.C. Zienkiewicz and G.S. Holister, Wiley, New York, N.Y., 1965.

42. Cauchy, A.L., *"Sur L'Equilibre et le Mouvement Interior des Corps Consideres Comme des Masses Continues,"* Ex. de Math. 4 = Oeuvres (2) 9, (1829), pp. 342-369.

43. Green, A.E., Rivlin, R.S., and Shield, R.T., *"General Theory of Small Elastic Deformations Superposed on Finite Elastic Deformations,"* Proc. R. Soc. London (A) 211 (1952), pp. 128-154.

44. Murnaghan, F.D., **A Revision of the Theory of Elasticity, Anais Acad. Brasil Ci,** 21 (1949), pp. 329-336.

45. Felippa, C.A., *"Refined Finite Element Analysis of Linear and Nonlinear Two-Dimensional Structures,"* Ph.D. Dissertation, Univ. of Calif., Berkeley, 1966.

46. Murray, D.W., and Wilson, E.L., *"Finite Element Postbuckling Analysis of Thin Elastic Plates,"* AIAA Journal, Vol. 7, No. 10, 1969.

47. Bergan, Pal, G., *"Nonlinear Analysis of Plates Considering Geometric and Material Effects,"* Ph.D. Dissertation, Univ. of Calif., Berkeley, 1971.

48. Yaghmai, S., *"Incremental Analysis of Large Deformations in Mechanics of Solids with Applications to Axisymmetric Shells of Revolution,"* Ph.D. Dissertation, Univ. of Calif., Berkeley, 1968.

49. Nemat-Nasser, S., and Shatoff, H.D., *"A Consistent Numerical Method for the Solution of Nonlinear Elasticity Problems at Finite Strains,"* Department of the Aerospace and Mechanical Engineering Sciences, Univ. of California, San Diego, January 1970.

50. Hill R., **The Mathematical Theory of Plasticity**, Oxford University Press, London, England, 1950.

51. Koiter, W.T., *"Stress-Strain Relations, Uniqueness and Variational Theorems for Elastic-Plastic Materials with a Singular Yield Surface,"* Quart. Appl. Math., 11, 1953, pp. 350-354.

52. Naghdi, P.M., *"Stress-Strain Relations in Plasticity and Thermoplasticity,"* Inst. Eng. Res., Univ. of Calif. (Berkeley), Ser. 131, Issue 9, March 1960, p. 18.

53. Bridgman, P.W., *"The Effect of Hydrostatic Pressure on the Fracture of Brittle Substances,"* J. Appl. Phys., 18, 246, 1947.

54. Prager, W., *"Non-Isothermal Plastic Deformation,"* K. Nederl, Wetensch, Proceedings 61, 1958, pp. 176-192.

55. Prager, W., *"The Theory of Plasticity - A Survey of Recent Achievements,"* Proc. Inst. Mech. Engrs., London, 169, 41, 1955.

56. Shield, R.T., and Ziegler, H., *"On Prager's Hardening Rule,"* Z. ang. Math. und Phys. (1958), pp. 260-276.

57. McConnell, A.J., **Applications of the Tensor Calculus, Dover, 1931.**

58. Marguerre, K., *"On the Large-Deformation Theory of the Curved Plate,"* International Congress of Applied Mechanics, Boston, 1938.

59. Fraeijs de Veubeke, *"A Conforming Finite Element for Plate Bending,"* Int. J. Solids Struct., 4, pp. 95-108, 1968.

60. Marçal, P.V., *"Large Deflection Analysis of Elastic-Plastic Plates and Shells,"* Tech. Rpt. No. 1, Naval Ship Research and Development Center, Brown University, 1969.

61. Zienkiewicz, O.C., **The Finite Element Method in Engineering Science**, McGraw-Hill, London, England, 1971.

62. Irons, B.M.R., and Draper, K.J., *"Inadequacy of Nodal Connections in a Stiffness Solution of Plate Bendings,"* AIAA J., Vol. 3, No. 5, May 1965.

63. Hurty, W.C., and Rubinstein, M.F., **Dynamics of Structures**, Prentice-Hall, Englewood Cliffs, New Jersey, 1964.

64. Hibbitt, D.H., Levy, N.J., and Marçal, P.V., *"On General Purpose Programs for Nonlinear Finite Element Analysis,"* presented at the ASME Winter Annual Meeting, New York, N.Y., November 1970.

65. Marçal, P.V., *"On General Purpose Programs for Finite Element Analysis, with Special Reference to Geometrical and Material Nonlinearities,"* presented at the Symposium on Numerical Solution of Partial Differential Equations, Univ. of Maryland, May 1970.

66. Marçal, P.V., and King, I.P., *"Elastic-Plastic Analysis of Two-Dimensional Stress Systems by the Finite Element Method,"* International Journal of Mechanical Science, Vol. 9, No. 3, 1967, pp. 143-155.

67. McNamara, J.F., *"Incremental Stiffness Method for Finite Element Analysis of the Nonlinear Dynamic Problem,"* Ph.D. Thesis, Division of Engineering, Brown University, August 1971.

68. Martin, H.C., **Introduction to Matrix Methods of Structural Analysis**, McGraw-Hill, New York, N.Y., 1966, pp. 93-97.

69. , *"Eigensystem Subroutine Package,"* Argonne National Laboratory, Argonne, Illinois, May 1972.

70. Forsberg, K., *"An Evaluation of Finite Difference and Finite Element Techniques for Analysis of General Shells,"* IUTAM Conference on High Speed Computing of Elastic Structures, Liege, Belgium, 1970.

71. Ahmad, S., Irons, B.M., and Zienkiewicz, *"Analysis of Thick and Thin Shell Structures by Curved Finite Elements,"* International Journal for Numerical Methods in Engineering, Vol. 2, pp. 419-451, 1970.

72. Zienkiewica, O.C., Taylor, R.L., and Too, J.M., *"Reduced Integration Technique in General Analysis of Plates and Shells,"* International Journal for Numerical Methods in Engineering, Vol. 3, pp. 275-290, 1971.

73. Pulos, J.G., and Salerno, V.L., *"Axisymmetric Elastic Deformations and Stresses in a Ring-Stiffened, Perfectly Circular Cylindrical Shell under Externall Hydrostatic Pressure,* David Taylor Model Basin Report 1497, September 1961.

74. Levy, S., *"Bending of Rectangular Plates with Large Deflections,"* NACA Technical Note No. 846, 1942.

75. Penning, F.A., and Thurston, G.A., *"The Stability of Shallow Spherical Shells under Concentrated Load,"* NASA CR-265, 1965.

76. Hartung, R.F., *"An Assessment of Current Capability for Computer Anlaysis of Shell Structures,"* Wright-Patterson Air Force Base, Ohio, Technical Report AFFDL-TR-71-54, April 1971.

77. Haisler, W.E., Stricklin, J.A., and Stebbins, F.J., *"Development and Evaluation of Solution Procedures for Geometrically Nonlinear Structural Analysis by the Direct Stiffness Method,"* presented at the AIAA/ASME 12th Structures, Structural Dynamics, and Materials Conference, Anaheim, California, April 1971.

INITIAL DISTRIBUTION

Copies	
1	DDR&E
1	OP 098T
1	OP 981D
1	OP 982F
1	OP 02
1	ONR 102-0S
1	ONR 439
1	ONR 439/N. Perrone
1	ONR 466
1	MAT 03T
1	USNA
1	NAVPGSCOL
1	USNROTC & NAVADMINU, MIT
1	NAVWARCOL
1	SHIPS 031
1	SHIPS 0342
1	SHIPS 03423
1	SHIPS 2052
1	PMS-381
1	PMS-393
1	NAVAIRDEVCEN/E. McQuillen
1	NAVAIRDEVCEN/P. Przybylek
1	NELC
1	NAVUSEACEN/Lib
1	NAVUSEACEN 6505/J. Stachiw
1	NAVWPNSCEN
1	CIVENGRLAB/J. Crawford
1	CIVENGRLAB/K. Gray
1	NOL
1	NWL/W. Strong
1	NWL/W. Werback
1	NPTLAB NUSC
1	NLONLAB NUSC
1	NAVSHIPYD CHASN
1	NAVSHIPYD MARE
1	NAVSHIPYD PTSMH
1	SUPSHIP GROTON
1	SUPSHIP NPT NEWS
1	SUPSHIP PASCAGOULA
1	SEC 6101

Copies	
1	SEC 6110
1	SEC 6111
1	SEC 6114
1	SEC 6122
2	SEC 6129
1	SEC 6140
1	SEC 6147C
12	DDC
1	PIB/J. Kempner
1	Brown U/P. Marçal
1	Brown U/R. Nickell
1	Brown U/H. Hibbitt
1	U Cal Berkeley/R. Clough
1	Catholic U/S. Heller
1	Cornell U/R. Gallagher
1	U Mass/W. Nash
1	Oklahoma State U/D. Boyd
1	Princeton U/A. Eringen
1	SWRI/R. DeHart
1	VPI/G. Swift
1	U Washington APL/Lib
1	Franklin Inst Res Lab/Z. Zudans
1	Gen Dyn Elec Boat
1	Ingalls Shipbuilding
1	Lockheed Res Lab/D. Bushnell
1	McDonnell-Douglas Astronautics/ E. Stanton
1	Newport News Shipbuilding
1	Westinghouse Adv Reactor/R. Mallett

CENTER DISTRIBUTION

Copies	Code
1	17
1	172
1	1721
25	1725
1	1727

UNCLASSIFIED
Security Classification

DOCUMENT CONTROL DATA - R & D

(Security classification of title, body of abstract and indexing annotation must be entered when the overall report is classified)

1. ORIGINATING ACTIVITY (Corporate author)	2a. REPORT SECURITY CLASSIFICATION
Naval Ship Research and Development Center Bethesda, Maryland 20034	UNCLASSIFIED
	2b. GROUP

3. REPORT TITLE

Incremental Analysis of Nonlinear Structural Mechanics Problems with Applications to General Shell Structures

4. DESCRIPTIVE NOTES (Type of report and inclusive dates)

Final

5. AUTHOR(S) (First name, middle initial, last name)

Rembert F. Jones, Jr.

6. REPORT DATE	7a. TOTAL NO. OF PAGES	7b. NO. OF REFS
September 1973	104	77

8a. CONTRACT OR GRANT NO.	9a. ORIGINATOR'S REPORT NUMBER(S)
b. PROJECT NO.	4142
c.	9b. OTHER REPORT NO(S) (Any other numbers that may be assigned this report)
d.	

10. DISTRIBUTION STATEMENT

This document has been approved for public release and sale; its distribution is unlimited.

11. SUPPLEMENTARY NOTES	12. SPONSORING MILITARY ACTIVITY
Doctoral dissertation, Catholic University of America	Naval Ship Systems Command (Code 0342)

13. ABSTRACT

The primary theme is the nonlinear behavior of shell structures. A general formulation that can be applied to all structures is derived and then specialized for application to shells through the development of a quadrilateral shell finite element.

The formulation is in incremental form and is derived in terms of the material coordinate system. The procedure evolved to solve the nonlinear equilibrium equations allows for the inclusion of all terms as opposed to previous incremental procedures where the equations are linearized. The derivation of the formulation and solution procedure is independent of the finite element method, but it is this method that is used to exercise and apply the formulation. An elementary nonlinear problem is first solved and then more complex problems are studied by using the formulation and solution procedure.

The quadrilateral shell element which is introduced uses the exact geometry of the shell surface in the computation of stiffness matrices and loads. A consistent method is used for transforming the element and its properties; this improves element effectiveness for application to branched and reinforced shells. The shell surface geometry is used in the enforcement of the continuity of displacements for satisfying the convergence requirements. The ability of the element to undergo rigid body motion without causing strains is examined by studying the eigenvalues of the stiffness matrix of an element.

14. KEY WORDS	LINK A		LINK B		LINK C	
	ROLE	WT	ROLE	WT	ROLE	WT
Thin Shells						
Large Deformations						
Nonlinear Deformations						
Plasticity						
Finite Elements						
Incremental Formulation						